

Parameter sensitivity of climate models and climate driven ecological systems

Hanneke Elisabeth Moolenaar

Promotor: Prof. dr. J. Grasman
Hoogleraar wiskundige en statistische methoden
Wageningen Universiteit

Co-promotor: Dr. F.M. Selten
Onderzoeker Klimaat Variabiliteit
Koninklijk Nederlands Meteorologisch Instituut

Samenstelling

promotiecommissie: Prof. dr. A.A.M. Holtslag
Wageningen Universiteit

Prof. dr. ir. G. van Straten
Wageningen Universiteit

Dr. ir. E.H. van Nes
Wageningen Universiteit

Dr. G.J.H. Burgers
Koninklijk Nederlands Meteorologisch Instituut

Parameter sensitivity of climate models and climate driven ecological systems

Parameter gevoeligheid van klimaatmodellen en
klimaat gedreven ecologische systemen

Hanneke Elisabeth Moolenaar

Proefschrift
ter verkrijging van de graad van doctor
op gezag van de rector magnificus
van Wageningen Universiteit,
Prof.dr. M.J. Kropff
op maandag 11 september 2006
des namiddags te vier uur in de Aula

ISBN 90-8504-452-9

Contents

1	Introduction	1
1.1	Background	1
1.1.1	Modelling the climate	2
1.1.2	Climate and ecosystem	3
1.1.3	Parameter sensitivity and climate modelling	5
1.1.4	Climate driven metapopulation models	6
1.2	Research objectives	7
1.3	Scope of the method	10
1.4	Outline of the thesis	12
	References	16
2	Finding the effective parameter perturbations in atmospheric models; the Lorenz 63 model as case study	21
2.1	Introduction	21
2.2	Lorenz 63 model	23
2.3	Finding the effective parameter perturbations	24
2.3.1	The direct method	24
2.3.2	The adjoint method	25
2.4	Conclusions and discussion	31
2.5	Acknowledgements	33
	Appendix	34
	References	36
3	Sensitivity to forcing parameters in the T21QG atmospheric model	37
3.1	Introduction	37
3.2	Climate sensitivity analysis using Empirical Orthogonal Functions	41
3.2.1	The T21QG-model	41
3.2.2	Empirical Orthogonal Function (EOF) analysis	42
3.2.3	Parameter sensitivity analysis with the T21QG atmospheric model	43
3.3	Searching effective forcing parameter perturbations using the adjoint equations	46
3.3.1	The tangent linear and the adjoint equations	47

3.3.2	The perturbed model	50
3.3.3	Simulation results	51
3.4	Comparison with other search methods	52
3.4.1	Random selection of perturbations	54
3.4.2	Alternative selection of singular vectors as perturbations	54
3.4.3	Perturbation in the direction of EOF1	54
3.5	Conclusions	56
3.6	Acknowledgements	59
	Appendix	60
	References	62
4	Mathematical conservation ecology: supporting a herbivore metapopulation	65
4.1	Introduction	65
4.2	The herbivore-predator model	69
4.3	A herbivore metapopulation exposed to climatologic fluctuations	71
4.4	Herbivore fluctuations in the presence of a predator	75
4.5	Herbivore conservation in case of a migrating predator	78
4.6	Conclusions	81
4.7	Acknowledgements	85
	References	86
5	Species conservation by optimal parameter change in a metapopulation model	91
5.1	Introduction	91
5.1.1	Species conservation and sensitivity analysis	92
5.1.2	Finding effective parameter changes	93
5.1.3	Overview	95
5.2	Distribution in time of the local population size	95
5.3	A method to select effective perturbations in a large parameter set	98
5.3.1	Tangent linear and adjoint equations	101
5.3.2	Singular vectors as parameter perturbations	104
5.3.3	Simulation results	106
5.3.4	Importance of the singular value	112
5.4	Random selection of parameter perturbations	113
5.5	Concluding remarks	116
5.6	Acknowledgement	119
	References	120
	Summary	123
	Samenvatting	127
	Word of thanks	131

Contents

iii

Curriculum Vitae

133

CHAPTER 1

Introduction

1.1 Background

The global climate system consists of dynamical processes taking place in atmosphere, oceans, cryosphere (ice-sheets), geosphere (land surface) and biosphere (living organisms). Among these components many physical, chemical and biological interactions occur in a wide range of space and time scales, making it a highly complex system. The state of the global climate is determined to a large extent by the amount of energy stored by the climate system; the most important source of energy is the Sun.

The atmosphere is the most unstable and rapidly changing component of the system, which makes it difficult to predict its state even in the near future. The atmosphere consists of gases and aerosols (solid and liquid particles). The gases are mainly nitrogen (78.1%), oxygen (20.9%) and argon (0.93%). However, greenhouse gases (less than 0.1%), such as carbon dioxide, methane and ozone play an important role in the Earth's energy budget by their influence on the absorption and transfer of electromagnetic radiation. The same holds for solid aerosols (like sulphate, dust, black carbon) and liquid aerosols (water droplets in clouds) that are transported by the atmospheric currents from their respective source regions leading to highly variable concentrations in space and time. In addition, the atmosphere contains a varying amount of water vapour that is also a strong absorber of long wave radiation and as such contributes to the greenhouse effect.

The atmosphere and the oceans are strongly coupled; they exchange heat, momentum and water. The circulation of the oceans is much slower than that of the atmosphere. The oceans store a much larger quantity of energy than the atmosphere and the flow of energy between the oceans and atmosphere is an important aspect of the global climate. The cryosphere consists of those regions of the globe, both land and sea, that are covered by snow and ice. It has a high albedo (reflectivity of the solar radiation), so that a large fraction of incoming solar heat is not absorbed. Vegetation at the land surface and the soil itself contribute substantially to the absorption of solar energy and to the water cycle. Also, the texture of the land surface influences the dynamics of

the atmosphere as the air flows over it. Lastly, the biosphere has a large impact on the atmospheric composition. It influences the fluxes of certain greenhouse gases. For further reading on the climate system we suggest the IPCC report, (2001) and Trenberth, (1992).

1.1.1 Modelling the climate

The different processes in the climate system are expressed in mathematical equations and solved numerically on a discrete set of points covering the Earth, forming a numerical model. The most complex of these are used to simulate the behaviour of the climate system and in particular its response to changing future conditions like the projected increase in the amount of greenhouse gases. They consist of connected sub-modules describing the various parts of the climate system and are based on the fundamental laws of physics: conservation of energy, conservation of momentum, conservation of mass and the ideal gas law. The most complex climate models consist of an atmospheric general circulation model (AGCM) that describes the three-dimensional velocity fields, temperature and composition of the atmosphere, coupled to an ocean general circulation model (OGCM) that describes the three-dimensional ocean currents and water properties, a land surface model (LSM) describing soil moisture and energy fluxes at various depths and snow and vegetation characteristics, a sea-ice model that describes the formation, transport and melting of sea-ice. The latest developments include a representation of the carbon cycle in biogeochemistry modules that describe the uptake, storage and release of carbon by living organisms on land and in the ocean in order to include the feedback of changes in biology in a warmer world on the CO_2 levels in the atmosphere.

When dealing with such complex models, with their different scales in time and space, the necessity of making simplifications is unavoidable. The mathematical equations are based on approximations, the model is discretized and the solution is approximated at a finite number of positions (grid-points). The more grid-points a model has, the more complex the model and the more computation time it takes to calculate the solution. However, taking more grid-points does not necessarily give a better prediction of the model behaviour in future time. Some processes cannot be resolved in a model; they occur on a scale smaller than the grid-size or are too complex or even not well understood. These processes are captured in the model by parameterizations. Model parameters are fixed constants and are estimated by using observed data and/or derived from fundamental physical principles. Estimates that are less accurate affect the solution of the system of equations.

Uncertainty in the outcome of climate models is widely recognized (e.g. IPCC 2001, Reilley et al., 2001, Forest et al., 2002, Allen, 2003, Murphy et al., 2004, Stocker, 2004). It hinders policy-making on the issue of climate change. Besides parameter uncertainty, there is uncertainty in the understanding of the physical processes that influence the climate as well as uncertainty in how climate is changed by humans (such as energy consumption and green-house gas emissions). Because of this uncertainty, a range of possible climate changes is usually given. This range may be too large

to decide about the best policy on for instance reduction of greenhouse gas emissions. Stocker (2004) suggests that rather than tuning a model such that it fits the observations the best, one should quantify the range of outcomes when changing parameter values within given realistic bounds. It will require improved climate models and a systematic analysis of uncertainties using probability concepts. Allen (2003) points out that model parameter changes that are unlikely should be ruled out when making probabilistic climate predictions. Also, when comparing the results of different models to define a range of possible outcomes, models should be weighed by some measure of their similarity to the real world.

Murphy et al. (2004) made a systematic attempt to determine the range of climate changes consistent with uncertainties in the modelling process. It is essential that with the GCM prediction a quantitative estimate of the uncertainty is given to make the result more useful for policy makers. Uncertainty in their mixed atmosphere-ocean model cannot be accurately determined from observations. The range of predictions should be seen as a lower limit of the uncertainty in the outcome. If uncertainty in structural elements of the model are also considered, such as resolution and level of detail in parameterizations, this limit could increase. Only a large ensemble of GCM predictions, in which parameters are chosen such that the widest range of uncertainties is captured, can provide a reliable specification of the spread of possible regional climate changes. In a first attempt to evaluate climate sensitivity due to anthropogenic climate change (assuming a doubled CO_2 concentration), Murphy et al. (2004) compiled an ensemble containing four million model versions with randomly chosen multiple parameter perturbations. They assumed that the impacts combine linearly and that each parameter has a uniform distribution within a range of values. They weighed the model predictions of climate sensitivity according to the likelihood that the simulation of present-day climate is consistent with observations (the members of the ensemble are not equally reliable). In this way they narrow the range of possible temperature increase. As a next step, they propose to sample multiple parameter perturbations since the assumption that individual parameter perturbations combine linearly is unlikely to be valid at a regional scale.

In relation to model uncertainty, Forest et al. (2002) analysed three key properties of the climate system in a climate model of intermediate complexity. These properties are climate sensitivity, defined as the equilibrium global-mean surface temperature change in response to a doubling of CO_2 concentration, the rate of heat uptake by the ocean and lastly anthropogenic aerosol forcing. Three independent climate observation series were taken. They then systematically changed the parameters under consideration to assess which simulation fits the three observed climate records the best. This study differs from the main stream of climate uncertainty research by the fact that observations are varied instead of just the model parameters.

1.1.2 Climate and ecosystem

The biosphere is the global ecological system that integrates all living organisms (animals, plants) including their interactions with the other components of the Earth's

climate system. The biosphere is composed of ecosystems acting at different smaller scales. An ecosystem consists of a community of living organisms and their local physical environment, functioning as a unit. The living and non-living elements of an ecosystem are connected through flows of energy and chemical processes. Plants, for instance, realize their food intake through photosynthesis (from water, carbon dioxide, and light), but also need nutrients from the soil. Thus, plants interact with both the atmosphere and the geosphere. The size and scale of an ecosystem can vary widely. It may be a whole forest or a small pond. There are no absolute boundaries between ecosystems. However, some entities may have well defined boundaries, such as deserts, mountains or oceans. Ecosystems change continuously over time following certain patterns. They also respond to environmental changes such as climate fluctuations and anthropogenically induced environmental changes. For further reading on ecosystems we refer to Begon et al. (2006) and Hanski (1999).

Fluctuation in ecological systems is a topic of high importance. It deals with the dynamics of (sub)populations of species and how these populations interact with their environment. By estimating the survival probability of a species living in a given part of its habitat, a contribution can be made to the development of conservation management strategies. It has led to methods such as population viability analysis (PVA). PVA is a collection of methods that evaluates the risk of extinction or decline of a biological population and its chance to recover (Burgman et al., 1993, Akçakaya et al., 1999, Akçakaya 2000a, 2000b, Akçakaya and Sjögren-Gulve, 2000, Brook et al., 2000).

Also in ecological modelling uncertainty is an important issue. Inaccurate and insufficient data hamper PVA and, like in climate research, ranges (lower and upper bounds) of parameters are used (Akçakaya 2000b, Akçakaya and Sjögren-Gulve, 2000). Sensitivity analysis can be used to reduce uncertainties. It could be helpful to make the appropriate choice when collecting more data (through fieldwork). Then it is important to know a priori which parameters are most sensitive and should therefore be given priority. When analysing the dynamics of a population, a parameter sensitivity analysis is often included (Conroy et al, 1995, Akçakaya, 2000b, 2000c, Moilanen, 2002, Drechsler et al, 2003). Small changes in the parameters could change the behaviour of a (sub)population considerably. Also, in terms of conservation management, it is of great value to analyse how certain changes in the parameter values may improve the conditions for a specified population, and therefore reduce the risk of extinction.

The climate influences ecological processes in various ways. Recently, more attention has been given to the influence of large-scale climate variability upon ecological processes, rather than only taking the local weather in account (Sæther, 1997, Mysterud et al., 2001, Stenseth et al., 2002). Of particular interest are the impacts of the North Atlantic Oscillation (NAO), e.g. Thompson and Grosbois, (2002), Arnott and Ruxton, (2002), Lusseau et al., (2004) and the El-Nino Southern Oscillation (ENSO), e.g. Pounds et al., (1999), Urban et al., (2000). These climatic patterns affect both terrestrial and marine vegetation and animal life. Stenseth et al. (2002) point out that interaction between biologists and climate researchers will lead to more insight in the response of ecosystems to climate variability and climate change. Uncertainties in

the understanding of the underlying mechanisms in both the climate system and the ecosystem as well as our restricted notion of their interactions limit the knowledge of today. Stenseth et al. (2002) highlight five important aspects when analysing the effects that climate variations can have on ecosystems. Firstly, delayed effects of climate are important in ecosystems. The year in which certain individuals are born may be of influence on for instance their size, which might have an effect on their life-span. Secondly, climate can have a different influence on sexes and age-classes. For instance, the development of a population is altered when a climatic process influences younger age classes more than older ones. Thirdly, due to climate change extreme events could occur more frequently, which are often more relevant to ecosystems than fluctuations in the mean climate. A severe winter with a longer frost period for instance can lead to damage and death in plants and animals. Fourth, large climate fluctuations might affect a particular organism, not only directly but also indirectly in a way that is not easily understood because of the complex structure of the cause-effect chain. We already mentioned the impact of the climatic patterns NAO and ENSO upon species, both terrestrial and marine. Fifth, it is important to recognize that climate effects may interact with ecological factors. For instance, a warm winter might favour a certain population and cause growth. A next warm winter might not have the same effect, because of density dependence.

1.1.3 Parameter sensitivity and climate modelling

Inaccurate or insufficient data can lead to uncertainty in the parameters which will influence the model output. Also, lack of knowledge of certain processes within a model could cause an inaccurate description of the model and its parameters. When it is known that certain parameters can not be estimated accurately, a parameter range should be given, rather than just one value. It is important to analyse to which small parameter perturbations the model is most sensitive. Thus, within uncertainty analysis of climate models, parameter sensitivity is an important topic. It might be that a parameter perturbation within the range given, has not much effect on the long term characteristics of the dynamical system. It is clear that we are interested in small changes in parameters or combination of parameters to which the model is highly sensitive. When these parameter perturbations, which we call effective parameter perturbations, are identified, and we know their range, one can quantify the range of possible model outcomes. Especially extreme climate predictions are of interest, which can be found more easy if the most effective parameter perturbations are already known. In order to quantify change in the dynamical characteristics with respect to a given reference climate, a simulation of the model with the modified parameter values over an infinite large time interval is required. The simulation should be long enough to make a good approximation of the climate and its variability. A possible shift in the parameters may have a natural cause or may be anthropogenically induced. The changes in the model output we focus on are the duration of certain preferred circulation patterns and the transition from one to another.

As we mentioned, in the atmospheric circulation, preferred large-scale flow pat-

terns, also referred to as weather regimes, occur (Reinhold and Pierrehumbert, 1982). The atmosphere can be thought of as a dynamical system and weather regimes as quasi-stable equilibria of the dynamical system. The atmosphere is a flow that moves from one equilibrium to another (Charney and DeVore, 1979). The climate can be identified by the strength by which the different regimes occur. Climate change can be looked at in terms of change in the regime behaviour. The space dependent state variables of the system such as temperature and pressure can be expressed in series of orthogonal spectral functions. In this way new state variables are introduced: the time dependent coefficients of these functions. Yet another transformation is commonly made. It uses Empirical Orthonogonal Functions (EOFs) to identify the preferred regimes, (Haines and Hannachi, 1995). The leading EOFs give the directions of the largest variability of the atmospheric circulation.

Important patterns in the atmosphere are for instance the NAO (north atlantic oscillation) and the PNA (pacific north-american oscillation). These patterns can be represented by EOFs. The NAO is important for the regional climate in Western Europe. A stronger NAO results in fewer easterlies and more westerlies which cause milder winters in Western Europe. By using the EOFs the dimension of the phase space can be reduced considerably and the data fields become more manageable. During a model integration over a large time interval the atmospheric flow can be projected onto the EOFs at each time step. This gives a time series of the anomalies into the direction of the EOFs. From these time series probability density functions (PDFs) can be made. Palmer (1999) pointed out that climate change causes change in the probability density of the regimes, rather than a change in the structure of the regimes. It is of importance to know which parameter perturbations cause the largest change in regime behaviour, and secondly how much change is possible given a predefined uncertainty in the parameter values.

1.1.4 Climate driven metapopulation models

A metapopulation is a set of local populations of a species, divided over different habitat patches. Migration between the patches may be possible. Metapopulation models describe the dynamics of the metapopulation of one or more (interacting) species. A wide spectrum of models is available, ranging from occupancy models on one hand, to individual based models on the other hand. In occupancy models (see e.g. Levins, 1970), the patches can be in two states only, they are either occupied or empty. The local dynamics of the population is not described. In individual based models (see e.g. DeAngelis and Gross, 1992) the behaviour of each member of the population individually as well as their interaction is described using mathematical expressions. These models are highly sensitive to parameter perturbations and prone to error growth. Moreover, extensive and large computations are needed in order to carry out an analysis (Levin, 1992, Pascual and Levin, 1999). In between occupancy and individual based models, full scale structured metapopulation models are situated. They describe the population dynamics as well as spatial dynamics, by modelling migration and correlation among populations. The metapopulation model formulated in this thesis is a

herbivore-predator model containing two patches. It has local population sizes as state variables. Furthermore, it allows an atmospheric input.

Populations do not grow smoothly until they have reached their carrying capacity, but tend to fluctuate. This is not only due to intrinsic processes and interactions, but also due to environmental influences. One important aspect is the effect of the climate upon the dynamics of the population. As mentioned earlier, the influence of large-scale climate variability upon ecosystems, and in particular upon the dynamics of a population, has gained growing attention (e.g. Sæther, 1997, Mysterud et al., 2001, Stenseth et al., 2002). Long term changes in the environment, such as climate change can affect ecological processes. To verify how much impact climate change can have, it is significant to have a better understanding of the influence of climate upon ecosystems and their interaction. Specific climate patterns, such as the NAO and ENSO, can be linked to the dynamic behaviour of specific populations. We name wild red deer on the west coast of Norway (Mysterud et al., 2001), bottlenose dolphins in the Moray Firth UK and killer whales in Johnstone Strait, Canada (Lusseau et al., 2004), or toads and frogs in highland forests at Monteverde, Costa Rica (Pounds et al., 1999).

As mentioned earlier, parameter sensitivity analysis is a useful instrument to have at hand when interpreting model results for practical purposes (Conroy et al, 1995, Akçakaya, 2000b, Moilanen, 2002, Drechsler et al, 2003). Small changes in parameters could change the behaviour of a metapopulation considerably. When only a range of parameters can be given, rather than one value, it is important to find out to which parameter changes the system is the most sensitive. It is of great value to analyse how changes in the parameter values may improve or deteriorate the conditions for a specified population. Results of such studies may be of use in conservation management. When a subpopulation reaches a low value, it becomes at risk of extinction. As a measure of this extinction risk, we take the fifth percentile of the population, for a model run over a large time interval. This fifth percentile is the value below which the population size is found 5 out of 100 times in a series taken at fixed time intervals. The way parameter changes act upon the fifth percentile may be an indication for the effect of certain conservation measures.

1.2 Research objectives

Climate research is carried out with large-scale computer models that calculate the fluctuations in the circulation of the atmosphere and ocean over a large timespan. These models contain numerous parameters. From a large number of these parameters the values are uncertain and only a possible range of values is known. Given this uncertainty, it is desirable to obtain the full spectrum of possible model outcomes. This requires a large amount of system evaluations.

In weather prediction a similar problem occurs. Uncertainty in the initial conditions of the state variables influences the quality of the forecast. One wants to quantify the (un)certainty of the forecast by replacing the individual forecast (reference solution) by a range of possible outcomes. However, it is not feasible to change the initial state

in all directions. This has led to the ensemble forecast where initial perturbations are selected that change the forecast with a high probability. Such perturbations can lie in the direction of the fastest growing components of the tangent linear system (this system holds in the neighbourhood of the reference solution). At the European Centre for Medium range Weather Forecasts (ECMWF) an ensemble prediction system (EPS) is used where initial conditions are perturbed in this direction, see e.g. Buizza and Palmer, (1995), Molteni et al., (1996), Buizza, (1997), Gelaro et al., (1998). Other ways are also possible to obtain a perturbation of the initial conditions that have a strong effect. At NCEP (National Centres for Environmental Prediction) a so called breeding method is used for ensemble forecasting. Bred perturbations have grown most rapidly during some period prior to the analysis, see e.g. Toth and Kalnay, (1993), Tracton and Kalnay, (1993), Toth and Kalnay, (1997). The full non-linear system is used to generate the breeding perturbations. Houtekamer and Derome (1995) compared the two methods along with a method where random observational errors are added to observe the impact on a data assimilation system.

In our study we deal with climate models for which a large computing time is needed in order to obtain quantitative information about the dynamical characteristics of a climate. A full scale climate model should include the dynamical interaction between atmosphere, oceans and continents. We restrict ourselves to the atmospheric flow and use a general circulation model (GCM) to compute statistical properties of the model at its chaotic attractor. Clearly, because of this chaotic behaviour, the model equations should be integrated over an infinite time interval to obtain exact results. For making a good approximation the time interval must be sufficiently large. This requirement makes it difficult to carry out a complete sensitivity analysis. In the process of working with models it is necessary to know which parameters have the strongest effect upon the outcome. We are interested in finding the most effective parameter perturbations in climate models as well as in ecological models with a climatologic input. A direct method (Dickinson and Gelinas, 1976), where parameters are perturbed at random, is computationally too expensive if the required number of evaluations is made. For each parameter perturbation a long run is needed to evaluate how much it affects the model output. There is no a priori indication about the right choice of an effective perturbation. Other existing methods such as simulated annealing (Kirkpatrick et al, 1983) fail to yield an answer within a reasonable computing time as well. Therefore, a new method is needed that finds effective parameter perturbations in an efficient way.

In this study, we investigate whether such parameter perturbations can be chosen on the basis of the short term behaviour of a model. We make use of the tangent linear and adjoint equations of the models (see Errico, 1997, for a clear introduction on this topic). Adjoint models have been commonly used for analysing the effect of perturbations in initial conditions in climate models (see Courtier et al., 1993, for an overview), and more recently for parameter perturbations (see e.g. Barkmeijer et al., 2003). The tangent linear equations are computed by linearizing the original (non-linear) model around a reference (unperturbed) orbit. These are used to compute the evolution of small perturbations along the reference orbit. For our purpose the state space of the tangent linear system needs to be extended with the parameter space. We

then may compute the error growth in the original state space caused by a perturbation in the parameter space over a short time interval over which the linearization applies. It is noted that in the extended system the original state variables start in the origin, while the parameters start from a sphere formed by all possible parameter perturbations of a given size. The parameters then remain constant in time. With the adjoint method we find the parameter perturbation that produces the largest change in state space in the end point. This change is quantified by the so-called singular value and is related to the exponent of the fastest growing component of the tangent linear system. The chaotic attractor is scanned for the points where this singular value has a large value. It is anticipated that the parameter perturbation corresponding to a singular value after it has peaked may also have a large effect over a time interval that is sufficiently large to compute the climate characteristics. Not every parameter perturbation obtained in this way may have a strong effect upon the climate, but it is expected that the success rate within this subset is much larger than selecting parameter perturbations completely at random. This difference in success rate is the main topic of this thesis. As we already remarked, a more systematic maximization procedure could not be found in the numerical literature, because of the large number of parameters and the extremely large time integration intervals for each parameter choice.

Corti and Palmer (1997) presented evidence that sensitivities based on short term integrations are relevant for changes in long term statistics. For a quasi-geostrophic atmospheric model, they calculated perturbations to initial conditions that maximize the projection of the perturbations after five days onto a particular flow pattern, for instance the NAO or PNA. Next they took the average of 2000 perturbations calculated this way. These average perturbations are added to the system as a time-invariant forcing. The result is that the PDF of the PNA pattern changes much from this forcing perturbation. Adjoint models are widely used for analysing sensitivities in initial conditions. In addition to references given above we mention Molteni and Palmer (1993), Oortwijn and Barkmeijer (1995) and Barkmeijer (1996). They can also be used to efficiently calculate the sensitivity of various model parameters (Hall and Cacuci, 1983). In the 2001 IPCC rapport it is stated that a systematic evaluation of the effect of parameter uncertainties on the climate simulation is urgently needed. Barkmeijer et al. (2001) made a first step using forcing singular vectors in a sensitivity study. They compared forcing singular vectors with initial condition singular vectors in 2-day forecasts.

To analyse parameter sensitivity in the context of an ecosystem model, Moilanen (2002) added random errors to parameter values and analysed the change it brought about in the output. For the purpose of conservation management Etienne (2004) studied possible protection measures for threatened species by analysing parameter dependence in metapopulation models: the roles of patch size and patch connectivity were investigated using a model based on a transition matrix. In population biology the adjoint method is rarely applied to differential equation models. In Lawson et al. (1995) we meet a study on a predator-prey model. Huiskes (2002) worked out a closely related technique based on automatic differentiation algorithms and applied it to problems of stock assessment in fishery. In biological models one has to deal with a set of ecological parameters and to make an evaluation of the effect of a parameter perturbation a

large computation may be needed. This will typically be the case if weather fluctuations have an effect on the biological populations. Then a large time interval has to be considered in order to account for the various weather conditions that may occur. So again we are in the situation that a systematic sensitivity analysis is not feasible because of the large computing time and the large number of parameters. The latter will certainly be the case for spatially distributed population models.

The sensitivity analysis we carry out for the ecological parameters is similar to the one we develop for the forcing parameters in the GCM model. Ecological models, and more specifically metapopulation models, often deal with species conservation management. Then one is interested in finding the parameter change that supports the population that has a large extinction risk. Our method selects directions of parameter change that have a large effect. Since we work with small parameter perturbations the outcome has the nice linear property that a large negative effect is accompanied by a large positive effect in the opposite direction. A large effect in state space does not mean automatically a large effect for the population with an extinction risk, but we expect to do better by restricting us to parameter perturbations that are effective in a short run, than just taking a random parameter change. In a way our sensitivity analysis is bent in the direction of becoming a conservation management tool.

1.3 Scope of the method

A systematic uncertainty analysis of climate models has not been developed up to the present because of the previously pointed out reason of the required large scale computing capacity. With this research, aimed at finding effective parameter perturbations, we explore the possible relationship that could exist between effective parameter perturbations of the climate and effective perturbations of the atmospheric circulation over a short time period (a few days) during which solutions near the reference orbit have a strongly divergent character. Before applying this to a realistic model, it is tested in a low dimensional model: the Lorenz 63 equations. The results (chapter 2) justify a further application to a large scale model with a more complicated chaotic attractor (chapter 3). This model is of a size that the random search method is the only existing alternative to be taken in consideration. However, the success rate of finding a parameter perturbation that yields a large climate change is very low. At this point the proposed method scores significantly better. Next a new class of problems is investigated that deals with climate driven natural processes. This time not the climate parameters will be perturbed but the process parameters. We aim at biological processes in particular interacting biological populations living in a fragmented habitat (chapters 4 and 5). Again, we start with a simple ecological model with only few parameters. Also for the climate a simple model is chosen, the Lorenz 84 equations. Once more, our method turns out to give better results than the random search method. The fact that the results hold for three different types of strange attractors, may indicate that the method holds for a class of systems with a certain type of chaotic attractor.

In search for an efficient method to find effective parameter perturbations, the

Lorenz 63 model is used as a test case. This model contains only two regimes. Both regimes can be related to an unstable equilibrium. We first followed Corti and Palmer (1997): using Lagrange multipliers, we calculated the parameter perturbation vector that gave the largest systematic perturbation into the direction of the vector that connects the two equilibria of the model. Giving the model as large a perturbation as possible into the direction of one regime might result in more frequent visiting in that particular regime. However, it turned out that these parameter perturbations were not so effective in causing change in the regime behaviour in a long simulation. A second attempt is made by first doing a random search. The Lorenz 63 model does not require much computation time, so a sufficiently large number of random perturbations can be made for the method to cover the full range of parameter perturbations. The most effective parameter perturbations are then selected. Use is made of a visualizing tool to see what effect these perturbations have. We follow the orbit of a set of systems that differ only in parameter values. The start is at a sphere of parameter perturbations and with the initial state being a point at the reference orbit. After a short integration of the system linearized at the reference orbit, the set of solutions is transformed from a point into an ellipsoid at end time in state space, with the end point of the reference orbit as centre. This ellipsoid shows the deviations from the reference orbit that are possible. So the deviations caused by the effective parameter perturbations lie somewhere within this ellipsoid. After observing different areas of the attractor, it turns out that the effective parameter perturbations coincide with the first singular vector at some points. This occurs at time intervals right after a short orbit had been through a highly sensitive stage (with a large singular value). Our hypothesis is that singular vectors that correspond to a low singular value directly after such a passage are likely to be effective parameters. This hypothesis has been tested in the Lorenz 63 model.

This method of finding effective parameter perturbations is thus based on empirical findings. We have no theory supporting the hypothesis, we only compare this newly developed adjoint method with a random method in various models. The method proved to be successful for the Lorenz 63 model. Since we can select parameter perturbations that are more likely to be effective by using only one reference run of the climate model, the method can be used in a large scale model with many parameters. It puts us in a position of finding effective parameter perturbations in more realistic climate models. We use the T21QG atmospheric model for this purpose. Our method has a higher success rate in finding effective parameter perturbations than the fully random method has. However it is evident that finding the most effective perturbation remains difficult within such a large scale model.

To extend the scope of our method we apply it to a different class of dynamical systems from the natural sciences: we select a herbivore-predator population model driven by a simple atmospheric system, the Lorenz 84 model. In this model only five biological parameters are perturbed, the same number of parameters as in the Lorenz 63 model. Once more, the adjoint method proves to be efficient in finding effective parameters that change the behaviour of the populations. From these one can make a further selection and choose the ones that support the herbivore population. A next step would be to test the method in a more complicated metapopulation model, with

far more parameters, which may be the subject of a subsequent study.

1.4 Outline of the thesis

In this thesis, we carry out a parameter sensitivity study in two atmospheric models: the Lorenz 63 model (Lorenz, 1963) and the quasi-geostrophic three-level T21QG model (Marshall and Molteni, 1993). Moreover, we consider a metapopulation model, the Rosenzweig-MacArthur system (Rosenzweig and MacArthur, 1963), which is driven by the Lorenz 84 atmospheric equations (Lorenz, 1984).

In chapter 2, the Lorenz 63 model is used as a case study. This model consists of three state variables and contains only two regimes. This makes it easy to analyse. With the original parameters, these two regimes are equally populated as it is verified in a long simulation. The first EOF is the vector connecting the two equilibria in the regimes and the PDF of the projection onto this EOF is a bimodal function. Parameter perturbations can cause asymmetry in the model. One regime can be visited more at the expense of the other and the dynamical behaviour becomes asymmetric: a climate change occurs. We study the effect of a 5% perturbation in each of the parameters.

A method is developed that selects parameter perturbations that are most likely to cause a large climate change. This selection is based on the short term dynamics. The PDF that expresses the degree of asymmetry as a result of random perturbations, is unimodal with a maximum at zero, i.e. no asymmetry. The most effective parameter perturbations, i.e. perturbations that cause the largest climate change are in the tail of the PDF. They are first found using a random method. We then make short term integrations with these. The integrations are so short that the linear approximation of the model is still sufficiently accurate. It turns out that at some points on the attractor, these parameter perturbations collide with the first singular vectors. This occurs in time intervals right *after* the short orbit has passed through a sensitive stage, that is after the singular value had grown to a very large value. Now we make 50000 long simulations, where this time the parameters are perturbed with the (scaled) singular vectors, selected on the basis of their singular value. We compare the two methods and it turns out that our method, which we call the adjoint method, is more efficient in selecting effective parameter perturbations. It hardly draws any perturbations that give no climate change.

After these findings in a simple atmospheric model, we test the adjoint method in a more realistic model, the quasi-geostrophic three-level T21QG model, described in chapter 3. The T21QG model integrates prognostic equations for potential vorticity. It consists of 1449 state variables and contains several regimes, which can be identified by computing the EOFs. The first EOF is closely related to the North Atlantic Oscillation (NAO), which is a pattern that is important for the climate in western Europe. Changes in the regime behaviour could indicate changes in the climate. In this study, only the forcing parameters will be perturbed. The forcing is determined by taking the average of a large number of vorticity tendencies using observed atmospheric fields. These average tendencies should be equal to zero, the forcing term is chosen such that it compensates the deviation from zero. Again, we assume that the uncertainty in the

forcing parameters is 5%.

We compare the random method with the adjoint method as developed in the context of the Lorenz 63 model. The vector containing the forcing parameters has a dimension of 1449 (equal to the dimension of the system). This is considerably higher than in the simple Lorenz 63 model. Since this model takes up more computational time, it is only feasible to make 1000 different model simulations for each parameter choice. To carry out these simulations we use the high performance computing facility at the European Centre for Medium range Weather Forecasts (ECMWF), where it is possible to make parallel runs. One run takes approximately 7 hours in real time and we are able to make 32 runs simultaneously. The change in climate is measured, using the first few Empirical Orthogonal Functions. For each integration step, the streamfunction can be plotted onto the EOFs, giving an anomaly in each EOF direction. A time series of the anomalies can be computed for each EOF. Then, PDFs can be made of these time series. A change in the PDF, such as a shift or a change in shape, indicates climate change. It turns out that the parameter perturbations causing the largest climate change in terms of the sum of the changes in the PDFs 1 to 6, also causes the largest change in just the PDF of EOF1. So changes in the PDF of the anomalies into the direction of the first EOF only can be used as an indicator of climate change. When comparing the random method with the adjoint method, it turns out that almost all parameter perturbations drawn with the random method yield hardly any climate change at all. The singular vectors found with the adjoint method are more effective in changing the regime behaviour, 35.7% of the perturbations found are more effective than any of the random perturbations. This means that the random method does not select parameter perturbations close to a highly effective perturbation. Clearly, the number of 1000 random runs is much too low. For this model the most effective perturbation might still not be within reach using the adjoint method. However, we show that, although hampered by the large size of the parameter set, the adjoint method reveals the possibility of a much larger climate change than the random method.

In chapters 4 and 5 we study a metapopulation model, which is coupled to the simple atmospheric Lorenz 84 model. It consists of two patches occupied by two populations having a prey-predator relation. The intrinsic growth rates and the carrying capacities are made separately dependent on climate fluctuations. The parameters that will be perturbed are the intrinsic growth rates of the herbivores, the death rates of the predators and the migration rates of the herbivores. Herbivore-predator interaction may show cyclic behaviour and phases of very low herbivore population size may occur, bringing the population in a critical state. Due to climate fluctuations or to the intrinsic cyclic dynamics of the herbivore-predator system the two herbivore subpopulations may for some time, separately or jointly, get at a low level. A parameter sensitivity study increases the value of the modelling effort as it reveals which elements of a model have a large effect upon the outcome. Also, in terms of conservation management, it is important to find out which (small) perturbations in parameters have the most influence on population sizes. When the means are at hand to improve conditions for certain populations, model analysis can help to find a useful solution. Changes in the survival chance of the populations for different parameter values are monitored using

fifth percentiles. The fifth percentile is the value below which 5 out of 100 values of the population size taken are found in a long time series with fixed time intervals. The higher this fifth percentile, the lower the extinction risk is. A rise in the fifth percentile indicates that the conditions for the corresponding species have improved.

In chapter 4 predator-prey models with different side conditions are investigated. We start with a model in which predators are not present and the herbivores can migrate between the patches. The carrying capacities depend on the climate fluctuations. We take two different, uncorrelated, time series of the climate for the patches and analyse the influence of the migration rate. It turns out that increasing the coupling between the patches, does not improve the local conditions for the species. The degree of coupling between the two patches does however influence the speed of recolonization in case of full local extinction. Next, predators are added to the model. The same time series of the climate is used for the two patches, and now the climate acts upon the intrinsic growth rates. The intrinsic growth rate of the herbivore in the second patch is three times as large as the one for the herbivore in the first patch. Furthermore, the carrying capacity of the herbivore is twice as large in patch 1. It turns out that this makes the second herbivore more vulnerable for extinction. The goal is to improve the conditions for the herbivore in patch 2 by increasing the migration rate of the herbivores and/or increasing the death rates of the predator at the two patches. Changing different parameters takes a certain amount of effort. Given the cost per unit of changing a parameter and given a fixed effort, an optimal solution can be found. For the parameter perturbation that improves the conditions for the herbivore the most, the predator in patch 1 appears to die out. Lastly the model is modified by allowing the predators to migrate as well. Increasing the death rate of the predator in patch 1 shows little effect, increasing it in patch 2 has a slightly positive effect. Increasing the migration rate of the herbivores has a positive effect on the herbivores in patch 2, but a negative effect on the herbivores in patch 1. Small values of the migration rate of the predators has a negative effect on the herbivores of both patches, but after it has exceeded a certain value, the effect stabilizes for the herbivore in patch 1 and has a positive effect on the herbivores in patch 2. Depending on which herbivore needs to be supported, a choice should be made. These findings show that conservation measures may bear the risk of unwanted side effects.

In chapter 5 again only herbivores can migrate between the two patches and the intrinsic growth rates are influenced by climate fluctuations. We now consider a set of five parameters that can be perturbed; the intrinsic growth rates of the herbivores, the death rates of the predators and the migration rate. We assume an uncertainty of 5% in the parameters. The adjoint method, as used in atmospheric models in chapters 2 and 3, is now tested on this metapopulation model. We want to find the parameter perturbations that influence the long term behaviour of the model the most. Our aim is the conservation of the herbivores, so we want to find the perturbations that favour their populations most in the assumption that this will result in a lower extinction risk. It turns out that the selected singular vectors improve the conditions for both herbivores. When comparing the adjoint method with the random method, it shows that the adjoint method draws parameter perturbations that are very effective. The selected singular

vectors lie within the range of most effective parameter perturbations. It is remarked that this climate driven metapopulation model is still of such a small scale that the best parameter perturbation can still be approximated using a numerical scheme such as the conjugate gradient method (see e.g. Press et al., 1986).

References

- Akçakaya H.R., Burgman, M.A., Ginzburg, L.R., 1999. Applied population ecology: principles and computer exercises using RAMAS EcoLab2.0, *2nd Edition*. Sinauer, Sunderland, MA.
- Akçakaya, H.R., 2000a. Viability analyses with habitat-based metapopulation models. *Population Ecology*, **42**, 45-53.
- Akçakaya, H.R., 2000b. Population viability analyses with demographically and spatially structured models. *Ecological Bulletins*, **48**, 23-38.
- Akçakaya, H.R. and Sjögren-Gulve, P., 2000. Population viability analyses in conservation planning: an overview. *Ecological Bulletins*, **48**, 9-21.
- Allen, M.R., 2003. Possible or probable? *Nature*, **425**, p242.
- Arnott, S.A. and Ruxton, G.D., 2002. Sandeel recruitment in the North Sea: demographic, climatic and trophic effects. *Marine Ecology Progress Series*, **238**, 199-210.
- Barkmeijer, J., 1996. Constructing fast-growing perturbations for the nonlinear regime. *Journal of the Atmospheric Sciences*, **53**, 2838-2851.
- Barkmeijer, J., Iversen, T. and Palmer, T.N., 2003. Forcing singular vectors and other sensitive model perturbations. *Quarterly Journal of the Royal Meteorological Society*, **129**, 2401-2424.
- Begon, M., Townsend, C.R., Harper, J.L., 2006. Ecology: from individuals to ecosystems. *Malden: Blackwell, 4th Edition*.
- Buizza, R. and Palmer, T.N., 1995. The singular vector structure of the atmospheric general circulation. *Journal of the Atmospheric Sciences*, **52**, 1434-1456.
- Buizza, R., 1997. Potential forecast skill of ensemble prediction and spread and skill distributions of the ECMWF ensemble prediction system. *Monthly Weather Review*, **125**, 99-119.
- Brook, B.W., O'Grady, J.J., Chapman, A.P., Burgman, M.A., Akçakaya, H.R., Frankham, R., 2000. Predictive accuracy of population viability analysis in conservation biology. *Nature*, **404**, 385-387.

- Burgman, M.A., Ferson, S., Akçakaya, H.R., 1993. Risk assessment in conservation biology. *Chapman and Hall, London*.
- Charney, J.G. and DeVore, J.G., 1979. Multiple flow equilibria in the atmosphere and blocking. *Journal of the Atmospheric Sciences*, **36**, 1205-1216.
- Conroy, M.J., Cohen, Y., James, F.C., Matsinos, Y.G., Maurer, B.A., 1995. Parameter estimation, reliability and model improvement for spatially explicit models of animal populations. *Ecological Applications*, **5**, 17-19.
- Corti, S. and Palmer, T.N., 1997. Sensitivity analysis of atmospheric low-frequency variability. *Quarterly Journal of the Royal Meteorological Society*, **123**, 2425-2447.
- DeAngelis, D.E., Gross, L.J., 1992. Individual-based models and approaches in ecology: populations, communities and ecosystems. *Chapman and Hall, New York*.
- Dickinson, R.P. and Gelinas, R.J., 1976. Sensitivity analysis of ordinary differential equation systems - a direct method. *Journal of Computational Physics*, **21**, 123-143.
- Drechsler, M., Frank, K., Hanski, I., O'Hara, R.B., Wissel, C., 2003. Ranking metapopulation extinction risk: from patterns in data to conservation management decisions. *Ecological Applications*, **13**, 990-998.
- Errico, R.M., 1997. What is an adjoint model? *Bulletin of the American Meteorological Society*, **78**, 2576-2591.
- Etienne, R.S., 2004. On optimal choices in increase of patch area and reduction of interpatch distance for metapopulation persistence. *Ecological Modelling*, **179**, 77-90.
- Forest, C.E., Stone, P.H., Sokolov, A.P., Allen, M.R. and Webster, M.D., 2002. Quantifying uncertainties in climate system properties with the use of recent climate observations. *Science*, **295**, 113-117.
- Gelaro, R., Buizza, R., Palmer, T.N., Klinker, E., 1998. Sensitivity analysis of forecast errors and the construction of optimal perturbations using singular vectors. *Journal of the atmospheric sciences*, **55**, 1012-1033.
- Haines, K. and Hannachi, A., 1995. Weather regimes in the Pacific from a GCM. *Journal of the Atmospheric Sciences*, **52**, 2444-2462.

- Hall, M.C.T., and Cacuci, D.G., 1983. Physical interpretation of the adjoint functions for sensitivity analysis of atmospheric models. *Journal of the Atmospheric Sciences*, **40**, 2537-2545.
- Hanski, I., 1999. *Metapopulation Ecology*, Oxford University Press.
- Houtekamer, P.L. and Derome, J., 1995. Methods for ensemble prediction. *Monthly Weather Review*, **123**, 2181-2196.
- Huiskes, M.J., 2002. Automatic Differentiation Algorithms in Model Analysis, *PhD Thesis*, Wageningen University.
- IPCC, 2001. Climate Change 2001: The Scientific Basis. Eds: Houghton, J.T., Y. Ding, D.J. Griggs, M. Noguer, P.J. van der Linden, X. Dai, K. Maskell, and C.A. Johnson. Contribution of Working Group I to the Third Assessment Report of the Intergovernmental Panel on Climate Change. *Cambridge University Press*.
- Kirkpatrick, C.D., Gerlatt Jr., Vecchi, M.P., 1983. Optimization by simulated annealing, *Science* **220**, 671-680.
- Lawson, L., Spitz, Y., Hoffman, E. and Long, R., 1995. A data-assimilation technique applied to a predator prey model, *Bulletin of Mathematical Biology*, **57**, 593-617.
- Levin, S.A., 1992. The problem of pattern and scale in ecology. *Ecology*, **73**, 1943-1967.
- Levins, R., 1970. Extinction. in: Some Mathematical Problems in Biology. Gertenhaber, M. (Ed.), *American Mathematical Society*, 75-107.
- Lorenz, E.N., 1963. Deterministic nonperiodic flow. *Journal of the Atmospheric Sciences*, **20**, 130-141.
- Lorenz, E.N., 1984. Irregularity: A fundamental property of the atmosphere. *Tellus*, **36A**, 98-110.
- Lusseau, D., Williams, R., Wilson, B., Grellier, K., Barton, T.R., Hammond, P.S. and Thompson, P.M., 2004. Parallel influence of climate on the behaviour of Pacific killer whales and Atlantic bottlenose dolphins. *Ecology Letters*, **7**, 1068-1076.
- Marshall, J. and Molteni, F., 1993. Towards a dynamical understanding of planetary-scale flow regimes. *Journal of the Atmospheric Sciences*, **50**, 1792-1818.
- Moilanen, A., 2002. Implications of empirical data quality to metapopulation model parameter estimation and application. *Oikos*, **96**, 516-530.

- Molteni, F. and Palmer, T.N., 1993. Predictability and finite-time instability of the northern winter circulation. *Quarterly Journal of the Royal Meteorological Society*, **19**, 269-298.
- Molteni, F., Buizza, R., Palmer, T.N. and Petroliagis, T., 1996. The ECMWF ensemble prediction system: Methodology and validation. *Quarterly Journal of the Royal Meteorological Society*, **122**, 73-119.
- Murphy J.M., Sexton, D.M.H., Barnett, D.N., Jones, G.S., Webb, M.J., Collins, M. and Stainforth, D.A., 2004. Quantification of modelling uncertainties in a large ensemble of climate change simulations. *Nature*, **430**, 768-772.
- Mysterud, A., Stenseth, N.C., Yoccoz, N.G., Langvatn, R. and Steinheim, G., 2001. Nonlinear effects of large-scale climatic variability on wild and domestic herbivores. *Nature*, **410**, 1096-1099.
- Oortwijn, J., and Barkmeijer, J., 1995. Perturbations that optimally trigger weather regimes. *Journal of the Atmospheric Sciences*, **52**, 3932-3944.
- Palmer, T.N., 1999. A nonlinear dynamical perspective on climate prediction. *Journal of Climate*, **12**, 575-591.
- Pascual, M., Levin, S.A., 1999. From individuals to population densities: searching for the intermediate scale of nontrivial determinism. *Ecology*, **80**, 2225-2236.
- Pounds J.A., Fogden, M.P.L., Campbell, J.H., 1999. Biological response to climate change on a tropical mountain. *Nature*, **398**, 611-615.
- Press, W.H., Flannery, B.P., Teukolsky, S.A., and Vetterling, W.T., 1986. Numerical Recipes. *Cambridge University Press*.
- Reilly, J. Stone, P.H., Forest, C.E., Webster, M.D., Jacoby, H.D., Prinn, R.G., 2001. Uncertainty and climate change assessment. *Science*, **293**, 430-433.
- Reinhold, B.B. and Pierrehumbert, R.T., 1982. Dynamics of weather regimes: quasi-stationary waves and blocking. *Monthly Weather Review*, **110**, 1105-1145.
- Rosenzweig, M.L. and MacArthur, R.H., 1963. Graphical representation and stability conditions of predator-prey interactions. *American Naturalist*, **97**, 209-223.
- Sæther, B.-E., 1997. Environmental stochasticity and population dynamics of large herbivores: a search for mechanisms. *Trends in Ecology and Evolution*, **12**, 143-149.

Stenseth, N.C., Mysterud, A., Ottersen, G., Hurrell, J.W., Chan, K.-S. and Lima, M., 2002. Ecological effects of climate fluctuations. *Science*, **297**, 1292-1296.

Stocker, T.F., 2004. Models change their tunes. *Nature*, **430**, 737-738.

Thompson, P.M. and V. Grosbois, 2002. Effects of climate variation on seabird population dynamics. *Directions in Science*, **1**, 50-52.

Toth, Z. and Kalnay, E., 1993. Ensemble forecasting at NMC: The generation of perturbations. *Bulletin of the American Meteorological Society*, **74**, 2317-2330.

Toth, Z. and Kalnay, E., 1997. Ensemble forecasting at NCEP and the breeding method. *Monthly Weather Review*, **125**, 3298-3319.

Tracton, M.S. and Kalnay, E., 1993. Operational ensemble prediction at the National Meteorological Center: Practical aspects. *Weather Forecasting*, **8**, 379-398.

Trenberth, K. E., 1992. Climate System Modeling. *Cambridge University Press*.

Urban, F.E., Cole, J.E., Overpeck, J.T., 2000. Influence of mean climate change on climate variability from a 155-year tropical Pacific coral record. *Nature*, **407**, 989-993.

CHAPTER 2

Finding the effective parameter perturbations in atmospheric models; the Lorenz 63 model as case study

Climate models contain numerous parameters whose numeric values are uncertain. In the context of climate simulation and prediction, a relevant question is what range of climate outcomes is possible given the range of parameter uncertainties. Which parameter perturbation changes the climate in some predefined sense the most? In the context of the Lorenz 63 model, a method is developed that identifies effective parameter perturbations based on short integrations. Use is made of the adjoint equations to assess the sensitivity of a short integration to a parameter perturbation. A key feature is the selection of initial conditions.

2.1 Introduction

Complex numerical models are used to make expectations for the earth's future climate. The reliability of these expectations is unknown. One contributing factor is the existence of uncertain model parameters which leads to uncertainties in the outcome of the simulations. Ideally one would like to quantify these uncertainties. In the last IPCC, 2001, it is stated that a systematic evaluation of the effect of parameter uncertainties on the simulation of the present climate and the transient climate response is urgently needed. A direct approach, perturbing parameters and making additional climate simulations, is infeasible due to computational constraints. Many expensive simulations are required since the simulated climate is bound to be more sensitive to some parameter changes than to others. It would therefore be of great practical use to be able to identify effective parameter perturbations a priori on the basis of short integrations. However, it is not at all clear that this is possible. Some previous studies shed light on this issue.

Corti and Palmer (1997) presented evidence that sensitivities based on short term integrations are relevant for changes in long term statistics. They calculated for a quasi-

geostrophic atmospheric model perturbations to initial conditions that maximize the projection of the perturbations after five days onto a particular pattern, the NAO or PNA in their case. Next they averaged these optimal perturbations of 2000 initial conditions. This averaged perturbation was put on the right hand side of the equation as an additional time-invariant forcing. The probability density function (PDF) of the amplitude of the PNA pattern was determined for the reference and the perturbed forcing from a long integration. The result was that the PDF of the PNA pattern changed a lot due to the forcing perturbation and more so than with a forcing perturbation in the direction of the PNA pattern itself. This result suggests that in order to find parameter or forcing perturbations to which the climate is sensitive, use can be made of the sensitivity of short term evolutions to such perturbations. In our terminology, forcing terms refer to parameters in the tendency equations that are not multiplied by state variables.

Lea et al., (2000) also worked on the idea that short term evolutions can be used for a sensitivity analysis of the climate. In the Lorenz 63 model (Lorenz, 1963) a brute force method was used to assess the effect of changes in parameter r on the climate mean. The climate sensitivity was then measured in terms of $\frac{\Delta \bar{z}_\infty}{\Delta r}$, where \bar{z}_∞ is the average value of variable z over a time-interval of length τ , as $\tau \rightarrow \infty$. They found that an intermediate time scale τ^* exists for which adjoint calculations to determine $\frac{\Delta \bar{z}_{\tau^*}}{\Delta r}$, ensemble averaged over a set of initial conditions, gives a reasonable estimate of $\frac{\Delta \bar{z}_\infty}{\Delta r}$. This result is another indication that it makes sense to try to identify effective parameter perturbations on the basis of short term integrations.

Hall (1986) showed the potency of using the adjoint equations to determine climate sensitivities by determining the sensitivity of the global mean surface air temperature for variation in different model parameters of an atmospheric model with prescribed sea surface temperatures. Using 10 day integrations, the sensitivities estimated with the use of adjoints agreed within 20% to the sensitivities obtained directly by rerunning the model. Question remains whether this 10 day estimate provides a reasonable estimate for the sensitivity of the temperature averaged over a 30 year period. Also, it is not clear if the adjoint equations yield to useful sensitivities for longer integrations, since the atmosphere is a chaotic system, of which the evolution sensitively depends on small changes in the initial condition.

In this paper we develop an efficient method that can identify parameter perturbations on the basis of short term integrations, that cause, with high probability, large changes in the simulated climate. This way, estimates can be obtained of the range of possible climate outcomes given the uncertainties in model parameters. Changes in the probability of certain types of circulations that have great influence on a regional climate are the main focus. The method is developed in the context of a simple numerical model used as a climate metaphore, namely the Lorenz 63 model, and, motivated by the studies mentioned above, is based on the effect of parameter perturbations on short term evolutions.

In Section 2.2 the modified Lorenz 63 model and its characteristics are described. In Section 2.3 we describe the methods that we used to identify effective parameter perturbations in the Lorenz 63 model. (Effective parameter perturbations are the para-

meter perturbations that change model simulations the most.) Section 5.5 contains the conclusions and discussion.

2.2 Lorenz 63 model

We take the Lorenz 63 model (Lorenz, 1963) as a climate metaphor. It is described by three differential equations, describing the time evolution of state variables x , y and z and contains three parameters, σ' , r' and b' . Following Palmer (1999), two additional parameters c'_x and c'_y are introduced to break the symmetry of the solution.

$$\begin{aligned}\dot{x} &= -\sigma'x + \sigma'y + c'_x, \\ \dot{y} &= -xz + r'x - y + c'_y, \\ \dot{z} &= xy - b'z.\end{aligned}\tag{2.1}$$

For certain parameter settings, the model solution consists of irregular transitions between two unstable equilibria, which might be thought of, in meteorological terms, as representing blocked or zonal flow regimes. If the parameters in the model are set at their standard values, $(\sigma', r', b', c'_x, c'_y) = (10, 28, \frac{8}{3}, 0, 0) = (\sigma_0, r_0, b_0, c_{x0}, c_{y0})$ the two regimes are equally populated. To characterize their population, we determine from a long simulation the probability density function (PDF) along the vector connecting the two regimes. Prior to this, the time series is low-pass filtered with a running mean of one time unit. The resulting PDF clearly shows the existence of equally populated regimes, see Figure 2.1.

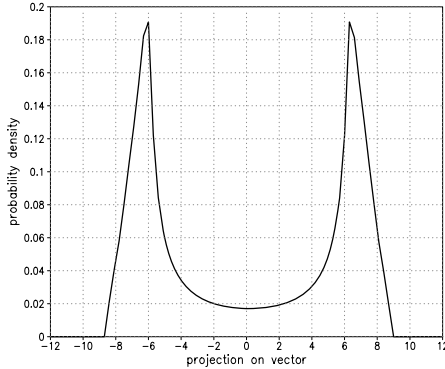


Figure 2.1: *Probability density function of low pass filtered time series of the projection onto the vector connecting the two regimes, for the Lorenz 63 model with standard parameter values.*

A parameter γ , measuring the asymmetry, is introduced. Its value is obtained by integrating the PDF over the left half of its domain, subtract it from 0.5 and multiply

by 2. A value of 0 corresponds to a symmetric PDF, which is obtained for the standard values, values of ± 1 are limiting values corresponding to the population of one regime only. Changes in the population of the regimes are of interest, since regime behaviour in climate models has a large influence on regional climates. When compared with blocked or zonal flows, more blocked flows near Europe causes dryer and warmer periods in summer or dryer and colder periods in winter for Western-Europe and more wet and stormy weather to the north and south of the blocking (Oortwijn et al. 1995).

We assume that the model parameters are uncertain within $\pm 5\%$ of their standard values (c'_x and c'_y can vary ± 1). For mathematical convenience, this is accomplished by choosing a new set of parameters, $(\sigma_0 + 0.5\sigma, r_0 + 1.4r, b_0 + \frac{2}{15}b, c_{x0} + c_x, c_{y0} + c_y)$, where the parameters σ, r, b, c_x, c_y can vary between $[-1, 1]$.

2.3 Finding the effective parameter perturbations

The question we wish to address is the following: what is the maximum value of γ possible, given the specified uncertainties in the parameters of the Lorenz 63 model. Or, in meteorological terms, does a model allow a climate solution with more blocked flows, leading to more frequent cold spells in winters in Europe for instance. One approach to determine this maximum value of γ , is by the use of the direct method (Dickinson et al., 1976).

2.3.1 The direct method

The direct method is a 'brute force' method; random parameter perturbations are drawn from a uniform distribution on a five-dimensional unit-sphere in parameter space, centered around the standard values $((\sigma_0, r_0, b_0, c_{x0}, c_{y0}) = (10, 28, \frac{8}{3}, 0, 0))$. Note that because of the special choice of the parameters, points on this unit-sphere correspond to parameter perturbations that lie within the specified range of 5% uncertainty. For each of these random perturbations, γ is estimated from a long integration (80000 time units). The length of 80000 time units allows γ to be estimated within an absolute error of about 0.001. A total of 50000 random parameter perturbations were evaluated. The values of γ obtained are displayed in the form of an estimate of the probability density function of γ in Figure 2.2 (solid line). The PDF estimate was obtained by dividing the range of γ , $[-0.10, 0.10]$ into 100 bins, counting the number of occurrences in each bin and finally divide by the total number of draws.

The PDF of γ is centered around zero, is uni-modal and is bounded from below by -0.08 and above by 0.08 . The maximum is found at zero, which means that the most probable climate solution, given the uncertainties in the parameters, has equal probabilities for both regimes. However, climate solutions are possible with 8% more occurrences of one regime. The PDF indicates that the chance of picking a parameter perturbation that leads to such an asymmetric solution is small. Most parameter perturbations lead to fairly symmetric solutions. This means that many draws are needed to estimate the range of possible values of γ . Therefore, it would be of great practical

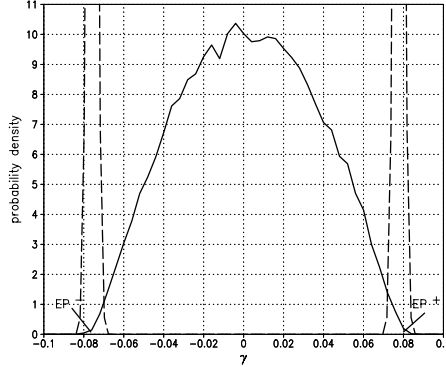


Figure 2.2: Probability density function of asymmetry γ of randomly chosen parameter perturbations (solid line), together with an idealized PDF (dashed line).

use to be able to draw effective parameter perturbations, that is perturbations that most effectively change γ , a priori, also since long simulations are computationally demanding. Ideally one would like to draw effective parameter perturbations only, as indicated by the idealized PDF in Figure 2.2 (dashed line). We wish to determine these on the basis of short model simulations. That this might be possible is based on the notion that systematic changes in short term evolutions change long term statistics.

2.3.2 The adjoint method

Effective parameter perturbations and short term integrations

To follow up on this idea, we choose two sets of effective parameter perturbations from the tails of the distribution of γ in Figure 2.2, which we call EP^+ and EP^- , and investigate the effect of these perturbations on short model evolutions in order to find a means to detect these effective parameter perturbations a priori on the basis of short model evolutions alone. Our short integrations take 2 time units. This is sufficiently long for a regime transition to take place as well as sufficiently short for the linear approximation to still be accurate enough in most cases. For a realistic atmospheric model, this range would be 3 to 5 days, (Oortwijn et al., 1995).

In Figure 2.3 two short term evolutions of two time units, for unperturbed parameters, referred to as a reference orbit are plotted. In 2.3 (a) and (c) we also plotted the end points of additional evolutions from the same initial condition but with randomly perturbed parameters (grey and black points). In 2.3 (b) and (c) the end points of orbits with the selected perturbed parameters EP^+ (black) and EP^- (grey) are plotted. The two regimes are indicated by the large grey and black dot. The black points in Figure 2.3 (a) and (c) are calculated using the non-linear equations (1), whereas the grey points in Figure 2.3 (a) and (c), and EP^+ and EP^- in 2.3 (b) and (d) are calculated

using a linear approximation of the equations around the reference orbit, referred to as the tangent linear equations.

Using the tangent linear equations, a cheap method exists to calculate the parameter perturbation yielding the largest deviation at the end of the reference orbit. The method is based on a Singular Value Decomposition (SVD) of the linear mapping of the parameter perturbation onto the changes in the end point of the reference orbit. The first right singular vector corresponds to the parameter perturbation and is mapped onto the first left singular vector which corresponds to the direction of largest change of the end point of the reference orbit. The corresponding singular value equals the length of the left singular vector. The method is described in the appendix and is very similar to the procedure to find the perturbation to the initial conditions yielding the largest change at the end of the reference orbit (Barkmeijer, 1996).

The linearly evolved random parameter perturbations (grey points) in Figures 2.3 (a) and (c) form an ellipsoid centered around the end point of the reference orbit (black line). The deviation of the black cloud from the grey one is an indication of the limited accuracy of the linearized solution. This accuracy depends on the magnitude of the deviations from the reference orbit (δg , see appendix) which grow in time, for some reference orbits faster than for others.

Focussing on the effective perturbations EP^+ and EP^- , we observed that for some reference orbits they don't lie in distinct areas of the cloud (Figure 2.3 (b)), but that for others EP^+ and EP^- are clearly separated and lie on the end points of the first left singular vector, as shown in Figure 2.3 (d). Thus for reference orbits like this one, the first right singular vector is likely an effective parameter perturbation.

The only problem is how to select orbits such as in Figure 2.3 (d) without any knowledge about EP^+ and EP^- . By shifting reference orbits in time one timestep after the other and examining the behaviour of EP^+ and EP^- , we discovered that the separation along the first singular vector takes place just after an episode when the first singular value has grown to very large values. As an illustration of this, we have plotted the first singular value for subsequent reference orbits in time in Figure 2.4. Every now and then the singular value exceeds 8000 and comes down again below 220. At this moment, EP^+ and EP^- are separated along the first left singular vector, and the first right singular vector is likely an effective parameter perturbation. This empirical finding gives us a recipe to draw potentially effective parameter perturbations a priori:

1. shift reference orbit in time
2. select reference orbit according to evolution of first singular value (after a period of extensive growth)
3. determine for that reference orbit the first singular vector using the adjoint method, use this as parameter perturbation

For the computation of the first singular vector and value corresponding to a reference orbit, one needs to calculate this reference orbit (this is a non linear integration of 2 time units), the tangent linear and the adjoint equations (both at the cost of 2 times a

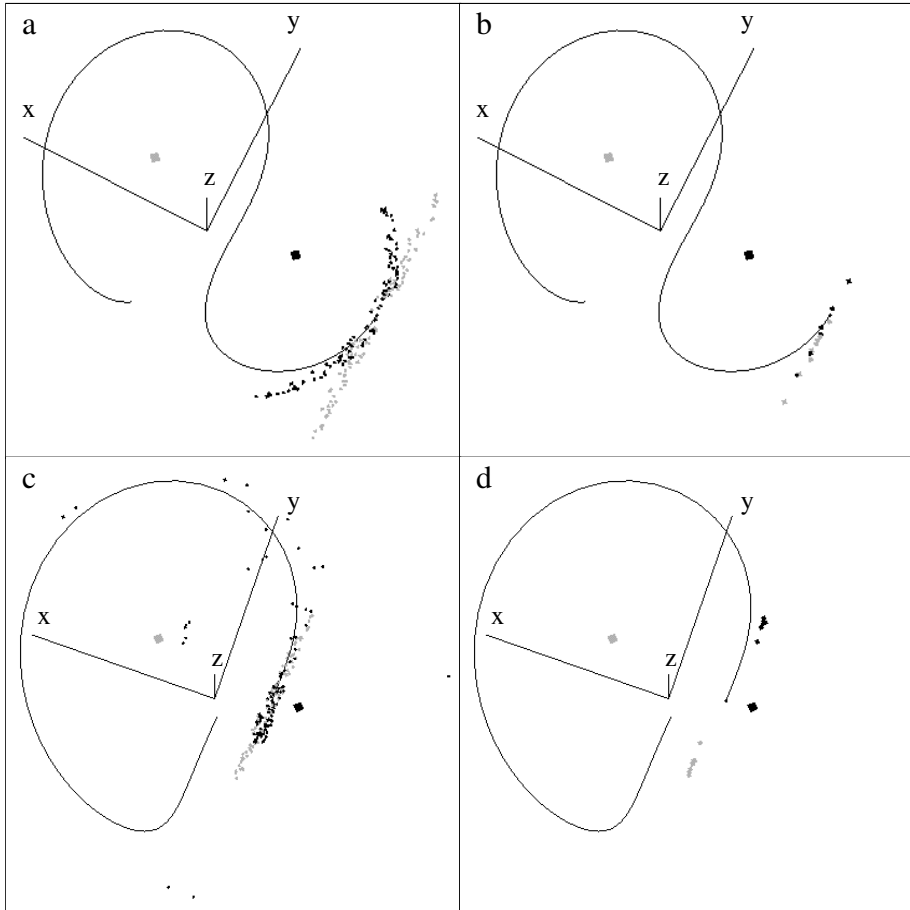


Figure 2.3: The black line is a reference orbit of 2 time units in the 3D space space of the Lorenz 63 model. The two regimes are indicated by the large grey and black dot. In (a) and (c) the grey and black points are resp. the linearly and non-linearly evolved random parameter perturbations, all from the same initial condition. In (b) and (d) the grey and black points are EP^- and EP^+ resp. In (b) EP^- and EP^+ don't lie in distinct area's. In (d) EP^- and EP^+ are clearly separated and lie on the ends of the first left singular vector. Note also that the change induced by the parameter perturbations is not directed along the vector connecting both regimes, but instead is almost perpendicular to it.

non linear integration of 2 time units). This is a total cost of 5 times a non linear integration of 2 time units. In Figure 2.4 it is shown that on average the first singular value exceeds 8000 4 times per 200 shifts of the reference orbit in time. So on average one needs to shift the reference orbit in time 50 times before finding a suitable initial condition. So the total cost to find an effective parameter perturbation is $50 \times 5 \times 2 = 500$ time units of a non linear integration, which is only a fraction of the 80000 time units needed for one long term non linear climate integration. Since this method of finding effective parameter perturbations has so little computational cost compared to one long term non linear integration, it is relevant to use this method to select effective parameter perturbations a priori instead of perturbing at random and making a long term integration for each of these perturbations.

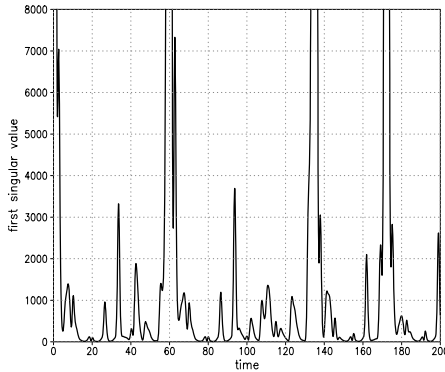


Figure 2.4: A plot of the first singular value which measures the maximum change possible in the end state of the reference orbit. The reference orbit has a duration of 2 time units and is shifted in time in discrete steps of 0.1 time unit.

Effectiveness of the adjoint method

To evaluate the effectiveness of the parameter perturbations determined from the first singular value of selected initial conditions as described above, we made long integrations of 80000 time units for a total of 50000 parameter perturbations and calculated γ for each one of these, as we did with the direct method. The PDF of γ is shown in Figure 2.5 (a).

The solid line is the PDF of γ of randomly chosen parameter perturbations, the dashed line is the PDF of γ of the potentially effective parameter perturbations. It is quite clear that the adjoint method applied to specially selected initial conditions draws almost no parameter perturbation that leads to a symmetrical PDF of the Lorenz 63 model ($\gamma = 0$) and has a much higher probability to draw effective parameter perturbations than the random method does. In Figure 2.5 (b) the cumulative distribution of both the direct (solid line) and adjoint (dashed line) method are shown. This is the

probability to draw a parameter perturbation that yields to $|\gamma| \geq x$. For example, the probability to draw parameter perturbations that gives an asymmetry higher than 6%, that is $|\gamma| \geq 0.06$ with the direct method is 7.7%, whereas with the adjoint method this probability is 17.8%, which is 2.29 times as high. This result is proof that sensitivities based on short integrations contain valuable information on the sensitivity of long term statistics to parameter perturbations, at least for the Lorenz 63 model.

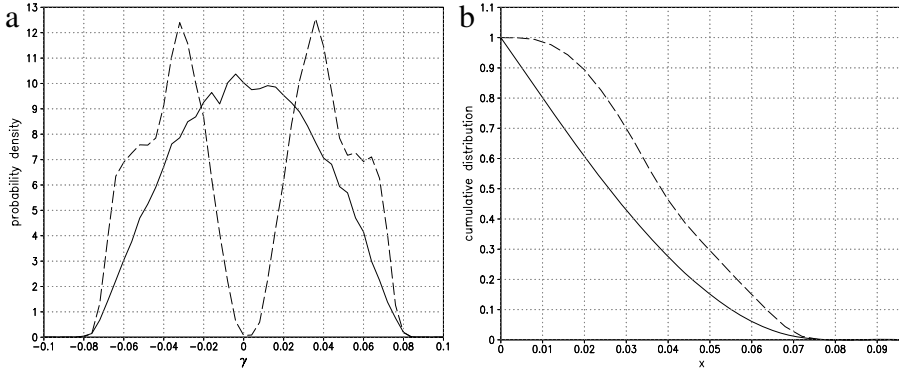


Figure 2.5: (a) Probability density function of the asymmetry γ . The solid line is the PDF of randomly chosen parameter perturbations, the dashed line is the PDF of parameter perturbations calculated with our adjoint method. (b) Cumulative distribution of both the direct (solid line) and adjoint (dashed line) method. This is the probability to draw a parameter perturbation that yields to $|\gamma| \geq x$.

Inspecting the PDF of the adjoint method in Figure 2.5 (a) again, it seems that there are two groups of parameter perturbations, one more effective than the other. These perturbations might be related to two sets of reference orbits from which they were calculated that lie on different areas of the attractor. In Figure 2.6 the 25000 initial values of the reference orbits are plotted that were used to calculate the perturbations (we used both the first singular vector and the opposite signed first singular vector as parameter perturbations to get 50000 draws).

We can divide the initial values broadly into two sets. Set 1 contains the initial conditions in the centre part, set 2 contains the two groups of initial values at the left and right side of the attractor. We made separate PDF's of γ of these two sets, see Figure 2.7. The dashed line is the same PDF as in Figure 2.5 (a), for all the initial conditions, the dotted dashed line is the PDF for set 1 and the dotted line for set 2. The reference orbits with initial values from set 1 yield more effective parameter perturbations than set 2. Unfortunately, this is an observation after the fact and cannot be used to make the adjoint method more effective.

We did an extra experiment to make sure that especially the initial conditions, selected after the reference orbit passed through a sensitive area on the attractor yield

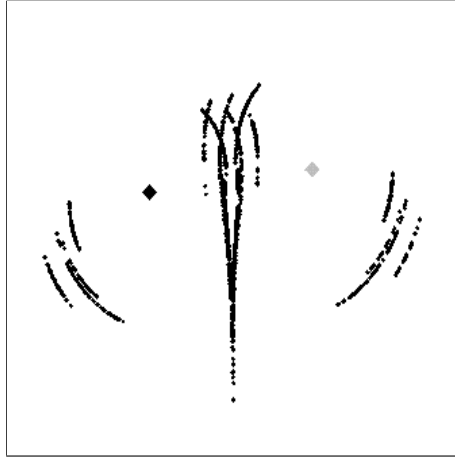


Figure 2.6: *Initial conditions of the reference orbits just after an episode when the first singular value has grown to very large values.*

effective parameter perturbations. For this, we took the first singular vector as parameter perturbation for reference orbits 0.1 time unit apart irrespective of the value of the first singular value. For 50000 perturbations γ was calculated on the basis of 80000 time unit long trajectories. This gave us the PDF of γ shown in Figure 2.8 (a) with a dotted dashed line. Clearly this method is not optimal to draw effective parameter perturbations. Although this method still gives less ineffective parameter perturbations than the random method, it also gives less effective ones. Furthermore, the peaks of the PDF correspond to smaller values of γ than the two highest peaks of the dashed PDF based on the selection of specific initial conditions.

In another experiment to verify the effectiveness of our adjoint method, we took only first left singular vectors as our parameter perturbations, with very large corresponding singular values (greater than 8000). Again, for 50000 perturbations γ was calculated on the basis of 80000 time unit long trajectories. This gave us the dotted PDF in Figure 2.8 (b). This is hardly an improvement of the previous PDF in Figure 2.8 (a). Although there are less parameter perturbations drawn that give a value γ close to 0, there are also no parameter perturbations that give a value $|\gamma|$ greater than 0.06.

Another interesting aspect is the contribution of the forcing parameters c_x and c_y to the asymmetry of the model. To illustrate this, we project the first singular vector onto the (c_x, c_y) -plane and calculated the percentage of this length compared to the total length of the first singular vector. We did this for all the singular vectors drawn with the adjoint method, that were used as parameter perturbations. We plotted a PDF of these percentages in Figure 2.9. The solid line represents the percentages of all the singular vectors drawn with the adjoint method, the dashed line represents the percentages of the singular vectors that cause an asymmetry higher than 6%. The solid line has two large

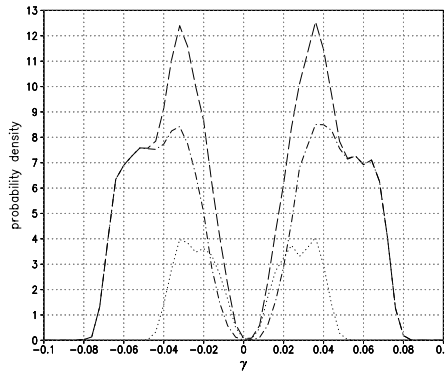


Figure 2.7: Probability density function of the asymmetry γ . The dashed line is the PDF of parameter perturbations of the adjoint method (as in Figure 2.5 (a)), for all initial conditions shown in Figure 2.6. The dotted dashed line is the PDF for the set of initial conditions in the centre part in Figure 2.6 (set 1) and the dotted line is the PDF for the set of initial conditions at the left and right side of the attractor in Figure 2.6 (set 2).

peaks, one around 45% and one around 92%. The dashed line has one peak around 92%. This does indicate that the forcing parameters c_x and c_y play an important role in causing asymmetry, however, it is also possible to cause large asymmetry with a contribution of c_x and c_y of for instance 60%, so it is useful to take all parameters in consideration when making perturbations.

To conclude, the adjoint method yields effective parameter perturbations for specific initial conditions that can be selected a priori based on the history of the behaviour of the first singular value.

2.4 Conclusions and discussion

In this study we set out to develop an efficient method to identify parameter perturbations that cause large changes in the simulated climate. The method is based on the sensitivity of short integrations to parameter perturbations. These sensitivities can be calculated efficiently using the adjoint method (Errico, 1997). The method is developed in the context of the Lorenz 63 equations. It turns out that for specific initial conditions, the parameter perturbations that give rise to the largest changes in the short term, also tend to be effective in changing the long term climate statistics as measured by the asymmetry of the PDF. A priori selection of these special initial conditions is possible. They tend to occur just *after* the trajectory has passed through a very sensitive area where small parameter perturbations can cause the largest changes in the short term evolution. We don't know why this is, but we do know that parameter perturbations for

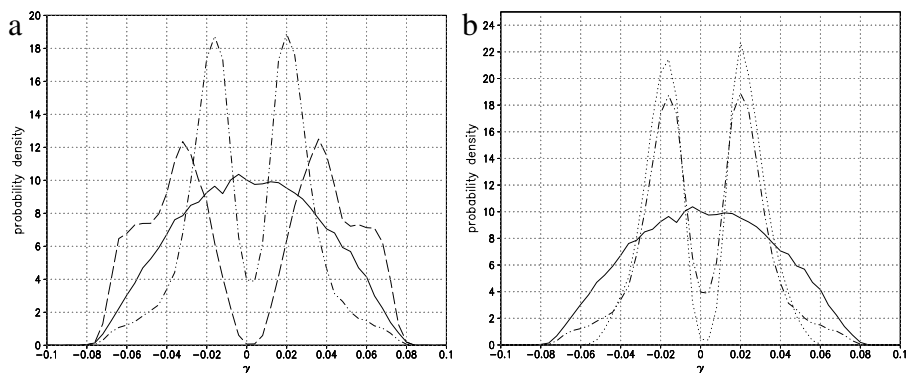


Figure 2.8: Probability density functions of the asymmetry γ . The solid line in (a) and (b) is the PDF for the direct method (as in Figures 2.2 and 2.5 (a)). In (a) and (b) the dotted dashed line is the PDF of γ taking as parameter perturbations the first singular vector of arbitrary initial conditions. The dotted PDF in (b) is the PDF where parameter perturbations correspond to first singular vectors with very large corresponding singular values only.

reference orbits with the largest short term sensitivities are not effective in perturbing the climate solution.

Since this method to select parameter perturbations within the specified uncertainties has a higher probability for drawing effective parameters than the direct method, it is more likely that a good estimate of the largest changes possible in the simulated climate can be obtained with this method when only making a few long term integrations. One provision must be made; adjoint equations of the model under consideration are needed to determine the short term sensitivities efficiently. Only few climate integrations can be made for realistic models due to computational constraints. It pays to identify potentially effective parameter perturbations a priori. Probably more so for higher dimensional systems. It is well known that for atmospheric models most perturbations to initial conditions are rather ineffective since they decay in most of the dimensions in the state space. For similar reason, most parameter perturbations are bound to be ineffective. There is a relatively low number of unstable directions.

The customary adjoint equations to estimate sensitivities of short term trajectories to changes in the initial conditions need to be expanded to include the effect of changes in parameters as well. A first step into this direction was taken by Barkmeijer et al., (2002) who included the effect of changes of the forcing terms in the right hand side of the tendency equations. The most effective changes to the forcing terms for a given reference orbit were coined forcing singular vectors.

In this study we have shown the relevance of short term sensitivities for the sensitivity of long term statistics for parameter changes. Also Corti and Palmer (1997)

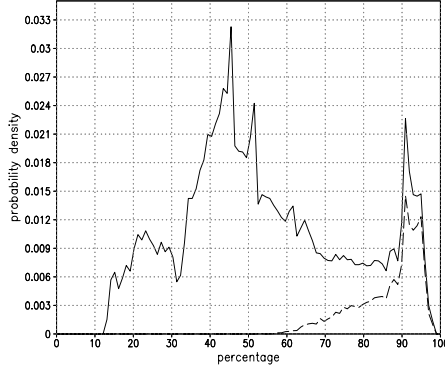


Figure 2.9: *PDF of the percentages of the length of the projection of the singular vector onto the (c_x, c_y) -plane compared to the length of the singular vector, drawn with the adjoint method.*

presented evidence that sensitivities based on short term integrations are relevant for long term statistics. In their study, they ensemble averaged over 2000 initial conditions the perturbation to the initial condition that changed the projection of the end point of a five day integration onto the PNA pattern the most and put their averaged perturbation as a forcing perturbation on the right hand side of the equations. Although they noted a large change in the PDF of the PNA pattern due to this forcing, question remains whether this is the maximum change possible given the size of the forcing perturbation. To answer this question in the context of the Lorenz 63 model, we did a similar analysis. We determined parameter perturbations that maximize the projection of the end points of the perturbed reference orbit onto the vector connecting both regimes. For a total of 50000 initial conditions, we determined the mean parameter perturbation. This mean perturbation was scaled to correspond to the specified uncertainty of 5%. This perturbation yields an asymmetry γ of only 5% of the maximum γ possible, indicating that just averaging optimal perturbations will not necessarily yield an effective parameter perturbation. On the contrary, our results indicate that the initial condition of the reference orbit matters.

Lastly, so far the method has only been tested in the context of the Lorenz 63 model. A natural next step is to evaluate the method in the context of a more realistic atmospheric model. Work along these lines is on its way.

2.5 Acknowledgements

We would like to thank J. Grasman for his interest and suggestions.

Appendix: The tangent linear equations

Usually, the tangent linear equations are derived for deviations in the state space variables only. Here we include perturbations in model parameters as well. For this purpose, we introduce the vector \mathbf{q} , which consists of the vector $\mathbf{x} = (x, y, z)$ in state space and the vector $\alpha = (\sigma, r, b, c_x, c_y)$ in parameter space, so

$$\mathbf{q} = \begin{pmatrix} \mathbf{x} \\ \alpha \end{pmatrix}$$

$$\dot{\mathbf{q}} = \begin{pmatrix} \dot{\mathbf{x}} \\ \dot{\alpha} \end{pmatrix} = \begin{pmatrix} \mathbf{F}_1(\mathbf{x}, \alpha) \\ \mathbf{F}_2(\alpha) \end{pmatrix} = \begin{pmatrix} \mathbf{F}_1(\mathbf{x}, \alpha) \\ \mathbf{0} \end{pmatrix} = \mathbf{F}(\mathbf{q})$$

The tangent linear equations are derived as follows:

$$\begin{aligned} \dot{\mathbf{q}} = \mathbf{F}(\mathbf{q}) &\Rightarrow (\mathbf{q}_r + \delta\mathbf{q}_r) = \mathbf{F}(\mathbf{q}_r + \delta\mathbf{q}_r) \approx \mathbf{F}(\mathbf{q}_r) + J\delta\mathbf{q}_r + \mathcal{O}(|\delta\mathbf{q}_r|^2) \\ &\Rightarrow \dot{\mathbf{q}}_r + \delta\dot{\mathbf{q}}_r \approx \mathbf{F}(\mathbf{q}_r) + J\delta\mathbf{q}_r \\ &\Rightarrow \delta\dot{\mathbf{q}}_r \approx J\delta\mathbf{q}_r \end{aligned}$$

where J is the Jacobi matrix, \mathbf{q}_r denotes the reference orbit and where:

$$J = \frac{\partial \mathbf{F}(\mathbf{q})}{\partial \mathbf{q}} \Big|_{\mathbf{q}_r} = \begin{pmatrix} \frac{\partial \mathbf{F}_1(\mathbf{x}, \alpha)}{\partial \mathbf{x}} & \frac{\partial \mathbf{F}_1(\mathbf{x}, \alpha)}{\partial \alpha} \\ \frac{\partial \mathbf{F}_2(\alpha)}{\partial \mathbf{x}} & \frac{\partial \mathbf{F}_2(\alpha)}{\partial \alpha} \end{pmatrix} \Big|_{\mathbf{q}_r} = \begin{pmatrix} \frac{\partial \mathbf{F}_1(\mathbf{x}, \alpha)}{\partial \mathbf{x}} & \frac{\partial \mathbf{F}_1(\mathbf{x}, \alpha)}{\partial \alpha} \\ \mathbf{0} & \mathbf{0} \end{pmatrix} \Big|_{\mathbf{q}_r},$$

the tangent linear equations of the Lorenz 63 model (1) read:

$$\begin{aligned} \delta\dot{x} &= -\sigma' \cdot (\delta x - \delta y) - (x - y) \cdot \delta\sigma' + \delta c'_x, \\ \delta\dot{y} &= (r' - z') \cdot \delta x - \delta y - x \cdot \delta z' + x \cdot \delta r' + \delta c'_y, \\ \delta\dot{z} &= y \cdot \delta x + x \cdot \delta y - b' \cdot \delta z - z \cdot \delta b', \\ \delta\dot{\sigma}' &= 0, \\ \delta\dot{r}' &= 0, \\ \delta\dot{b}' &= 0, \\ \delta\dot{c}'_x &= 0, \\ \delta\dot{c}'_y &= 0. \end{aligned}$$

For a given reference orbit of duration T the tangent linear equations project perturbations in vector \mathbf{q} at initial time onto perturbations in \mathbf{q} at final time. Formally, this linear transformation can be represented by a matrix R : $\delta\mathbf{q}(T) = R(0, T) \cdot \delta\mathbf{q}(0)$, also referred to as the tangent linear propagator. We only wish to assess the influence of parameter perturbations on the flow, not of perturbations in the initial conditions, which means that $\delta\mathbf{x}(0) = \mathbf{0}$ and $\delta\alpha(0) \neq \mathbf{0}$. To achieve this, projection matrices P_1 and P_2 are introduced which project vector \mathbf{q} into parameter space or state space respectively:

$$P_1 \mathbf{q} = P_1 \begin{pmatrix} \mathbf{x} \\ \alpha \end{pmatrix} = \begin{pmatrix} \mathbf{0} \\ \alpha \end{pmatrix}$$

$$P_2 \mathbf{q} = P_2 \begin{pmatrix} \mathbf{x} \\ \alpha \end{pmatrix} = \begin{pmatrix} \mathbf{x} \\ \mathbf{0} \end{pmatrix}$$

Using these matrices, a forward integration of the tangent linear equations can be rewritten as:

$$P_2 R P_1 \delta \mathbf{q}(0) = \delta \mathbf{x}(T) \equiv S \delta \mathbf{q}(0)$$

When $\delta \mathbf{q}(0)$ is limited to a hypersphere; $\delta \mathbf{x}(T)$ lies on an ellipsoid. Now, for the length of vector $\delta \mathbf{x}(T)$ we can write

$$\langle \delta \mathbf{x}(T), \delta \mathbf{x}(T) \rangle^{1/2} = \langle S \delta \mathbf{q}(0), S \delta \mathbf{q}(0) \rangle^{1/2} = \langle S^T S \delta \mathbf{q}(0), \delta \mathbf{q}(0) \rangle^{1/2}$$

where \langle, \rangle defines an euclidian inner product and S^T is the transposed of S . This length is maximized when $\delta \mathbf{q}(0)$ is the eigenvector of $S^T S$ with the largest eigenvalue. It corresponds to the vector of parameter perturbations that evolves into the major axis of the ellipsoid at time T . The square root of the eigenvalue corresponds to the length of the major axis and is an indication of the sensitivity of the reference orbit to changes in the parameters.

In the literature, this vector is called the first right singular vector, the corresponding eigenvalue the first singular value. This terminology stems from the singular value decomposition of S , (see for instance Press et al (1986)). An arbitrary ($m \times n$) matrix S can be written as: $S = U W V^T$, where U is a column-orthonormal ($m \times n$) matrix (containing the left singular vectors), W is an ($n \times n$) diagonal matrix with positive and zero elements (the singular values) and V^T is the transposed of orthonormal ($n \times n$) matrix V (containing the right singular vectors). These singular vectors are eigenvectors of $S^T S$:

$$S^T S V = (U W V^T)^T (U W V^T) V = V W U^T U W V^T V = V W^2 V^T V = V W^2$$

with eigenvalues equal to the squares of the singular values W . Matrix S projects the right singular vectors onto the left singular vectors:

$$S V = U W V^T V = U W.$$

Thus the left singular vectors are the axes of the ellipsoid.

References

- Barkmeijer, J., 1996. Constructing fast-growing perturbations for the nonlinear regime. *J. Atmos. Sci.*, **53**, 2838-2851.
- Barkmeijer, J., Iversen, and T., Palmer, T.N., 2002. Forcing singular vectors and other sensitive model structures. *Quart. J. Roy. Meteor. Soc.*, **128**, 2401-2424.
- Corti, S. and Palmer, T.N., 1997. Sensitivity analysis of atmospheric low-frequency variability. *Q.J.R. Meteorol. Soc.*, **123**, 2425-2447.
- Dickinson, R.P. and Gelinas, R.J., 1976. Sensitivity analysis of ordinary differential equation systems - a direct method. *J. Comp. Phys.*, **21**, 123-143.
- IPCC, 2001. Climate Change 2001: The Scientific Basis. Eds: Houghton, J.T., Y. Ding, D.J. Griggs, M. Noguer, P.J. van der Linden, X. Dai, K. Maskell, and C.A. Johnson. Contribution of Working Group I to the Third Assessment Report of the Intergovernmental Panel on Climate Change. *Cambridge University Press*, pp 511.
- Errico, R.M., 1997. What is an adjoint model? *Bull. Amer. Soc.*, **78**, 2576-2591.
- Hall, M.C.G., 1986. Application of adjoint sensitivity theory to an atmospheric general circulation model. *J. Atmos. Sci.*, **43**, 2644-2651.
- Lea, D.J., Allen, M.R. and Haine, T.W.N., 2000. Sensitivity analysis of the climate of a chaotic system. *Tellus*, **52A**, 523-532.
- Lorenz, E.N., 1963. Deterministic nonperiodic flow. *J. Atmos. Sci.*, **20**, 130-141.
- Oortwijn, J., and Barkmeijer, J., 1995. Perturbations that optimally trigger weather regimes. *J. Atmos. Sci.*, **52**, 3932-3944.
- Palmer, T.N., 1999. A nonlinear dynamical perspective on climate prediction. *Journal of Climate* **12** 575-591.
- Press, W.H., Flannery, B.P., Teukolsky, S.A., and Vetterling, W.T., 1986. Numerical Recipes. *Cambridge University Press*, §2.6.

CHAPTER 3

Sensitivity to forcing parameters in the T21QG atmospheric model

The way uncertainty in model parameters is handled determines for a large part the quality of a climate forecast. It is important to specify and quantify the effect of these uncertainties. In the context of the three-level quasi-geostrophic spectral T21QG model, the sensitivity to forcing parameters is studied. It is relevant to identify the vector of parameter perturbations that yields the largest climate change. A method is presented that uses short term dynamical behaviour to identify the perturbations to the forcing parameters that will affect the long term behaviour the most and result in the largest change in the simulated climate. Climate change will be looked at in terms of change in the strength of preferred circulation patterns. The tangent linear and adjoint equations are applied to consecutive short non-linear integrations to determine the vector of parameter perturbations leading to the largest error growth in the state variables over this short time interval. The model equations are extended with the parameter vector with vanishing time derivative for this purpose. The vector of parameter perturbations leading to largest error growth is called the first singular vector. The corresponding singular value is a measure of this growth. Its value depends on the initial condition as the sensitivity of the model solution to parameter perturbations varies over the attractor. The first singular vector is potentially an effective parameter perturbation leading to a large climate change when it is selected just after the system has passed through a period of maximum error growth. This method to select forcing parameter perturbations on the basis of the short term behaviour of the model, is compared with a random selection of these perturbations. The rate of success of the selection method based on short integrations is shown to be much larger.

3.1 Introduction

Uncertainty in the outcome of climate models is widely recognized (e.g. IPCC 2001, Reilley et al., 2001, Forest et al., 2002, Allen, 2003, Murphy et al., 2004, Stocker,

2004). A contributing factor is uncertainty in the model parameters. Many of the model parameters are not exactly known so an uncertainty analysis should be part of a study on the long term dynamics of the climate. We are especially interested in the range of possible outcomes of the climate model, given a parameter uncertainty. It would be an advantage to efficiently find the parameter perturbations that yield the extreme outcomes. These parameter perturbations are called effective parameter perturbations. It would save computing time if these can be found on the basis of the short term behaviour of the model. For this purpose, the tangent linear and adjoint equations are introduced. The question then is, to what extent can the short term behaviour of the model be used to determine the long term statistics. For this purpose a method is developed that detects the vector of parameter perturbations to which the system has the highest sensitivity.

In Moolenaar and Selten (2004) this method of finding effective parameter perturbations has been tested using the Lorenz 63 equations (Lorenz, 1963). The behaviour on the chaotic attractor of this system was analysed by model runs that had a fixed length and that were sufficiently short in time to allow a linear analysis based on the adjoint equations. For each reference run the optimal parameter perturbation was computed leading to the largest error growth. It turned out that for specific points at the attractor this most effective parameter perturbation is frequently also a highly effective parameter perturbation leading to large changes in the climate. When calculating consecutive short runs, the effective perturbations were found just after the reference run had passed through a phase of strong error growth.

Adjoint models are powerful tools to estimate the sensitivity of model output with respect to input, such as initial conditions and parameters. In particular, they can be used to efficiently calculate the sensitivity to variations in any of the model's parameters (Hall and Cacuci, 1983). Errico (1997) gives a good description of the adjoint model and its applications. With the adjoint equations singular vectors can be calculated. These calculations are carried out over a sufficiently short time period, during which the linearization is still holds. Singular vectors, also referred to as optimal finite-time perturbations, were first introduced by Lorenz (1965).

Since the adjoint method developed in Moolenaar and Selten (2004), chapter 2 in this thesis, proved to be an efficient method in the Lorenz 63 model, we now want to test it in a more realistic atmospheric model. Our choice is the T21QG model. This model has been used for adjoint sensitivity analysis with respect to uncertainty in initial conditions, see e.g. Molteni and Palmer (1993), Oortwijn and Barkmeijer (1995) and Barkmeijer (1996). As in the Lorenz 63 model, the T21QG model shows regime behaviour. Whereas the Lorenz 63 model only has two preferred regimes, the T21QG model contains several preferred flow regimes. Both models show sensitivity to initial conditions. The sensitivity to the perturbation of parameters depends on the state of the model. Consequently, the dynamics of the T21QG model show sufficient similarities with the Lorenz 63 model to apply the adjoint method for finding effective parameter perturbations. In the Lorenz 63 model all model parameters were perturbed, whereas in the T21QG model only the forcing parameters are chosen.

The T21QG model is a spectral model. Such models are commonly used for a

numerical analysis of the atmospheric circulation. In the spectral model (a type of Galerkin method) each dependent variable is expressed in a (truncated) sum of orthogonal functions, the spherical harmonics. By this method, partial differential equations are transformed into a set of ordinary differential equations for the coefficients of the orthogonal functions, see i.e. Haltiner and Williams, (1980) and Press et al, (1986). Spherical harmonics are described in Appendix A.

In the atmospheric circulation, preferred large-scale flow patterns, also referred to as weather regimes, occur (Reinhold and Pierrehumbert, 1982). Regimes are usually defined by local maxima in the multi-dimensional Probability Density Function (PDF) of states. An important part of the low-frequency variability of the atmosphere can be captured in a low-dimensional space (D'Andrea and Vautard, 2001). The low-frequency variability can be decomposed into Empirical Orthogonal Functions (EOFs). The leading EOFs give the directions of the most variance and span the state space that contains these regimes, (Haines and Hannachi, 1995, Marshall and Molteni, 1993). For a long integration, the streamfunction can be projected onto the EOFs at fixed time intervals (of one day). The amplitudes of these projections vary in time and PDFs of the timeseries of the amplitudes can be approximated. Palmer (1999) hypothesized that climate change due to a small imposed forcing will result in changes of these PDFs in which the regimes remain present, while their duration and alternation may change. We will use the PDFs of the dominant EOFs as a measure of climate change since these EOFs are important for the local climate.

Fleming (1993) recognized the importance of determining the uncertainty in forcing in climate models. He states that there is a need to establish a scientific methodology for identifying and quantifying the impacts of uncertainty. Using a Monte Carlo approach for this purpose is not feasible for large systems due to the required number of runs and the number of forcing parameters that are uncertain. However, because it is important to analyse parameter uncertainty, he still considers it as a practical method to start with. In order to make a comparison for our method based on local error growth with a standard method such as the Monte Carlo method, we carry out a search for effective parameter perturbations by taking the best one from a set of randomly selected perturbations.

Dymnikov and Gritsoun (2001) did a study in determining a climate system's sensitivity to small perturbations to an external forcing using a two-layer quasi-geostrophic atmospheric model. They added an external forcing considered in the subspace of the first 30 EOFs (Empirical Orthogonal Functions). They calculated the first and second right singular vector of the response operator matrix which according to the linear theory should correspond to the optimal forcing perturbations leadint to the largest change in the model's average state. This matrix evaluates the response of the average state of the model to the perturbation. It is obtained from a 30000 day model run using the response formula of Leith (1975) which is based on the fluctuation-dissipation theorem (Kraichnan, 1959). They carried out two integrations of 10000 days that were perturbed with respectively the first and second (scaled) right singular vector as a forcing perturbation. The perturbed runs were compared with the unperturbed run by the changes in the average state of the system. It proved to be a good prediction of the

response of the model to the small constant perturbations of external forcing. In our study we are interested in changes in the PDFs of the dominant circulation structures, not just the average state. Moreover, our method also applies to parameters that occur in products with state variables in the governing equations.

To provide a reliable specification of the spread of possible regional climate changes, a large ensemble of climate predictions is needed, in which parameters are chosen such that the widest range of uncertainties is captured (Murphy et al. (2004)). In a first attempt to evaluate climate sensitivity due to anthropogenic climate change (assuming a doubled CO_2 concentration), Murphy et al. (2004) compiled an ensemble containing four million model versions, of an atmospheric model coupled to a mixed-layer ocean, with randomly chosen multiple parameter perturbations. Parameters that cannot be accurately determined from observations are perturbed within an uncertainty range, specified by experts. It is assumed that the impacts combine linearly and that each parameter has a uniform distribution within a range of values. They weighed the model predictions of climate sensitivity according to the likelihood that the simulation of present-day climate is consistent with observations (the members of the ensemble are not equally reliable). In this way they narrow the range of possible future global mean temperature increase. As a next step, they propose to sample multiple parameter perturbations since the assumption that individual parameter perturbations combine linearly is unlikely to be valid at a regional scale. To increase the ensemble size, they will make use of results from <http://www.climateprediction.net> where computers of members of the public are used for simulation runs.

Stainforth et al., (2005) present results from the 'climateprediction.net' experiment. They emphasize that ensembles of climate prediction are needed to assess both chaotic climate variability and model response uncertainty. Within a multi-thousand member ensemble, parameters are altered within a range considered plausible by experts, although they do stress that experts are known to underestimate uncertainty and these ranges cannot be considered as absolute ranges. Two or three alternate values are used per parameter and a simulation may have several parameters perturbed. Each member of the ensemble quantifies the response of the model to a doubling of CO_2 concentrations. They find that, when assessing the possible temperature change, most simulations cluster around the value of the unperturbed model, suggesting most parameter perturbations have little effect. This could be due to a limited impact of relevant processes on sensitivity, the parameter ranges may have been estimated too small and/or multiple perturbations may compensate each other when averaged. However, they do show a large range of possible climate outcomes and that high sensitivities should not be omitted. In future experiments a model with a fully dynamic ocean will be used.

In Section 3.2 the T21QG model is described and it is explained how EOF analysis can be used for a parameter sensitivity analysis of the climate. In Section 3.3 the model will be perturbed and the previously described adjoint method is applied to the T21QG model. A set of 1000 climate runs is made, each with a perturbed forcing that is expected to be effective with a high probability. These perturbations are selected from short runs of the linearized system at the specific points of the attractor where the singular value falls back from an extremely large value. In Section 3.4 the results of

Section 3.3 are compared with other methods for searching effective parameter perturbations, among which a random selection method. Section 5.5 contains the conclusions of this study.

3.2 Climate sensitivity analysis using Empirical Orthogonal Functions

3.2.1 The T21QG-model

In the extratropics, the atmospheric circulation can be well approximated by quasi-geostrophic equations. The quasi-geostrophic equations are filtered prognostic equations (gravity waves are absent) and can be written in terms of only one variable, the quasi-geostrophic potential vorticity. Here, the quasi-geostrophic (QG) T21QG-model is used, which is a spectral, 3-level model, as described by Marshall and Molteni (1993).

For the potential vorticity a series expansion in spherical harmonics is made. The time dependent coefficients of this expansion are the state variables of the model. The series of spherical harmonics used in the representation of horizontal fields has a triangular truncation at total wavenumber 21 (T21). The model integrates prognostic equations for QG potential vorticity (PV) at 200 hPa (level 1), 500 hPa (level 2) and 800 hPa (level 3),

$$\frac{\partial q_k}{\partial t} = -J(\psi_k, q_k) - D_k(\psi_k) + S_k, \quad k = 1, 2, 3., \quad (3.1)$$

where q is the potential vorticity (PV) and ψ the streamfunction, D is a linear operator that represents dissipation, S is an artificial forcing, J the Jacobian, $J(\psi, q) = (\frac{\partial \psi}{\partial \lambda} \frac{\partial q}{\partial \mu} - \frac{\partial \psi}{\partial \mu} \frac{\partial q}{\partial \lambda})$, where λ is longitude and μ is the sine of latitude, and k is the index for the different levels. Equation (3.1) is the vertical discretization of the quasi-geostrophic potential vorticity equation (Holton, 1992)

$$(\frac{\partial}{\partial t} + \mathbf{V}_\psi \cdot \nabla)(\nabla^2 \psi + f + f_0^2 \frac{\partial}{\partial p} \sigma^{-1} \frac{\partial \psi}{\partial p}) = 0, \quad (3.2)$$

where \mathbf{V}_ψ is the non-divergent velocity, f_0 is f at reference latitude $45^\circ N$, $f = 2\Omega \sin \phi$ and Ω is the earth's angular velocity, σ is a static stability parameter and p is pressure. The dissipative and forcing terms have been added to represent the effect of diabatic processes. The dissipative terms are described in detail in Appendix B. The relative vorticity is the Laplacian of the streamfunction. Here PV is defined as

$$\begin{aligned} q_1 &= \nabla^2 \psi_1 + f - R_1^{-2}(\psi_1 - \psi_2), \\ q_2 &= \nabla^2 \psi_2 + f - R_1^{-2}(\psi_1 - \psi_2) - R_2^{-2}(\psi_2 - \psi_3), \\ q_3 &= \nabla^2 \psi_3 + f(1 + \frac{h}{H_0}) - R_2^{-2}(\psi_2 - \psi_3), \end{aligned} \quad (3.3)$$

where $f = 2\Omega \sin \phi$ is the planetary vorticity, R_1 ($= 700$ km) and R_2 ($= 450$ km) are Rossby radii of deformation appropriate to the 200-500 hPa level and the 500-800 hPa level respectively, h is the orographic height and H_0 ($= 9$ km) is a scale height. At each level the quasi-geostrophic potential vorticity has 483 independent spectral components, so that the model has 1449 degrees of freedom. It is assumed that the multi-level field of PV is a linear function of the multi-level streamfunction, which is invertible under appropriate boundary conditions.

3.2.2 Empirical Orthogonal Function (EOF) analysis

EOF analysis deals with a given set of data, in our case a time series of streamfunction values evaluated on a grid covering the northern hemisphere. One of the first to introduce EOFs in meteorology was Lorenz (1956). It has turned out to be an effective means of representing climatological fields. It gives information on the variability of the studied data. Out of this data set, a set of vectors can be formed. This set of vectors is centred at the mean of all the points in the data set. The first vector is a unit vector that indicates the direction for which the variance is maximized. The second vector indicates the direction of second most variance, and is a unit vector orthogonal to the first vector and so on. These vectors are the eigenvectors of the covariance matrix V of the data set and are termed Empirical Orthogonal Functions (EOFs). The EOFs form the orthonormal system, $\{\mathbf{e}_1, \mathbf{e}_2, \dots, \mathbf{e}_p\}$. This theory is fully explained in Preisendorfer(1988).

Each data set in a p -dimensional space, denoted by a vector $\mathbf{z}(t) = (z_1(t), \dots, z_p(t))$ can be described by its projection onto the EOFs \mathbf{e}_i :

$$\mathbf{z}(t) = \sum_{i=1}^p a_i(t) \mathbf{e}_i, \quad (3.4)$$

where the amplitudes (or principal components) $a_i(t)$ are given by $a_i(t) = [\mathbf{z}(t), \mathbf{e}_i]$ with $[\cdot, \cdot]$ the Euclidian innerproduct. When projecting a streamfunction onto the EOFs, the time mean needs to be subtracted from the streamfunction, since the EOFs are centred at the time mean, resulting in $\mathbf{z}(t) = \psi(t) - \overline{\psi(t)}$. The a_i are the coordinates of the points in the EOF space. The total variance of the dataset is equal to the sum of the eigenvalues of the matrix spanned by the EOFs:

$$Var(\psi) = \sum_{i=1}^p \overline{z_i(t)^2} = \sum_{i=1}^p \overline{[\sum_{j=1}^p a_j(t) e_{ji}]^2} = \sum_{i=1}^p \overline{a_i(t)^2} = \sum_{i=1}^p \lambda_i, \quad (3.5)$$

where use has been made of the fact that the EOF amplitudes are uncorrelated in time, $\overline{a_i a_j} = 0$ for $i \neq j$.

The eigenvalues corresponding to the EOFs fall off very quickly, see Figure 3.1 a). Given are the eigenvalues of the first 100 EOFs of the T21QG model calculated from 100000 daily fields of 500 hPa streamfunction over the northern hemisphere. It is observed that most information about the variability is contained in the first leading

EOFs. Figure 3.1 b) shows us the cumulative variance. We can see that the first 10 EOFs contain 55% of the information about the variability. By projecting the data along these dominant EOFs (truncate summation (3.4) at a certain $n < p$), we can reduce the dimension of the full EOF space considerably and still retain a good global view of the dynamical range of the system. A special property of the EOFs is that for a given truncation n , no other basis set can explain more of the average variance (Lorenz, 1956, North et al., 1982).

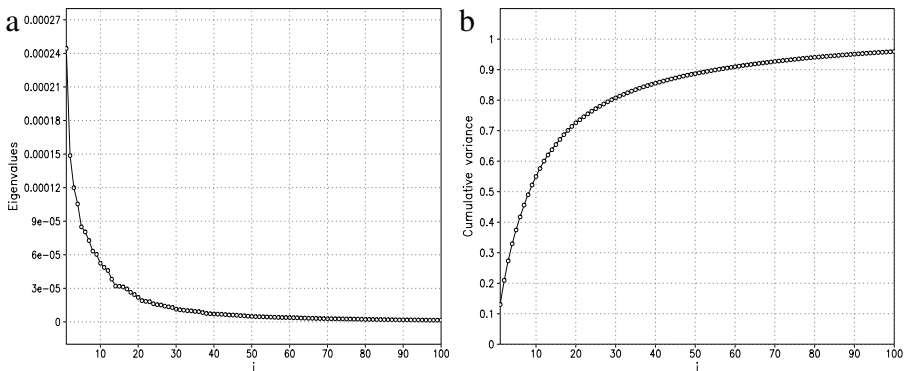


Figure 3.1: a) Eigenvalues of the covariance matrix V for the first 100 EOFs of the T21QG model, b) Cumulative variance, see (3.5).

3.2.3 Parameter sensitivity analysis with the T21QG atmospheric model

The leading EOFs are an indication for the presence of preferred flow regimes. In the T21QG model EOF1 is strongly related to the North Atlantic Oscillation (NAO) and EOF2 may represent the Pacific North American pattern (PNA). The NAO is important for the regional climate in Western Europe. A stronger NAO results in fewer easterlies and more westerlies which cause milder winters in Western Europe (Hurrell, 1995). We will examine the effect of forcing parameter perturbations on the preferred flow regimes. An important question is formulated as follows: do parameter changes have influence on the NAO and therefore on the climate in Western Europe? Analysis of the EOFs can give us information on the statistics of the changed climate. In Figure 3.2 EOF1 - EOF4 of the T21QG model are shown.

In the Lorenz 63 model the degree of asymmetry of the model was used as a parameter to measure the change in the behaviour of the attractor (Moolenaar and Selten,

2004). At each time step, the state of the attractor was projected onto the vector connecting the two equilibria. This vector corresponds to EOF1 of the Lorenz 63 model. The two equilibria indicate regimes. They were visited at irregular time intervals. Such dynamics has the meteorological interpretation of regime behaviour. From these projection values a PDF for the coefficients was calculated over a large time interval. Since there are only two regimes in the Lorenz 63 model, the PDF is a bimodal function, where both modes occur with equal probability for unperturbed parameters. When perturbing the parameters, one mode can grow at the expense of the other mode, indicating asymmetry in the model and in the PDF. In the T21QG model regime behaviour is found that can be related to the real atmosphere as mentioned above. The PDFs of the first a_i 's will reflect these preferences. In order to study the sensitivity to changes in the forcing parameters S_k of (3.1) we have to identify a measure for the change in the behaviour of the T21QG model. We will use the amplitudes a_i of the projections of the streamfunction onto the EOFs. Only the level 500 hPa will be analysed. For a long term integration for each day a_1 , the amplitude of the projection onto EOF1 at level 500 hPa, is calculated and then binned, thus creating the PDF1 of a_1 . Each PDF_i is divided into 100 bins, each bin has the length 0.002 and $\sum_{j=1}^{nbin} PDF_i(j) = 1$. It describes the intensity of the anomaly in the direction of EOF1. The same is done for a_2 to a_6 . In Figure 3.3 the PDFs of a_1 to a_6 for an unperturbed climate integration of 100000 days are shown.

The time mean of these PDFs is equal to 0:

$$\begin{aligned} [(\psi(t) - \overline{\psi(t)}), \mathbf{e}_i] &= a_i(t) \Rightarrow \\ \overline{[(\psi(t) - \overline{\psi(t)}), \mathbf{e}_i]} &= \overline{a_i(t)} \Rightarrow \\ [(\overline{\psi(t)} - \overline{\psi(t)}), \mathbf{e}_i] &= \overline{a_i(t)} \Rightarrow \\ [0, \mathbf{e}_i] &= \overline{a_i(t)} \Rightarrow \\ \overline{a_i(t)} &= 0, \end{aligned}$$

where $[\cdot, \cdot]$ is the Euclidian inproduct:

$$[x, y] = \sum x_i y_i, \quad (3.6)$$

and the overbar indicates the time mean. Such PDFs can also be made for a climate integration with perturbed forcing parameters. Systematic changes in time of the EOF amplitudes indicate climatic change (North et al. 1982, Selten, 1997). It produces a shift in the PDF.

We introduce parameters β_i , ($i = 1, 2, 3, 4, 5, 6$) to indicate the measure of change in the simulated climate:

$$\beta_i = \sum_{j=1}^{nbin} (PDF_i(j) - \widetilde{PDF_i(j)})^2, \quad (3.7)$$

where $\widetilde{PDF_i(j)}$ is the probability density of a_i in bin j for the perturbed integration and $PDF_i(j)$ is the probability density of a_i in bin j for the integration with standard parameters. Changes in the PDFs of the a_i 's indicate changes in the strength of

the preferred patterns of the streamfunction. These changes are influential for the regional climate. It is of interest to find the largest changes possible. This is indicated by those PDFs, made with perturbed parameters, that differ the most from the standard PDFs. The parameters β_i will indicate the measure of change of these PDFs. Larger β_i 's mean larger change in the climate. These β_i 's are one way of measuring climatic change. Different changes may result in a same β_i value. A PDF can just shift in its horizontal range, or change shape; become wider or smaller or change in skewness. Not all climate changes are reflected in these β_i 's, because different types of time series may have identical PDFs.

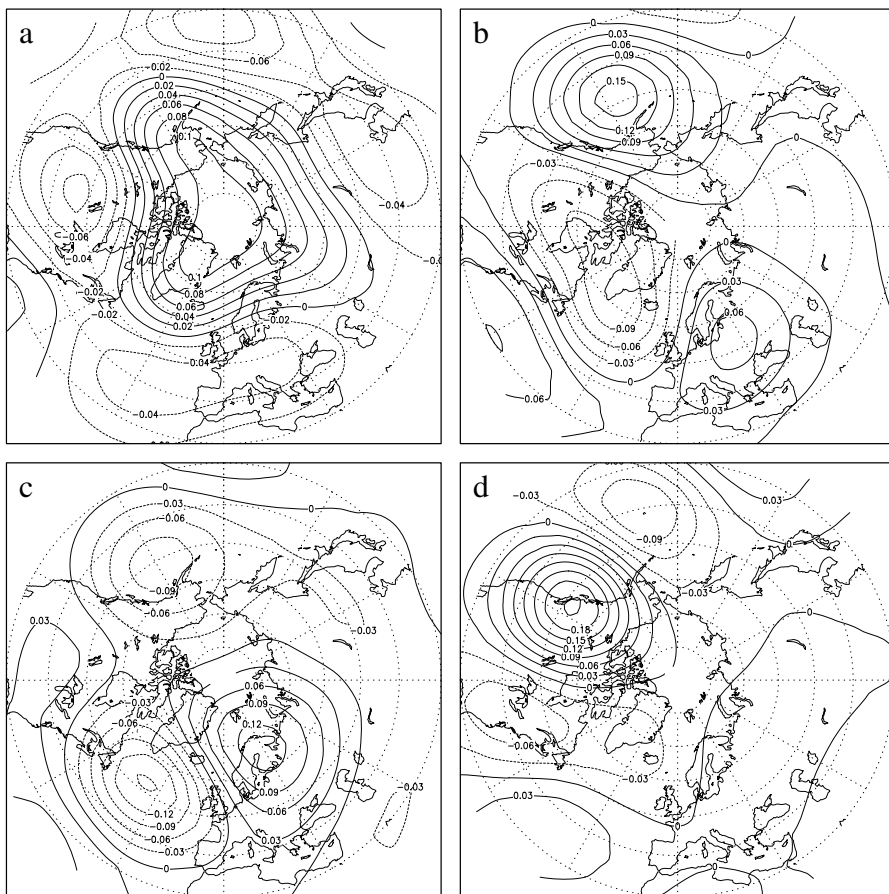


Figure 3.2: EOF 1 (a), EOF 2 (b), EOF3 (c) and EOF 4 (d) of the T21QG model, of 500 hPa streamfunction (normalized units).

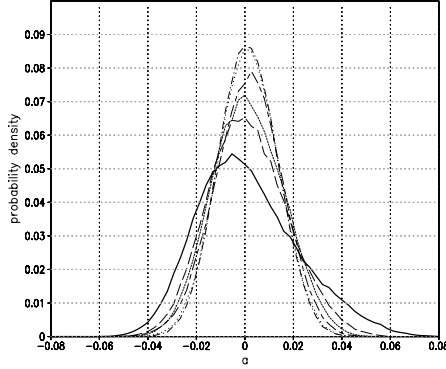


Figure 3.3: PDF's of the amplitudes a_1 (solid), a_2 (long dash), a_3 (short dash), a_4 (long short dash), a_5 , (dots) and a_6 (dot dash). It is noted that for all PDFs the time mean equals zero, see (3.6).

3.3 Searching effective forcing parameter perturbations using the adjoint equations

The T21QG model is written in terms of the potential vorticity q_k at each of the three levels k (equation (3.1)). The forcing terms S_k are determined (following Roads, 1987) by computing the potential vorticity tendencies, using a large number of observed atmospheric fields and by averaging these tendencies. These average tendencies should be equal to zero; the forcing term S is chosen such that it compensates the deviation from zero. This is equivalent to assuming that the sample of fields used in such a computation represents a statistically stable climatology. Averaging the potential vorticity tendencies gives:

$$\overline{\frac{dq_k}{dt}} = -\overline{J(\psi_k, q_k)} - \overline{D_k(\psi_k)} + \overline{S_k} \quad (3.8)$$

$$\frac{d}{dt}(\overline{q_k}) = -\overline{J(\psi_k + \psi'_k, \overline{q_k} + q'_k)} - D_k(\overline{\psi_k} + \psi'_k) + \overline{S_k} \quad (3.9)$$

$$\begin{aligned} &= -\overline{J(\psi_k, \overline{q_k})} - \overline{J(\psi_k, q'_k)} - \overline{J(\psi'_k, \overline{q_k})} - \overline{J(\psi'_k, q'_k)} - D_k(\overline{\psi_k}) + \overline{S_k} \\ 0 = \overline{\dot{q}_k} &= -\overline{J(\psi_k, \overline{q_k})} - D_k(\overline{\psi_k}) - \overline{J(\psi'_k, q'_k)} + S_k, \end{aligned} \quad (3.10)$$

where overbar denotes averaged values and apostrophe denotes the deviation from the averaged value. For the forcing S_k we now have that this equals the opposite of the averaged tendencies, so:

$$S_k = \overline{J(\psi_k, \overline{q_k})} + D_k(\overline{\psi_k}) + \overline{J(\psi'_k, q'_k)}. \quad (3.11)$$

For these computations daily analysed streamfunction fields from the winter season are used obtained from the European Centre for Medium range Weather Forecasts

(ECMWF).

Two important questions are raised: do small changes in the forcing parameters affect the simulated climate and is there an efficient way of finding the most effective forcing parameter perturbations? As in a previous study (Moolenaar and Selten, 2004), we want to compare random perturbations with perturbations chosen with the use of the first singular vector, as mentioned in the introduction. One difference is that instead of taking all model parameters into account, we now only allow an uncertainty in the forcing parameters. We will use the algorithm to calculate forcing singular vectors as devised by Barkmeijer et al, (2003). They compared forcing singular vectors with initial condition singular vectors in 2-day forecasts.

3.3.1 The tangent linear and the adjoint equations

To calculate the forcing singular vectors, the tangent linear and the corresponding adjoint model need to be extended with the equations with respect to the forcing parameters, which are elements of the parameter vector \mathbf{S} .

As mentioned in Section 3.2.1 it is assumed that the multi-level field of PV is a linear function of the multi-level streamfunction, which is invertible under appropriate boundary conditions. A time derivative of the streamfunction can be derived by applying the linear operator on both sides of equation (3.1). We obtain a system of the form

$$\dot{\psi} = \mathbf{F}_1(\psi, \mathcal{S}), \quad (3.12)$$

whereby \mathcal{S} is the forcing in terms of streamfunction. This streamfunction vector ψ is next extended with the vector \mathcal{S} in the forcing parameter space, resulting in vector \mathbf{y} :

$$\mathbf{y} = \begin{pmatrix} \psi \\ \mathcal{S} \end{pmatrix}. \quad (3.13)$$

The tendency equations then become:

$$\dot{\mathbf{y}} = \begin{pmatrix} \dot{\psi} \\ \dot{\mathcal{S}} \end{pmatrix} = \begin{pmatrix} \mathbf{F}_1(\psi, \mathcal{S}) \\ \mathbf{F}_2(\mathcal{S}) \end{pmatrix} = \begin{pmatrix} \mathbf{F}_1(\psi, \mathcal{S}) \\ \mathbf{0} \end{pmatrix} = \mathbf{F}(\mathbf{y}). \quad (3.14)$$

The tangent linear equations are derived by linearizing the tendency equations (3.14) around a non-linear reference orbit \mathbf{y}_r :

$$\begin{aligned} \dot{\mathbf{y}} = \mathbf{F}(\mathbf{y}) &\Rightarrow (\mathbf{y}_r + \delta\mathbf{y}_r) = \mathbf{F}(\mathbf{y}_r + \delta\mathbf{y}_r) \approx \mathbf{F}(\mathbf{y}_r) + J_b\delta\mathbf{y}_r + \mathcal{O}(|\delta\mathbf{y}_r|^2) \\ &\Rightarrow \dot{\mathbf{y}}_r + \delta\dot{\mathbf{y}}_r \approx \mathbf{F}(\mathbf{y}_r) + J_b\delta\mathbf{y}_r \\ &\Rightarrow \delta\dot{\mathbf{y}}_r \approx J_b\delta\mathbf{y}_r, \end{aligned} \quad (3.15)$$

where J_b is the Jacobi matrix:

$$\begin{aligned} J_b = \frac{\partial \mathbf{F}(\mathbf{y})}{\partial \mathbf{y}} \Big|_{\mathbf{y}_r} &= \begin{pmatrix} \frac{\partial \mathbf{F}_1(\psi, \mathcal{S})}{\partial \psi} & \frac{\partial \mathbf{F}_1(\psi, \mathcal{S})}{\partial \mathcal{S}} \\ \frac{\partial \mathbf{F}_2(\mathcal{S})}{\partial \psi} & \frac{\partial \mathbf{F}_2(\mathcal{S})}{\partial \mathcal{S}} \end{pmatrix} \Big|_{\mathbf{y}_r} = \begin{pmatrix} \frac{\partial \mathbf{F}_1(\mathbf{r}, \mathcal{S})}{\partial \mathbf{r}} & \frac{\partial \mathbf{F}_1(\mathbf{r}, \mathcal{S})}{\partial \mathcal{S}} \\ \mathbf{0} & \mathbf{0} \end{pmatrix} \Big|_{\mathbf{y}_r} \\ &= \begin{pmatrix} J_a & \mathbf{I} \\ \mathbf{0} & \mathbf{0} \end{pmatrix} \Big|_{\mathbf{y}_r}, \end{aligned} \quad (3.16)$$

where \mathbf{I} is the identity matrix since the parameter vector only contains the forcing terms, \mathbf{O} is the zero matrix and J_a is the Jacobian matrix that is obtained by linearizing equation (3.12) along a reference solution when only the streamfunction is a variable, rather than both the streamfunction and the forcing parameters.

The tangent linear equations integrate a small perturbation ($\delta\mathbf{y}_r(0)$) forward in time over a sufficiently short period. This can be formulated with the propagation matrix R :

$$\delta\mathbf{y}_r(T) = R(0, T) \cdot \delta\mathbf{y}_r(0). \quad (3.17)$$

The perturbation is set fixed at initial time, $\langle \delta\mathbf{y}_r(0), \delta\mathbf{y}_r(0) \rangle = 1$, where \langle, \rangle is the Kinetic Energy inner product, applied at each level separately and added together

$$\langle x, y \rangle = \int \int \nabla x \nabla y d\Sigma, \quad (3.18)$$

which is related to the Euclidian inner product by

$$\langle \delta\mathbf{y}_r(0), \delta\mathbf{y}_r(0) \rangle = [\mathbf{T}\mathbf{y}_r(0), \mathbf{y}_r(0)], \quad (3.19)$$

with T a diagonal matrix. Since only perturbations in the forcing parameters are considered and not perturbations in the initial conditions, this can be rewritten as:

$$\delta\mathbf{y}_r(0) = \begin{pmatrix} \delta\psi(0) \\ \delta\mathcal{S}(0) \end{pmatrix} = \begin{pmatrix} 0 \\ \delta\mathcal{S}(0) \end{pmatrix} \Rightarrow \langle \delta\mathcal{S}(0), \delta\mathcal{S}(0) \rangle = 1. \quad (3.20)$$

This can be formally written with the use of a projection matrix P_2 , which projects vector \mathbf{y} onto (forcing) parameter space:

$$P_2\mathbf{y} = P_2 \begin{pmatrix} \psi \\ \mathcal{S} \end{pmatrix} = \begin{pmatrix} \mathbf{0} \\ \mathcal{S} \end{pmatrix}. \quad (3.21)$$

The solution of the tangent linear equations at end time (T) yields the approximate deviation from the reference orbit, $\delta\mathbf{y}_r(T)$. Because $\delta\mathcal{S}$ remains constant in time, we have:

$$\delta\mathbf{y}_r(T) = \begin{pmatrix} \delta\psi(T) \\ \delta\mathcal{S}(T) \end{pmatrix} = \begin{pmatrix} \delta\psi(T) \\ \delta\mathcal{S}(0) \end{pmatrix}, \quad (3.22)$$

and we only have to look at the evolution of $\delta\psi$. This can be formally written with the use of a projection matrix P_1 , which projects vector \mathbf{y} onto state space:

$$P_1\mathbf{y} = P_1 \begin{pmatrix} \psi \\ \mathcal{S} \end{pmatrix} = \begin{pmatrix} \psi \\ \mathbf{0} \end{pmatrix}. \quad (3.23)$$

Combining these matrices, a forward integration of the tangent linear equations can be rewritten as:

$$\begin{pmatrix} \delta\psi(T) \\ \mathbf{0} \end{pmatrix} = P_1\delta\mathbf{y}_r(T) = P_1R\delta\mathbf{y}_r(0) = P_1RP_2 \begin{pmatrix} \mathbf{0} \\ \delta\mathcal{S}(0) \end{pmatrix} \equiv M \begin{pmatrix} \mathbf{0} \\ \delta\mathcal{S}(0) \end{pmatrix}. \quad (3.24)$$

In summary, using the tangent linear equations, a unit hypersphere in parameter space, centred at the initial state of the reference orbit, evolves into the deviation of the reference orbit in state space. In Figure 3.4 a schematic picture is drawn of this error growth. The sphere on the left represents the unit hypersphere in parameter space at initial time ($t = 0$), centred at the standard parameter values. The hypersphere evolves into the ellipsoid at the right, which lies in the state space. The dashed line is the reference orbit, calculated with non-linear equations, that starts at the centre of the hypersphere and evolves to the centre of the ellipsoid at end time ($t = T$). The first major axis of the ellipsoid shows the largest deviation from the reference orbit and equals the first singular vector. The solid line represents an orbit calculated with the tangent linear equations. It starts at the first right singular vector and evolves into the first left singular vector. So this first right singular vector in parameter space is the parameter perturbation that will yield the largest error growth in state space.

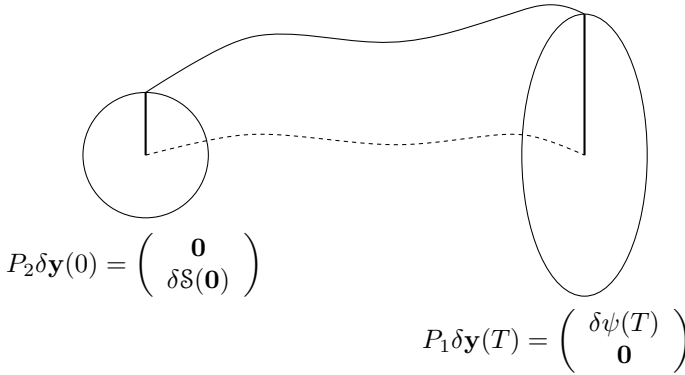


Figure 3.4: Schematic picture of the evolution of the first right singular vector (in parameter space) into the first left singular vector (in state space).

We want to find the parameter perturbation $\delta\mathcal{S}$ that causes the largest error growth at end time. This is the vector $\delta\mathcal{S}$ that maximizes the ratio

$$\frac{[\delta\psi(T), T\delta\psi(T)]^{1/2}}{[\delta\mathcal{S}(0), T\delta\mathcal{S}(0)]^{1/2}} = \frac{[M\delta\mathcal{S}(0), TM\delta\mathcal{S}(0)]^{1/2}}{[\delta\mathcal{S}(0), T\delta\mathcal{S}(0)]^{1/2}} = \frac{[M^*TM\delta\mathcal{S}(0), \delta\mathcal{S}(0)]^{1/2}}{[\delta\mathcal{S}(0), T\delta\mathcal{S}(0)]^{1/2}}, \quad (3.25)$$

where matrix T is here to denote the kinetic energy innerproduct, M^* is the adjoint of M and is found as a solution of the following generalized eigenvalue problem

$$M^*TM\delta\mathcal{S} = \lambda T\delta\mathcal{S}. \quad (3.26)$$

with largest eigenvalue λ and is called the first singular vector. Using $v = T^{1/2}\delta\mathcal{S}$ this can be rewritten into the following symmetric eigenvalue problem:

$$T^{-1/2}M^*TMT^{-1/2}\mathbf{v} = \lambda\mathbf{v} \quad (3.27)$$

which is solved using the Lanczos algorithm (Parlett, 1980). The operators M and M^* are not explicitly known but are evaluated using forward and backward integrations with the tangent linear and adjoint equations as described by Barkmeijer et al. (2003), (equations 13-16).

3.3.2 The perturbed model

To denote the uncertainty in the forcing in streamfunction \mathcal{S} we add the forcing term f and obtain

$$\mathcal{S}_k + f_k, \quad k = 1, 2, 3 \quad (3.28)$$

as a new forcing at each level k . Using f without subscript to denote the forcing perturbation at all three levels simultaneously $f = \delta\mathcal{S}$; it is the perturbation of \mathcal{S} and the length of f will be 5% of the length of \mathcal{S} .

When using first singular vectors as the forcing perturbation f , the vector will be scaled as follows:

$$\langle f, f \rangle^{1/2} = 0.05 \langle \mathcal{S}, \mathcal{S} \rangle^{1/2}. \quad (3.29)$$

To be more precise:

$$f_k = 0.05 \frac{\langle \mathcal{S}, \mathcal{S} \rangle^{1/2}}{\langle \tilde{f}, \tilde{f} \rangle^{1/2}} \tilde{f}_k, \quad (3.30)$$

where \tilde{f} is the singular vector (before scaling). The scaling is the same on each of the three levels, preserving the structure of the singular vector. However, when using random perturbations, f will be scaled on each level k separately:

$$\langle f_k, f_k \rangle^{1/2} = 0.05 \langle \mathcal{S}_k, \mathcal{S}_k \rangle^{1/2}, \quad k = 1, 2, 3. \quad (3.31)$$

This can be interpreted as using certain weights in the norm. Moreover, equation (3.29) still holds. With these weights, we assume the same level of uncertainty in the forcing at each level.

The search for the perturbation vector f that results in the largest climate change is carried out in the same way as in Moolenaar and Selten (2004) for the Lorenz 63 model: with the use of an adjoint method forcing parameter perturbations that are likely to be effective are selected. The scheme is as follows:

- calculate a short reference orbit
- calculate, with the use of the tangent linear and adjoint equations the corresponding first singular vector, along with the first singular value
- shift the reference orbit a timestep (one day) forward, calculating the corresponding first singular vector and the first singular value again
- look at the evolution of the singular value and select the singular values that occur *after* the trajectory has gone through a sensitive area, that is *after* the first singular value has grown to a large value and use the corresponding first singular vector as forcing parameter perturbation

The short term integrations that we use to calculate the first singular vector and the corresponding first singular value, are 5 days long. This is long enough for the perturbation to grow sufficiently, and short enough for the linearity to be sufficiently accurate. When a reference orbit and its corresponding first singular vector and value are calculated, the next reference orbit is calculated starting at the second day of the previous orbit, so the integration interval is shifted one day forward.

When the singular vectors have been calculated, these can be added as a forcing onto the climatological forcing \mathcal{S} . Both the climatological forcing and the added forcing are scaled with the kinetic energy norm, this norm is constructed by adding the norms of each of the three levels.

3.3.3 Simulation results

The first singular value fluctuates considerably, as can be seen in Figure 3.5. Peaks mark the passage of a time interval in which the system is sensitive to parameter perturbations. For a peak, we require that the first singular value exceeds the value of 500000. In Moolenaar and Selten (2004) we found that the singular vector that has just passed through a sensitive area, is likely to be an effective parameter perturbation. So, we want to draw the singular value at the moment it has a first local minimal value after the peak.

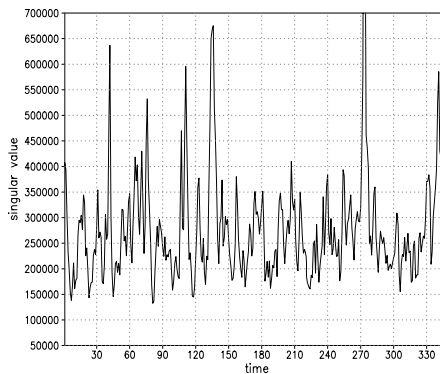


Figure 3.5: *Evolution of the first singular value for 5 day long reference runs.*

100000 day long integrations are made with 1000 specifically chosen first singular vectors as perturbations on the forcing parameters (as described in a previous section). For each of these perturbed integrations the PDFs of a_1 to a_6 (PDF1 to PDF6) are calculated along with β_1 to β_6 . A PDF of this β_1 is then calculated. Since the simulations with the largest $\beta_{total} = \beta_1 + \beta_2 + \beta_3 + \beta_4 + \beta_5 + \beta_6$, were also the ones with the largest β_1 , we only take a look at the PDF of β_1 . Apparently the shift in the projection onto EOF1 is usually the largest one. In Figure 3.6 the PDF of β_1 is shown (solid

line). It falls very rapidly, but there is a long tail consisting of 25 integrations with $\beta_1 > 0.02$. So searching effective forcing parameter perturbations with the adjoint method does lead to success, admitted that this is only the case for part of the selected singular vectors. The largest value found for β_1 is 0.05. PDF1 to PDF6 of a_1 to a_6 resp. (the amplitudes of the projections on the EOF1 to EOF6 resp.) of the simulation made with the singular vector as parameter perturbation that gave the largest β_1 are shown in Figure 3.7. Unfortunately, when comparing plots of different singular vectors, the 25 singular vectors that resulted in a $\beta_1 > 0.02$, they did not show any specifics in common that could distinguish them from the other, less effective, singular vectors.

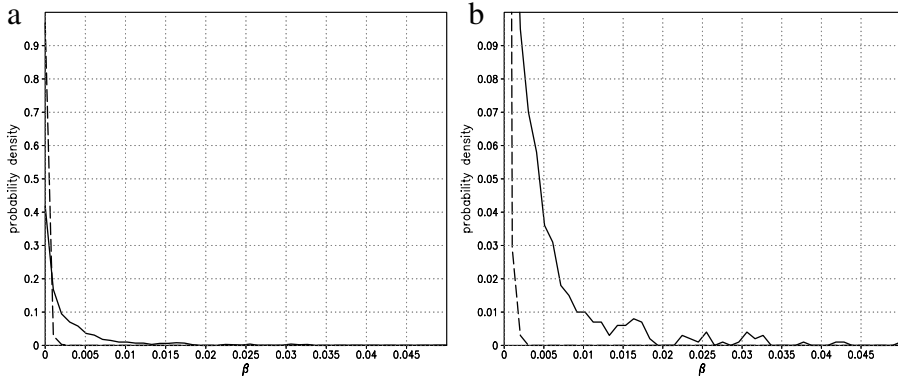


Figure 3.6: PDF of β_1 for the adjoint method (solid line) and the random method (dashed line). a) total PDF b) zoom in of PDF. The random method is explained in Section 3.4.1.

3.4 Comparison with other search methods

Other methods, such as simulated annealing (Kirkpatrick et al, 1983), fail to give an answer within a reasonable computing time due to the long integration time of one run in combination with the large number of parameters that are varied. In order to find the optimal solution, a perturbed run needs to be made for each parameter. When the number of parameters exceeds the number of runs that are feasible, this method becomes too computationally expensive.

In order to see if the adjoint method draws effective forcing parameter perturbations, we need to compare our chosen parameters with the best of randomly chosen perturbed forcing parameters. We want to do this as 'random' as possible and also with as less information about the pattern of the forcing vector as possible. Furthermore, we will select in the evolution, the singular value at the peak itself instead of the value at the bottom after the peak, see Section 5.3.3. We will find out whether this yields comparable results. Finally, we add forcing perturbations in the direction of EOF1 to

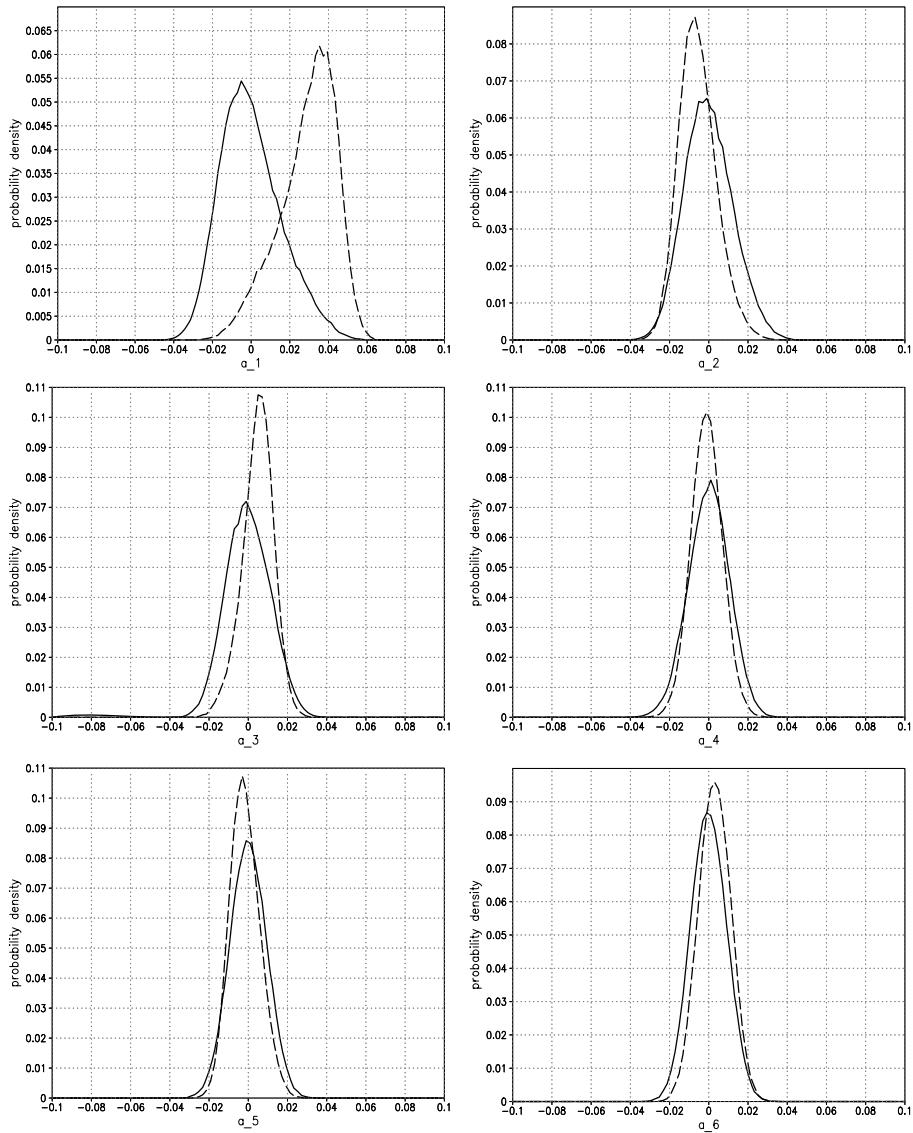


Figure 3.7: Standard (solid line) and perturbed (dashed line) PDF1-PDF6. $\beta_1 = 5.0 \cdot 10^{-2}$, $\beta_2 = 8.9 \cdot 10^{-3}$, $\beta_3 = 1.7 \cdot 10^{-2}$, $\beta_4 = 4.2 \cdot 10^{-3}$, $\beta_5 = 4.3 \cdot 10^{-3}$ and $\beta_6 = 4.6 \cdot 10^{-3}$. This perturbation gave the largest shift in PDF1 (and therefore the largest β_1).

evaluate if this causes an increase in the strength of the circulation pattern corresponding to EOF1.

3.4.1 Random selection of perturbations

For each level, we draw a random vector from a uniform hypersphere in parameter space, which will then be scaled to 5% of the climatological forcing, as described in Section 3.3.2. The scaling will be weighed, by requiring that f_k is 5% of \mathcal{S}_k at each level. In this way we assume equal uncertainty in streamfunction forcing \mathcal{S} at each level.

Again 100000 day long integrations are made, but this time with randomly chosen parameter perturbations. The PDF of β_1 for these integrations is shown in Figure 3.6 (dashed line). The largest β_1 found with this random method, equals 0.0025. This is 20 times smaller than the largest β_1 found with the adjoint method. From the vector perturbations found with the adjoint method, 35.7% yielded a larger β_1 than this largest β_1 found with a random parameter vector perturbation. PDF1 to PDF6 of a_1 to a_6 resp. of the simulation made with the random vector as parameter perturbation that gave the largest β_1 are shown in Figure 3.8.

3.4.2 Alternative selection of singular vectors as perturbations

From the experiments carried out with the Lorenz 63 model (Moolenaar and Selten, 2004), it was concluded that the first singular vectors that correspond to a first singular value that occurs just after a high peak, are likely to be effective parameter perturbations, and are more likely to be effective than the first singular vectors corresponding to the first singular values in the high peaks. To verify this in the T21QG model, 1000 long integrations were made with the first singular vectors with singular values in the peaks (values larger than 500000). Again, the PDF of β_1 was calculated and can be seen in Figure 3.9. This PDF (dotted line) is quite similar to the previous one made with the adjoint method (solid line). However, the largest value for β_1 found here is some degree smaller, namely 0.037. In this experiment only 8 β_1 's larger than 0.02 are found as opposed to 25 in the previous case. So this tells us that singular vectors corresponding to singular values in a high peak are slightly less likely to be effective than singular vectors corresponding to singular values just after a high peak.

3.4.3 Perturbation in the direction of EOF1

As a last experiment, we add a forcing perturbation in the direction of EOF1. This will have an effect on EOF1, but is this the forcing perturbation with the most effect on EOF1? To answer this question, a 100000 day integration was made with EOF1 as forcing parameter perturbation. It was scaled on each level individually with 5% of the climatological forcing. This gave us $\beta_1 = 0.018$, which is not the largest β_1 we found by far. When scaling the perturbation with 10%, β_1 had the value of 0.05, which equals the largest β_1 found with the specific first singular vectors as forcing parameter

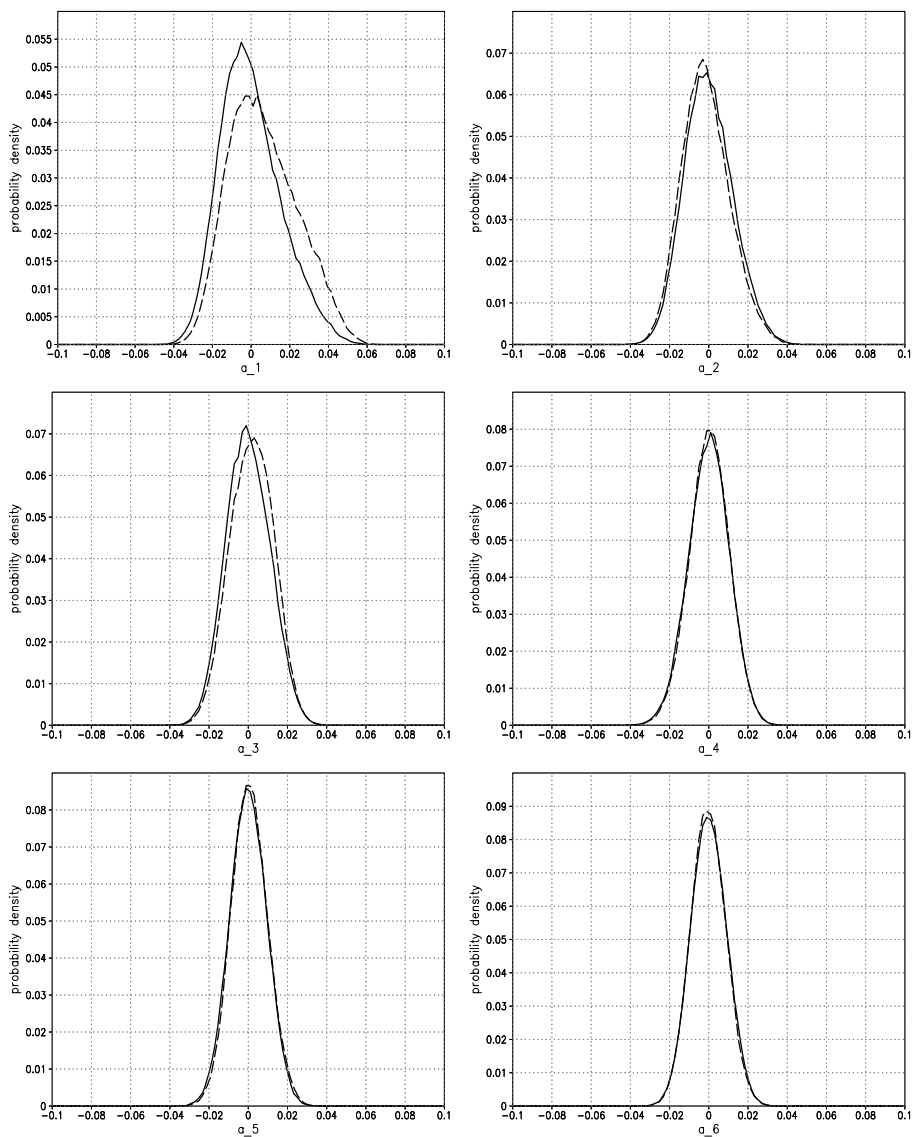


Figure 3.8: Standard (solid line) and perturbed (dashed line) PDF1-PDF6. $\beta_1 = 2.5 \cdot 10^{-3}$, $\beta_2 = 4.4 \cdot 10^{-4}$, $\beta_3 = 1.1 \cdot 10^{-3}$, $\beta_4 = 7.1 \cdot 10^{-5}$, $\beta_5 = 1.1 \cdot 10^{-4}$ and $\beta_6 = 6.8 \cdot 10^{-5}$. This perturbation gave the largest shift in PDF1 with the random draws.

perturbation, but then with 5% scaling. So we can conclude that a forcing in the direction of EOF1 will not result in the largest change in EOF1. Our method is capable of finding a forcing perturbation that is more effective. In Figure 3.10 PDF1 to PDF6 of a_1 to a_6 of the simulation made with EOF1 as forcing parameter perturbation are shown. The solid lines are the standard (unperturbed) PDFs, the dashed lines are the PDFs perturbed with EOF1 scaled with 5%, and the dotted lines are the PDFs perturbed with EOF1 scaled with 10%. Note the change in skewness which was also apparent for the most effective parameter perturbation (Figure 3.7).

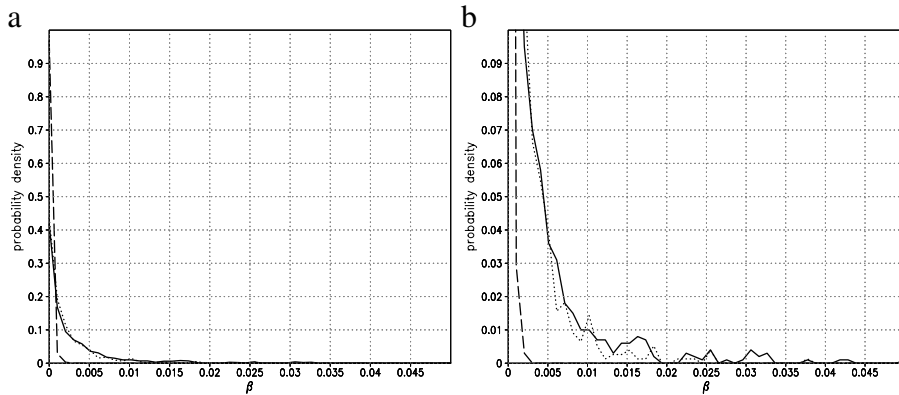


Figure 3.9: PDF of β_1 for the *sv1* after a peak (solid line), the random perturbations (dashed line) and for the *sv1* in a peak (dotted line) a. a) total PDF b) zoom in of PDF.

3.5 Conclusions

This study is a continuation of Moolenaar and Selten (2004), where a method for finding effective parameter perturbations in atmospheric models was tested in the simple Lorenz 63 model. The goal of this method is to find those perturbations that cause the largest change in the climate statistics. Therefore, such a model has to be integrated over a large time interval. Optimization methods, that require an extremely long computer time to evaluate the effect of a new set of parameter values, cannot produce the solution that results in the maximum climate change within a reasonable computing time. In the above study, a method was presented that uses short time integrations of the adjoint equations and selects perturbations that have a good chance to be effective in changing the climate. To judge the result a comparison with a random selection method was made.

In this study we applied, as a next step, the same method to a more realistic atmospheric model, the T21QG model. The parameter vector that is perturbed by a small vector of given size, consists of the forcing parameters and has a dimension 1449. It is clear that we may not expect that a random method produces acceptable results in such a case. The parameter space is large and the combinations of perturbing these parameters are numerous.

Using the adjoint equations 1000 singular vectors were selected from a large number of consecutive short runs and it was checked if a parameter perturbation, having the same direction, turned out to be effective in changing the climate. The selection was based on the first singular value. At the moment it had dropped after a high peak, the first singular vector was selected. So we have chosen the points on the attractor where the trajectory has just passed a phase where it is highly sensitive to perturbations.

The T21QG model shows regime behaviour. These regimes can be identified by the first few EOFs. The change β_1 in the distribution of the amplitude of the first EOF over a large simulation run is used as a measure for the change of the climate. The largest β_1 found was 0.05 with the adjoint method and 0.0025 with a random selection of 1000 parameter perturbations. From the vectors found with the adjoint method 35.7% yielded a larger β_1 than this largest β_1 found with a random parameter vector perturbation.

As mentioned before, finding the most effective solution is for the present model not within reach even with a converging scheme at hand. We are dealing with a large variable space (consisting of a large parameter space and a large state space). Therefore, a large percentage of the parameter perturbations is expected to be ineffective. Although we are not as successful as Moolenaar and Selten (2004), where for the Lorenz 63 model most selected parameter perturbations were effective, we still found that 2.5% of the parameter perturbations here, selected with the adjoint method, gave a value above $\beta_1 = 0.02$, while for the random method none of the 1000 runs came above this value, see Figure 3.6. We can also phrase the result differently: the random method comes in 97% of the cases with an ineffective perturbation ($\beta_1 < 0.001$), while for the adjoint method the percentage is 43%.

It is important to verify how much change small parameter perturbations can cause in the simulated climate. To get an insight in how much effect such perturbations can have, it is important to identify the parameter perturbations that yield the largest climate change. We have shown that, although still hampered by the large size of the parameter space and the ensemble set, the adjoint method reveals a much larger possible magnitude of climate change, than a random method is capable of. We selected 1000 parameter perturbations with each method. With the adjoint method many parameter perturbation vectors were found that yield far more change in the simulated climate than the most effective randomly chosen vector.

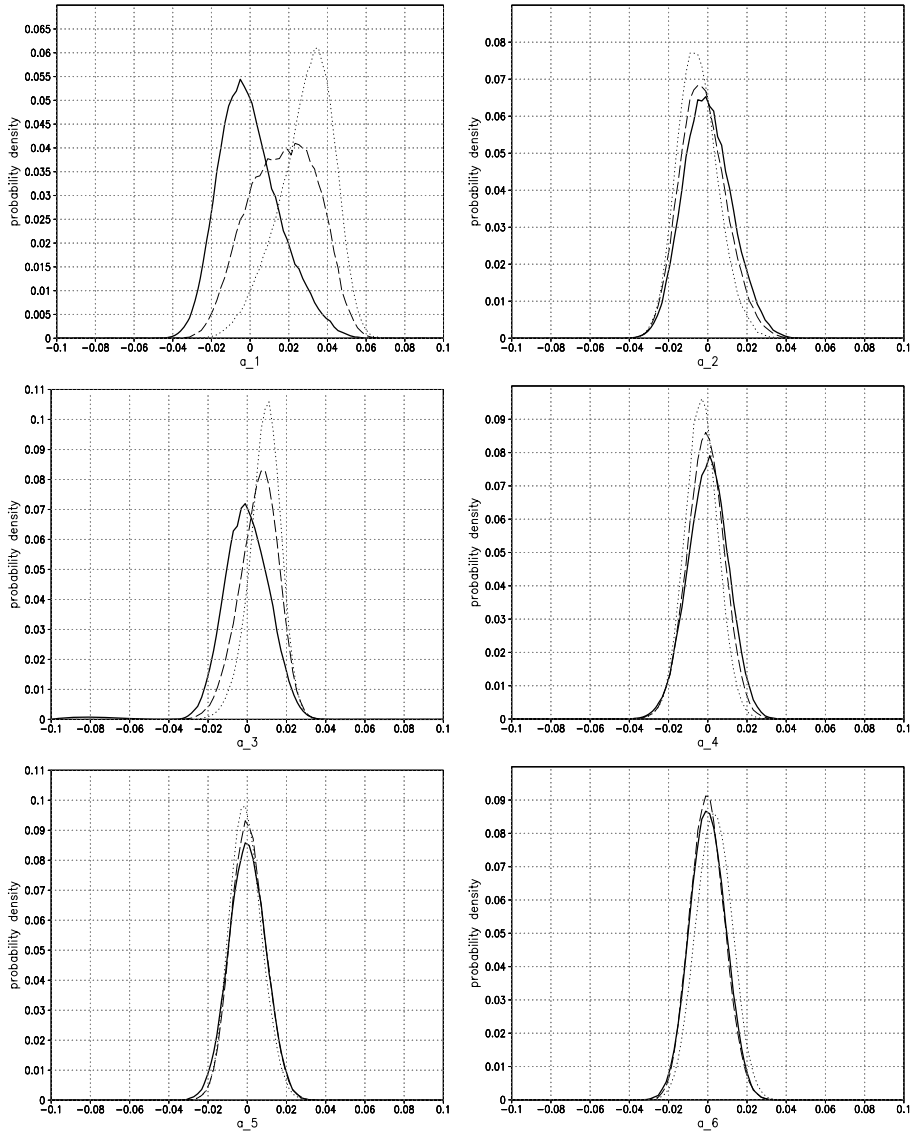


Figure 3.10: Standard PDF1-PDF6 (solid line) and perturbed with EOF1, scaled with 5% (dashed line) and with 10% (dotted line) PDF1-PDF6. For 5% scaling: $\beta_1 = 1.8 \cdot 10^{-2}$, $\beta_2 = 1.1 \cdot 10^{-3}$, $\beta_3 = 1.2 \cdot 10^{-2}$, $\beta_4 = 9.2 \cdot 10^{-4}$, $\beta_5 = 3.5 \cdot 10^{-4}$ and $\beta_6 = 1.6 \cdot 10^{-4}$. For 10% scaling: $\beta_1 = 5.0 \cdot 10^{-2}$, $\beta_2 = 5.5 \cdot 10^{-3}$, $\beta_3 = 3.2 \cdot 10^{-2}$, $\beta_4 = 6.3 \cdot 10^{-3}$, $\beta_5 = 1.4 \cdot 10^{-3}$ and $\beta_6 = 3.9 \cdot 10^{-3}$.

3.6 Acknowledgements

We would like to thank J. Barkmeijer for his help and for allowing us to use his code to calculate the forcing singular vectors. Also thanks to J. Greenaway for his help with running the model on the ECMWF computing facilities.

Appendix A: Spherical harmonics

The spherical harmonic $Y_{mn}(\lambda, \phi)$, $-n \leq m \leq n$, is a function of the two coordinates λ, ϕ on the surface of a sphere. ϕ is taken as the polar (colatitudinal) coordinate with $\phi \in [-\frac{1}{2}\pi, \frac{1}{2}\pi]$, and λ as the azimuthal (longitudinal) coordinate with $\lambda \in [0, 2\pi)$. The spherical harmonics are orthogonal for different m and n , and they are normalized so that their integrated square over the sphere is unity:

$$\int_0^{2\pi} d\lambda \int_{-1}^1 d(\sin \phi) Y_{m'n'}^*(\lambda, \phi) Y_{mn}(\lambda, \phi) = \delta_{n'n} \delta_{m'm}. \quad (3.32)$$

Here $*$ denotes the complex conjugate and δ_{mn} is the Kronecker delta. Spherical harmonics satisfy the spherical harmonic differential equation, which is given by the angular part of Laplace's equation in spherical coordinates. Mathematically, the spherical harmonics are related to associated Legendre polynomials (P_n^m) by the equation

$$Y_{mn}(\lambda, \phi) = \sqrt{\frac{2n+1}{4\pi} \frac{(n-m)!}{(n+m)!}} P_n^m(\sin \phi) e^{im\lambda}. \quad (3.33)$$

The spherical harmonics form a complete orthonormal basis, so an arbitrary real function $f(\lambda, \phi)$ can be expanded in terms of real or complex spherical harmonics.

Appendix B: Dissipative terms in the T21QG model

We describe here the dissipative terms in equations 3.3, closely following Marshall and Molteni, (1993). The dissipative terms $-D_1, -D_2, -D_3$ at the three pressure levels 200, 300 and 500 hPa respectively, take the form:

$$\begin{aligned} -D_1 &= TR_{12} - H_1 \\ -D_2 &= -TR_{12} + TR_{23} - H_2 \\ -D_3 &= -TR_{23} - EK_3 - H_3. \end{aligned} \quad (3.34)$$

The effect of temperature relaxation between levels 1 and 2 is represented by the term:

$$TR_{12} = \tau_R^{-1} R_1^{-2} (\psi_1 - \psi_2), \quad (3.35)$$

where τ_R is a radiative time scale of 25 days. The corresponding term for temperature relaxation between levels 2 and 3 is given by:

$$TR_{23} = -\tau_R^{-1} R_2^{-2} (\psi_2 - \psi_3). \quad (3.36)$$

Ekman dissipation is expressed as the vorticity tendency due to a linear drag on the wind at 800 hPa:

$$EK_3 = (a \cos \phi)^{-1} \left(\frac{\partial}{\partial \lambda} [k(\lambda, \phi, h)v_3] - \frac{\partial}{\partial \phi} [k(\lambda, \phi, h)u_3 \cos \phi] \right), \quad (3.37)$$

where λ is longitude, ϕ latitude, h the orographic height, a the average earth radius, and

$$u_3 = -a^{-1} \frac{\partial \psi_3}{\partial \phi}, \quad v_3 = (a \cos \phi)^{-1} \frac{\partial \psi_3}{\partial \lambda}. \quad (3.38)$$

The term k is the drag coefficient and is dependent on the land-sea mask and on the orographic height:

$$k(\lambda, \phi, h) = \tau_E^{-1} [1 + \alpha_1 LS(\lambda, \phi) + \alpha_2 FH(h)], \quad (3.39)$$

where $\tau_E = 3$ days, $\alpha_1 = \alpha_2 = 0.5$, $LS(\lambda, \psi)$ is the fraction of land within a grid box, and

$$FH(h) = 1 - \exp -h/(1000m). \quad (3.40)$$

Finally,

$$H_i = c_H \nabla^8 q'_i, \quad (3.41)$$

where q'_i is the PV minus planetary vorticity and orographic component, and the coefficient

$$c_H = \tau_H^{-1} a^8 (21 \cdot 22)^{-4} \quad (3.42)$$

is such that spherical harmonics of total wavenumber 21 are damped with time scale $\tau_H = 2$ days.

References

- Allen, M.R., 2003. Possible or probable? *Nature*, **425**, p242.
- Barkmeijer, J., 1996. Constructing fast-growing perturbations for the nonlinear regime. *Journal of the Atmospheric Sciences*, **53**, 2838-2851.
- Barkmeijer, J., Iversen T. and Palmer, T.N., 2003. Forcing singular vectors and other sensitive model perturbations. *Quarterly Journal of the Royal Meteorological Society*, **129**, 2401-2424.
- D'Andrea, F. and Vautard, R. 2001. Extratropical low-frequency variability as a low-dimensional problem. I: A simplified model. *Quarterly Journal of the Meteorological Society*, **127**, 1357-1374.
- Dymnikov, V.P. and Gritsoun, A.S., 2001. Climate model attractors: chaos, quasi-regularity and sensitivity to small perturbations of external forcing. *Nonlinear Processes in Geophysics*, **8**, 201-209.
- Errico, R.M., 1997. What is an adjoint model? *Bulletin of the American Meteorological Society*, **78**, 2577-2591.
- Fleming, R.J., 1993. The dynamics of uncertainty: application to parameterization constants in climate models. *Climate Dynamics*, **8**, 135-150.
- Forest, C.E., Stone, P.H., Sokolov, A.P., Allen, M.R. and Webster, M.D., 2002. Quantifying uncertainties in climate system properties with the use of recent climate observations. *Science*, **295**, 113-117.
- Haines, K. and Hannachi, A., 1995. Weather regimes in the pacific from a GCM. *Journal of the Atmospheric Sciences*, **52**, 2444-2462.
- Hall, M.C.T., and Cacuci, D.G., 1983. Physical interpretation of the adjoint functions for sensitivity analysis of atmospheric models. *Journal of the Atmospheric Sciences*, **40**, 2537-2545.
- Haltiner, G.J. and Williams, R.T., 1980. Numerical prediction and dynamic meteorology. *Wiley, New York*
- Holton, J.R., 1992. An introduction to dynamic meteorology. *3d Edition. Academic Press*.
- Hurrell, J.W., 1995. Decadal trends in the North Atlantic Oscillation: Regional temperatures and precipitation. *Science*, **269**, 676-689.

- IPCC, 2001. Climate Change 2001: The Scientific Basis. Eds: Houghton, J.T., Y. Ding, D.J. Griggs, M. Noguer, P.J. van der Linden, X. Dai, K. Maskell, and C.A. Johnson. Contribution of Working Group I to the Third Assessment Report of the Intergovernmental Panel on Climate Change. *Cambridge University Press*.
- Kirkpatrick, C.D., Gerlatt Jr., Vecchi, M.P., 1983. Optimization by simulated annealing. *Science*, **220**, 671-680.
- Kraichnan, R.H., 1959. Classical fluctuation-relaxation theorem. *Physical Review*, textbf113, 1181-1182.
- Leith, C.E., 1975. Climate response and fluctuation dissipation. *Journal of the Atmospheric Sciences*, **32**, 2022-2026.
- Lorenz, E.N., 1956. Empirical orthogonal functions and statistical weather prediction. *Scientific Report No. 1, Department of Meteorology, MIT*, 49 pp.
- Lorenz, E.N., 1963. Deterministic nonperiodic flow. *Journal of the Atmospheric Sciences*, **20**, 130-141.
- Lorenz, E.N., 1965. A study of the predictability of a 28-variable atmospheric model. *Tellus* **17**, 321-333.
- Marshall, J. and Molteni, F., 1993. Towards a dynamical understanding of planetary-scale flow regimes. *Journal of the Atmospheric Sciences* **50**, 1792-1818.
- Molteni, F. and Palmer, T.N., 1993. Predictability and finite-time instability of the northern winter circulation. *Quarterly Journal of the Royal Meteorological Society*, **19**, 269-298.
- Moolenaar, H.E. and Selten, F.M., 2004. Finding the effective parameter perturbations in atmospheric models: the LORENZ63 model as case study. *Tellus* **56A**, 47-55.
- Murphy J.M., Sexton, D.M.H., Barnett, D.N., Jones, G.S., Webb, M.J., Collins, M. and Stainforth, D.A., 2004. Quantification of modelling uncertainties in a large ensemble of climate change simulations. *Nature*, **430**, 768-772.
- North, G.R., Bell, T.L., Cahalan, R.F., Moen, J.M., 1982. Sampling errors in the estimation of empirical orthogonal functions. *Monthly Weather Review* **110**, 699-706.
- Oortwijn, J., and Barkmeijer, J., 1995. Perturbations that optimally trigger weather regimes. *Journal of the Atmospheric Sciences*, **52**, 3932-3944.

Palmer, T.N., 1999. A nonlinear dynamical perspective on climate prediction. *Journal of Climate*, **12**, 575-591.

Parlett, B.N., 1980. The Symmetric Eigenvalue Problem. Series in computational mathematics. *Prentice-Hall*.

Preisendorfer, R.W., 1988. Principal component analysis in meteorology and oceanography. *Elsevier Science*.

Press, W.H., Flannery, B.P., Teukolsky, S.A., Vetterling, W.T., 1986. Numerical Recipes. *Cambridge University Press*.

Reilly, J. Stone, P.H., Forest, C.E., Webster, M.D., Jacoby, H.D., Prinn, R.G., 2001. Uncertainty and climate change assessment. *Science*, **293**, 430-433.

Reinhold B.B. and Pierrehumbert, R.T., 1982. Dynamics of weather regimes: quasi-stationary waves and blocking. *Monthly Weather Review*, **110**, 1105-1145.

Roads, J.O., 1987. Predictability in the extended range. *Journal of the Atmospheric Sciences*, **44**, 3495-3527.

Selten, F.M., 1997. Baroclinic empirical orthogonal functions as basis functions in an atmospheric model. *Journal of the Atmospheric Sciences*, **54**, 2099-2114.

Stainforth, D.A., Aina, T., Christensen, C., Collins, M., Faull, N., Frame, D.J., Kettleborough, J.A., Knight, S., Martin, A., Murphy, J.M., Piani, C., Sexton, D., Smith, L.A., Spicer, R.A., Thorpe, A.J., Allen, M.R., 2005. Uncertainty in predictions of the climate response to rising levels of greenhouse gases. *Nature*, **433**, 403-406.

Stocker, T.F., 2004. Models change their tunes. *Nature*, **430**, 737-738.

CHAPTER 4

Mathematical conservation ecology: supporting a herbivore metapopulation

A herbivore-predator metapopulation model is investigated. Different situations are described in a model with two patches. The predator may be absent, and if it is present only herbivores may migrate between the patches. For all variants we include the influence of the climate by letting either the intrinsic growth rates or the carrying capacities depend on climatic fluctuations. These climatic fluctuations at both patches can be chosen to be either correlated or uncorrelated. We investigate the risk of extinction for the herbivores by varying the migration rates and the death rates of the predators. The risk of extinction is measured in terms of the fifth percentiles of the subpopulations. This is the value below which the subpopulation is found 5 out of 100 times in a series of values taken at fixed time intervals. The different migration rates and the death rates of the predators are varied. With a given cost per unit of changing a parameter and a given fixed total effort, the optimal solution can be found. It is concluded that general rules for conservation management are hard to formulate. Unwanted side effects may occur; improvement for one species may result in a decrease of the population size of some other species, even to the point of extinction. This shows that e.g. biodiversity may be influenced in a way that is not easy to foresee.

4.1 Introduction

Modelling the dynamics of an ecological system starts with the definition of the state variables and parameters and with the choice whether or not to include spatial structure. In this study the simplest form of spatial distribution is considered: a metapopulation model consisting of two patches. Within a patch no spatial variation is present and the total biomass of a species within the patch is defined as a state variable. Our investigation differs from the mainstream of metapopulation studies (Hanski, 1999) in the sense

that not the number of occupied patches acts as state variable (Levins, 1969); we consider population sizes. In a patch occupancy model such as the Levins model a patch is either occupied or empty and the local dynamics are not specified. When allowing a detailed spatial structure and local population dynamics in a patch, the model becomes considerably more complex. Individual based models do specify the local dynamics, see e.g. DeAngelis and Gross, (1992). From each member of the population individually they simulate the behaviour, such as movements within their habitat, growth and development, as well as reproduction and death. They distinguish themselves from less detailed models in which characteristic quantities of the entire population are averaged and their changes in time are computed. Individual based models are very complex, highly sensitive to parameter perturbations and prone to error growth. Furthermore, large simulations are needed to be able to analyse the systems (Levin, 1992, Pascual and Levin, 1999). The local dynamics may affect the viability and extinction risk of a subpopulation. For instance, the migration rate may depend on the local dynamics. It can therefore be useful to consider local dynamics when using a metapopulation model for conservation management of endangered species (Harding and McNamara, 2002, Lopez and Pfister, 2001).

The model used in this study does not deal with a single species metapopulation as most studies, see e.g. Etienne (2002) and Holt et al. (2005), but describes predator-prey interaction (Kareiva, 1987; Taylor, 1990). Furthermore the influence of climate fluctuations upon the subpopulations is taken into account. With other studies we have in common that our assessment of survival of a local population based on a model study is followed by possible management strategies to conserve species that have a large risk to disappear in parts of their (fragmentized) habitat.

Understanding why a biological population may fluctuate is the main goal of many ecological studies. By defining an ecological system with state variables in one of the above ways and with parameters quantifying properties such as population growth and species interaction we can go deeper into the question. A possible answer that deserves to be examined right away is that a fluctuating input yields a fluctuating output. In other words, time dependent parameters give rise to time dependent state variables, e.g. chaos in means chaos out. In Hsieh et al. (2005) such ecological systems are said to track the input (climate). In a simple herbivore-predator system consisting of two state variables and with constant parameters, fluctuations may arise in the form of a periodic solution. Like any pendulum its future states can be approximated as good as one wishes provided that sufficient accurate information about the parameters and the present state is available. Fluctuation can also be formulated differently. We may think of deviations of the system evolution from a computed solution satisfying the deterministic model and its initial conditions with an arbitrary high accuracy. In more complex systems with constant parameters chaotic solutions may turn up. Then the actual state variables will deviate from such a computed solution and will fluctuate irregularly within some range. The numerical solution then still gives an idea of the dynamics. It will be a concatenation of intervals where parts of the chaotic attractor are followed for some unknown length of time in some unknown order. This is an example of fluctuations due to the nonlinear structure of the system (Grasman and Van Straten,

1994). If the model contains stochastic elements e.g. multiplicative noise, then we may have a tracking type of fluctuation in which the distribution of possible states at a time is more or less Gaussian with the state of the system without noise as mean. It can also be that such a path is left and that the system may tend to the basin of attraction of a different stationary state of the corresponding deterministic system. It may visit all or some of these basins in an irregular way. Essential is that different stationary solutions can exist. This also requires a system with a nonlinear structure.

Population fluctuations may not only be due to intrinsic processes and interactions, but may as well arise from environmental influences. One important aspect is the influence of climate upon the dynamics of a population. Recently, more attention has been given to the influence of large-scale climate variability upon ecological processes than just taking the local weather into account (Sæther, 1997, Mysterud et al., 2001, Stenseth et al., 2002). Of particular interest are the impacts of the North Atlantic Oscillation (NAO), e.g. Mysterud et al., 2001, Thompson and Grosbois, (2002), Arnott and Ruxton, (2002), Lusseau et al., (2004) and the El-Nino Southern Oscillation (ENSO), e.g. Pounds et al., (1999), Urban et al., (2000). These climatic patterns affect both terrestrial and marine vegetation and animal life. We mention some examples. Mysterud et al. (2001) compared wild red deer living at the west coast of Norway with domestic sheep, which stay indoors during winter and have a steady supply of energy. They found that the winter climate variability, for which the NAO is mainly responsible, influences the food supply in summer and therefore influences the body weight of the wild red deer. Lusseau et al. (2004) suggest that climate variations have an effect upon prey availability and therefore influence the population size of bottlenose dolphins in the Moray Firth UK and that of killer whales in Johnstone Strait, Canada. Pounds et al. (1999) state that the disappearance of toads and frogs in highland forests at Monteverde, Costa Rica is caused by an increase in the average altitude of dry-season mist. This increase is caused by atmospheric warming, which is related to changes in sea surface temperature (ENSO). Also, long term changes in the environment, such as climate change may affect ecological processes. To get a good idea of how large the impact of climate change can be, it is necessary to have a good understanding of the way ecosystems are influenced by the climate with its natural variability.

Interaction between biologists and climate researchers is needed to gain more insight in the response of ecosystems to climate variability and climate change (Stenseth et al., 2002). Uncertainties in our understanding of underlying mechanisms in both the climate system and in ecosystems, and the way they interact, limit the knowledge of today. Stenseth et al. (2002) highlight five important aspects when analysing the effects that climate variations can have on ecosystems. Firstly, delayed effects of climate are important in ecosystems. The year in which certain individuals are born may be of influence on for instance their size, which might have an effect upon their lifespan. Secondly, climate can have a different influence on sexes and age-classes, e.g. the development of a population is altered when a climatic process influences younger age classes more than older ones. Thirdly, due to climate change extreme events could become more frequent, which are often more relevant to ecosystems than fluctuations in the mean climate. A severe winter with a longer frost period for instance can lead to

68 Mathematical conservation ecology: supporting a herbivore metapopulation

damage and death in plants and animals. Fourth, climate variability might directly or indirectly affect a particular organism, although the underlying mechanisms and their consequences may be complex. Fifth, it is important to recognize that climate and ecosystems may interact in a nonlinear way. For instance, a warm winter might favour a certain population and cause growth, but the next warm winter might not have that same effect, because of density dependence.

In the current literature the option of having a theoretically formulated system with chaotic dynamics of itself is widely studied (Cushing et al., 2003). The construction of bifurcation diagrams plays an important role in this literature. They indicate the type of solutions that occur as a function of the parameters. Examples of real world chaotic processes are more scarce (Becks et al., 2005). Fluctuations due to random noise making the nonlinear system visit the attraction basins of different stationary solutions is a less studied topic. A related problem is that of extinction of a population. Then by random fluctuations a population with even a positive growth coefficient may still die out globally or locally (Grasman and HilleRisLambers, 1997).

To bring a population near extinction, deterministic as well as stochastic forces may be responsible (Burgman et al., 1993). We will consider the first case: from e.g. herbivore-predator interaction, cycles with a phase of a very low herbivore population size may occur, bringing the population in a critical state. A catastrophic external force then may wipe away the herbivore. This last event is not part of our model. Ginzburg et al. (1982) and Gilpin (1990) make a similar distinction between almost extinction and full extinction. We also allow climatic fluctuations leading to periods with low herbivore population sizes, but these fluctuations are not that large that this population may get extinct.

Estimating the survival probability of a species in its habitat is part of a population viability analysis (PVA) and of conservation management. PVA is a collection of methods in model studies, used to identify threats faced by species. It evaluates the risk of extinction or decline of a biological population and its chance to recover (Burgman et al., 1993, Akçakaya et al., 1999, Akçakaya, 2000a, 2000b, Akçakaya and Sjögren-Gulve, 2000). Uncertainty in parameters (due to inaccurate and insufficient data) hamper PVA and parameter ranges (lower and upper bounds) are used (Akçakaya 2000b, Akçakaya and Sjögren-Gulve, 2000). Parameter sensitivity analysis can also be used in quantifying uncertainties. It could be helpful to make a choice when gaining more data (through fieldwork). Then it is important to know a priori which parameters are most sensitive and should therefore be given priority. When sensitivities within a model are known, the model prediction has more value for policy makers in the field of conservation management. It may come within reach to improve conditions of a certain endangered population, for instance by enhancing migration. Sensitivity analysis on specified parameters is a way to find effective solutions to reduce the risk of extinction.

We study a herbivore-predator metapopulation model for two patches between which the two species may migrate. In our model we include the influence of climate fluctuations upon the herbivore population. For the climate we take a simple model of the atmospheric circulation, the Lorenz-84 equations (Lorenz, 1984). Any climate time

series could have been taken as well. The aim of this study is to analyse how changes in parameter values may affect the conditions for the herbivore population. We are particularly interested in improving the conditions, making the probability of survival higher for the herbivores.

Due to climate fluctuations or to the intrinsic cyclic dynamics of the herbivore-predator system the two herbivore subpopulations may for some time, separately or jointly, get at a low level. In such a period a herbivore subpopulation may get extinct from a catastrophic event. As mentioned before such a sudden extinction event is not part of our model. Instead of taking the minimum value of the herbivore as a measure of a low subpopulation level we take the fifth percentile. It is the value below which the subpopulation is found 5 out of 100 times in a series of values taken at fixed time intervals. The risk of extinction is more or less the product of the probabilities that the population is at a low level and that a catastrophe (e.g. an epidemic disease) takes place, see Akçakaya (1992) for a more detailed discussion of such an event. Consequently, the time interval, that the population is small, must have a certain width in order to give a catastrophic event a chance. The fifth percentile is a better choice than the minimum for that reason.

In the next section the predator-prey model we use is specified. In the following sections, different variants of the model are investigated. We consider the situation that at the two patches the predator is absent. The herbivore may move from one patch to the other. The climate fluctuations at the two patches are assumed to be uncorrelated. The type of coupling between the two herbivore populations is based on the carrying capacities and the actual size of the subpopulations. The fifth percentile, as defined before, is a measure for the risk of local extinction of the herbivore. It will be analysed whether or not the strength of the coupling is playing a role. In Section 4.4 the predator is present at both patches but cannot migrate between them. Measures to conserve the herbivore are evaluated. More specifically the death rate of the predator and the strength of coupling between the patches are varied. The situation that also the predator may migrate between the patches is studied in Section 4.5. In Section 4.6 the results are discussed and interpreted in terms of species conservation policies.

4.2 The herbivore-predator model

There are many studies on herbivore-predator models, we select the Rosenzweig- MacArthur model (1963):

$$\begin{aligned}\frac{dh}{dt} &= d\left(1 - \frac{h}{K}\right)h - \frac{hp}{h+c}, \\ \frac{dp}{dt} &= \frac{hp}{h+c} - bp,\end{aligned}\tag{4.1}$$

where h and p are, respectively, the amount of herbivore- and predator biomass. It is a commonly used system (Sherratt et al. (1997), Rai and Anand (2004), Huang and Diekmann (2001), Janssen (2001)). The parameters are the intrinsic growth rate

70 Mathematical conservation ecology: supporting a herbivore metapopulation

d , the carrying capacity K of the herbivore, the death rate b of the predator and c , the reciproke of the slope at the origin of the functional response. Both Huang and Diekmann (2001) and Janssen (2001) used this model in a two-patch variant where only predators were allowed to migrate. They gave both patches equal parameter values.

Assuming that we start with strictly positive values for p and h , we may arrive at three types of limit solutions for $t \rightarrow \infty$:

- (a) a stable boundary equilibrium $(h, p) = (K, 0)$ meaning that the predator gets extinct
- (b) a stable internal equilibrium $(h, p) = (bc/(1 - b), cd(1 - b - bc/K)/(b - 1)^2)$
- (c) a stable limit cycle.

Taking the herbivore parameters d and K as varying parameters and fixating the predator related parameters at

$$c = 0.01 \quad \text{and} \quad b = 0.8, \quad (4.2)$$

we may find the above limit solutions. For a bifurcation diagram, system (4.1) is linearized around the equilibria. The eigenvalues of the Jacobian are expressed in d and K . Two important bifurcations only depend on the value of K ; the transition of the boundary equilibrium to the internal equilibrium is at $K = 0.4$ and the transition of the internal equilibrium to a stable limit cycle is at $K = 0.9$. The bifurcation diagram is depicted in Figure 4.1.

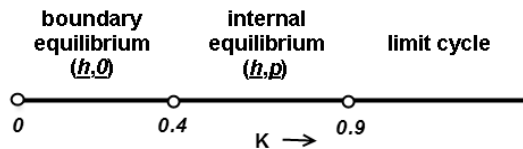


Figure 4.1: *Bifurcation diagram: types of stable limit solutions as a function of K .*

For a metapopulation model with two patches different configurations are possible. The herbivore parameters may be identical or different at the two patches. The predator may be absent at both patches or at one of them, and it may or may not migrate between them. The climate fluctuations may be identical at both patches or fluctuate at their own or be correlated in some way.

4.3 A herbivore metapopulation exposed to climatologic fluctuations

The influence of climate fluctuations upon the herbivore population is modelled by making the intrinsic growth rate d and/or the carrying capacity K time dependent. Furthermore, we consider the situation that the herbivores form a metapopulation living at two connected patches between which they can migrate. In the absence of predators the amount of biomass of the populations at the two patches satisfy

$$\begin{aligned}\frac{dh_1}{dt} &= d_1(t)\left(1 - \frac{h_1}{K_1(t)}\right)h_1(t) + w\left(\frac{h_2}{K_2(t)} - \frac{h_1}{K_1(t)}\right), \\ \frac{dh_2}{dt} &= d_2(t)\left(1 - \frac{h_2}{K_2(t)}\right)h_2(t) - w\left(\frac{h_2}{K_2(t)} - \frac{h_1}{K_1(t)}\right).\end{aligned}\quad (4.3)$$

Choosing this type of coupling between the two subpopulations we see that for constant carrying capacities K_i , the stable stationary solutions $h_1(t) = K_1$ and $h_2(t) = K_2$ hold for all $w \geq 0$ assuming positive intrinsic growth rates $d_i(t)$. There is a nett flow from patch 2 to patch 1 if $h_2/K_2 > 1$ and $h_2/K_2 > h_1/K_1$, which is quite natural. If $h_2/K_2 < 1$, there is no strong reason to leave patch 2. However, if $h_2/K_2 > h_1/K_1$, perspectives in patch 1 might be better. So if this information is available, which is possible because an equal exchange is not ruled out, a nett flow to patch 1 is still feasible. The same argument holds for a flow in the opposite direction. In conclusion the above coupling mechanism suits well for modelling a migration process. Nevertheless it is certainly worth to consider other dispersion mechanisms due to specific forms of behaviour (Reed et al., 2005).

We study the external influence upon the carrying capacities K_i given by a function of time $q(t)$ that mimics the fluctuations of the weather over a large time interval. We will use the Lorenz 84 equations for that purpose. In the study of a real world metapopulation an existing time series could have been taken as well. The Lorenz 84 system is a strongly truncated spectral model of the atmospheric circulation, being a system of three coupled nonlinear differential equations (Lorenz, 1984):

$$\begin{aligned}\frac{dx}{dt} &= e(-y^2 - z^2 - \alpha x + \alpha F), \\ \frac{dy}{dt} &= e(xy - \beta xz - y + G), \\ \frac{dz}{dt} &= e(\beta xy + xz - z).\end{aligned}\quad (4.4)$$

The component x represents the strength of the zonal flow (westerly-wind current) and the components y and z respectively the amplitudes of the cosine and sine phases of a chain of large superposed waves. The parameter F is a forcing from the north-south temperature gradient and G a forcing from the continent-ocean temperature contrast. In the original form $e = 1$. By our choice of e the time scale of the climate model is

72 Mathematical conservation ecology: supporting a herbivore metapopulation

such that the effect of the fluctuations upon the ecological system is large. The system exhibits chaotic dynamics for a large set of values in the parameter space. We choose

$$\alpha = 0.25, \quad \beta = 4, \quad e = 0.025, \quad F = 8 \quad \text{and} \quad G = 1. \quad (4.5)$$

The way of coupling this atmospheric model to the system (4.3) is as follows:

$$K_1(t) = \frac{1/2}{q_1(t)}, \quad K_2(t) = \frac{1}{q_2(t)}, \quad q_i(t) = z(t; x_0^{(i)}, y_0^{(i)}, z_0^{(i)}) + \gamma, \quad (4.6)$$

where $\gamma = 2.5$, so $z + \gamma > 0$ always holds (z ranges between -2.0 and 2.1). The state $(x_0^{(i)}, y_0^{(i)}, z_0^{(i)})$ denotes the starting point on the chaotic attractor of the Lorenz-84 system taken for patch i . Our choice of the function $q_i(t)$ is quite arbitrary. We made it such that the fluctuations stay within certain bounds so that the effect in the population sizes becomes notable but does not lead to explosive fluctuations in the population sizes. Figure 4.2 shows the evolution of the carrying capacities K_1 and K_2 which depend on the climatic fluctuations according to (4.6). For patches close together the same starting value may be taken, while for patches at a larger distance from each other different starting values would be more appropriate. If we want to keep a correlation between the $q_1(t)$ and $q_2(t)$, see Gilpin (1990), we have to take for the second patch the same solution as for the first with just the value of z shifted in time, so

$$q_2(t) = q_1(t + \Delta), \quad (4.7)$$

where Δ is a chosen small time difference. For uncorrelated time series, different initial conditions should be chosen,

$$(x_0^{(1)}, y_0^{(1)}, z_0^{(1)}) \neq (x_0^{(2)}, y_0^{(2)}, z_0^{(2)}). \quad (4.8)$$

Due to the chaotic behaviour (sensitive dependence on initial conditions) two solutions with even the slightest difference in starting value will get completely uncorrelated after some time. Here, we choose unrelated time series of q_1 and q_2 , meaning the two patches are in different time regimes of the external source of fluctuation. To obtain two different time series, we made two runs of the Lorenz 84 model (4.4) with different starting points, so that (4.8) holds. We keep the intrinsic growth rates constant. These parameters and the migration rate are set at

$$d_1 = 1, \quad d_2 = 3 \quad \text{and} \quad w = 0.5. \quad (4.9)$$

In Figure 4.3 the fluctuations of the herbivore subpopulations are depicted, for a time interval of 1000 time units. We are interested in the effect of the degree of coupling w between the two subpopulations upon the size of these populations in times that the external influence makes it hard for them (population size at a level much lower than the all time average). From a long run of 5000 time units, where each time unit consists of 100 integration steps, time series $\{h_1(t_j)\}$ and $\{h_2(t_j)\}$ are produced. We compute the histograms of the values that h_1 and h_2 take in these series to quantify the

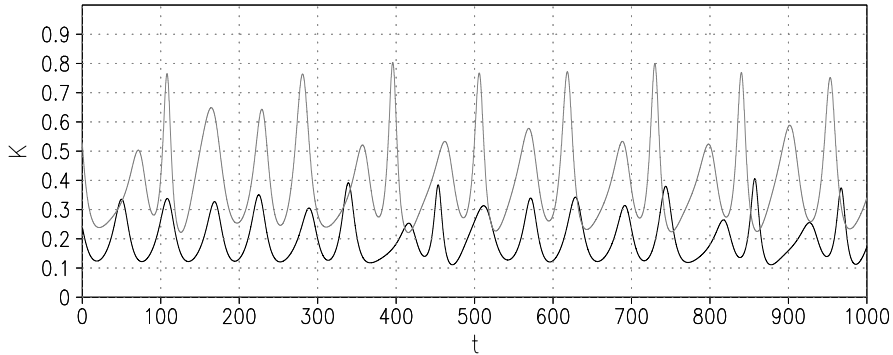


Figure 4.2: The evolution of carrying capacities K_1 and K_2 given by (4.6) as they depend upon the climatic fluctuations.

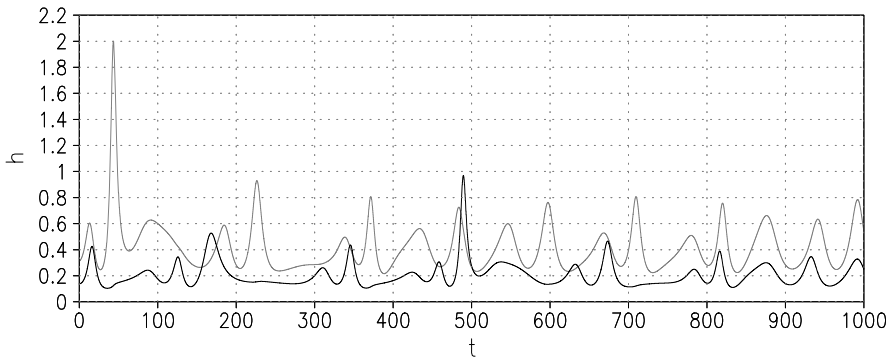


Figure 4.3: The size of the two herbivore subpopulations as a function of time, (black h_1 , grey h_2) for the system given by (4.3)-(4.4) and (4.9).

distribution in time of the herbivore populations, see Figure 4.4. From the two series $\{h_1(t_j)\}$ and $\{h_2(t_j)\}$ the fifth percentile r_i is computed. It means that 5% of the values of $\{h_i(t_j)\}$ lies below r_i . The lower r_i the more the population at patch i is at risk. As a measure for the risk of a local extinction we use the above defined fifth percentiles r_i . Thus, the size of the subpopulation is the only factor that is taken in consideration. Of course properties important for survival, such as the recovery speed of the herbivore subpopulation, depend on the local parameters d_i and K_i . However, these are already to a certain degree taken up in the indicator because a high recovery speed would lead to shorter time intervals of low subpopulation values resulting in a higher fifth percentile value. In Tabel 4.1 the fifth percentile of the two populations are given, as well as the minimum, mean and maximum.

When varying the migration rate w it turns out that the degree of coupling does not

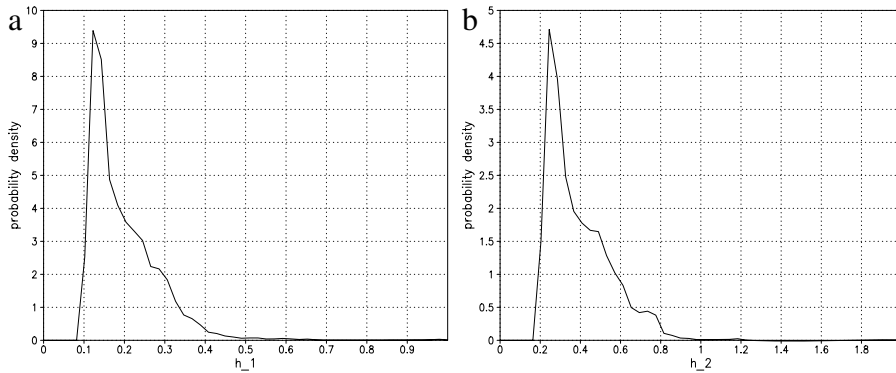


Figure 4.4: Histograms of the two subpopulations a) h_1 , b) h_2 , calculated with an integration of 5000 time units long.

	min	fifth percentile	mean	max
h_1	0.104	0.120	0.206	0.984
h_2	0.216	0.238	0.406	2.000

Table 4.1: Minimum, fifth percentile, mean and maximum for h_1 and h_2 for an integration of 5000 time units long, with $w = 0.5$.

play any role: for all $w \geq 0$ we find the same values, $r_1 = 0.120$ and $r_2 = 0.238$. This does not mean that automatically the degree of coupling is not important for the presence of species at a patch. If a catastrophe has completely wiped away the local population, then the speed of recolonization is an important factor. It may depend upon the strength of coupling w . We investigate this by making runs with for the herbivore starting subpopulations $h_1(t_0) = 0$ and $h_2(t_0) = K_2(t_0)$. The time needed for the subpopulation at patch 1 to arrive at 50% of its actual carrying capacity $K_1(t)$ is registered for different values of w , starting at 0.1 and for each new run increased by 0.1. Clearly for $w = 0$ this value is infinitely large. In Figure 4.5 it is seen how this arrival time (in terms of time units) decreases as the coupling is increased. It is worth to find out why the values r_1 and r_2 do not change with w . It is easily seen that the sum $h_1(t) + h_2(t)$ does not depend on w and that $h_i(t)$ will approximately follow $K_i(t)$ so that the net migration rate will be small. However, from these facts one cannot infer that r_i does not depend on w . It is also possible that the fluctuations are present at the third decimal or at higher ones.

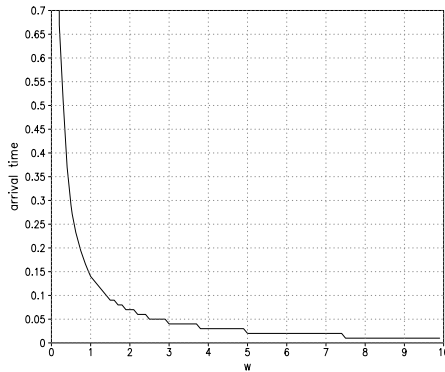


Figure 4.5: Arrival time at the level of 50% of the actual carrying capacity for the subpopulation at patch 1 as a function of the strength of coupling w . At the initial time we have $h_1(t_0) = 0$ and $h_2(t_0) = K_2(t_0)$.

4.4 Herbivore fluctuations in the presence of a predator

We now consider the situation that a predator is present at both patches. It is assumed that, contrary to the herbivore, it cannot migrate between the patches. Furthermore, the external fluctuations remain present. Now they will act upon the intrinsic growth rates and will be equal for both patches. The system then changes into

$$\begin{aligned}
 \frac{dh_1}{dt} &= d_1(t)\left(1 - \frac{h_1}{K_1}\right)h_1 - \frac{h_1 p_1}{h_1 + c_1} + w\left(\frac{h_2}{K_2} - \frac{h_1}{K_1}\right), \\
 \frac{dp_1}{dt} &= \frac{h_1 p_1}{h_1 + c_1} - b_1 p_1, \\
 \frac{dh_2}{dt} &= d_2(t)\left(1 - \frac{h_2}{K_2}\right)h_2 - \frac{h_2 p_2}{h_2 + c_2} - w\left(\frac{h_2}{K_2} - \frac{h_1}{K_1}\right), \\
 \frac{dp_2}{dt} &= \frac{h_2 p_2}{h_2 + c_2} - b_2 p_2,
 \end{aligned} \tag{4.10}$$

with

$$b_1 = b_2 = 0.8, \quad c_1 = c_2 = 0.1, \quad w = 0.5 \tag{4.11}$$

and

$$d_1(t) = q(t), \quad d_2(t) = 3q(t), \quad K_1 = 0.5, \quad K_2 = 1, \tag{4.12}$$

with $q(t)$ as in (4.6). In Figure 4.6 we see the dynamics of the herbivore and predator populations. The evolution during the first 500 time units is shown. When looking at a longer evolution of p_1 (not shown), it shows a trend of gradual growth until a sudden collapse after which it roughly repeats itself. Figure 4.7 shows the evolution of the intrinsic growth rate d_1 over the same time period. Remember that $d_2 = 3d_1$.

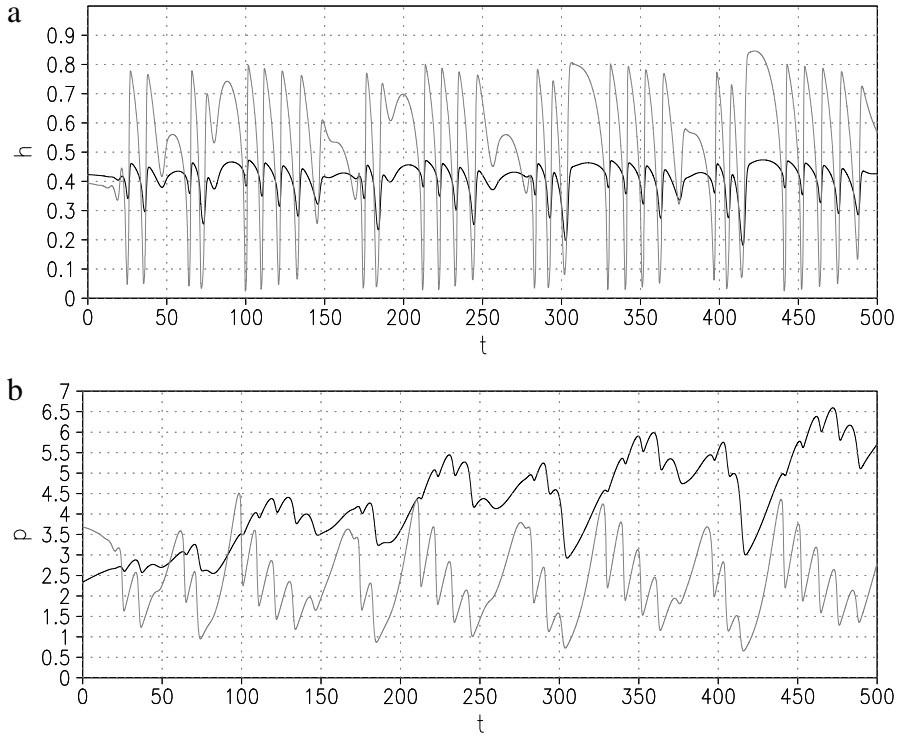


Figure 4.6: *The behaviour of the herbivore and predator populations in case of identical climatologic conditions at both patches. Part of the stationary solution of (4.10) is depicted. a) h_1 (black line) and h_2 (grey line), b) p_1 (black line) and p_2 (grey line). Note that the value of p_1 is multiplied with a factor 100. The behaviour of p_1 gives the impression that the solution is still in its spin up. This is not the case: long periods with an increasing trend are followed by a sudden collapse.*

Making a 5000 time unit long run with the system (4.10) we compute the fifth percentile r_i of the herbivore data at both patches. The result shows that the population at the second patch is the most vulnerable to extinction:

$$r_1 = 0.294, \quad r_2 = 0.0780. \tag{4.13}$$

In Table 4.2 minimum, fifth percentile, mean and maximum for h_1 , p_1 , h_2 and p_2 are given. We also computed the histograms of the herbivores for this run, which are shown in Figure 4.8.

Two ways to improve the situation are taken in consideration: the migration coefficient w can be increased as well as the predator's death rate b_2 . Both lead to an increase of r_2 . The element of a conservation management strategy is brought in by assuming that the effort to increase the death rate with one unit costs c_b and that for the

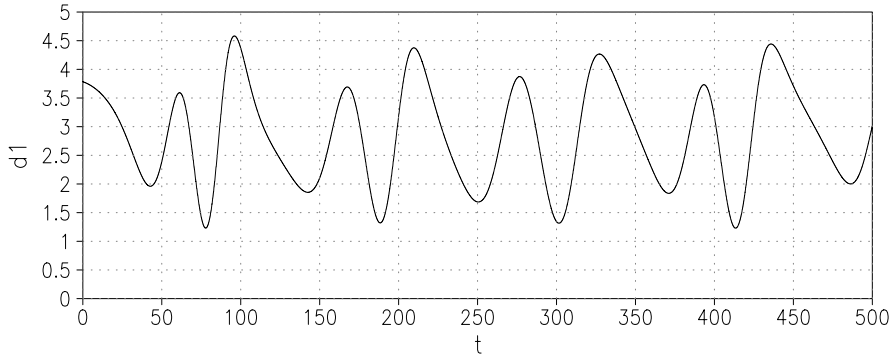


Figure 4.7: The evolution of intrinsic growth rate d_1 as it depends upon climatic fluctuations. (d_2 is three times d_1).

	min	fifth percentile	mean	max
h_1	0.0998	0.294	0.408	0.479
p_1	0.0102	0.0146	0.0423	0.0810
h_2	0.0233	0.0780	0.518	0.883
p_2	0.269	0.979	2.36	4.57

Table 4.2: Minimum, fifth percentile, mean and maximum for h_1 , p_1 , h_2 and p_2 for an integration of 5000 time units long, with unperturbed parameters.

migration coefficient this cost is c_w . Moreover, a fixed amount of effort C is available for improving the conditions for the herbivore metapopulation. Instead of one of the two options we may consider a mixed approach. So with the constraint

$$c_b(b_2 - 0.8) + c_w(w - 0.5) = C. \quad (4.14)$$

we look for values b_2 and w that produce the largest improvement of r_2 . In Figure 4.9 a) we see the results of r_2 for the choice $C = 0.05$, $c_b = 10$ and $c_w = 0.1$. Now (4.14) can be rewritten:

$$10(b_2 - 0.8) + 0.1(w - 0.5) = 0.05 \quad \Rightarrow \quad b_2 = 0.81 - 0.01w. \quad (4.15)$$

So when increasing w by a stepsize 0.005, b_2 decreases with stepsize 0.00005. An optimum is found for

$$b_2 = 0.80365 \quad \text{and} \quad w = 0.635 \quad \text{with} \quad r_2 = 0.1066. \quad (4.16)$$

It is noted that for this value of w , and larger values, the predator population at patch 1 gets extinct. This extinction coincides with a rapid decrease in the fifth percentile

78 Mathematical conservation ecology: supporting a herbivore metapopulation

for the herbivore in patch 1. This change in r_1 is more drastic than the change in r_2 , as can be seen in Figure 4.9 b). Apparently an increasing migration corridor along with an decreasing death rate for the predator in patch 2 result in a decline in the herbivore subpopulation in patch 1 which coincides with a rapid decrease in the predator subpopulation in that patch, eventually leading to extinction.

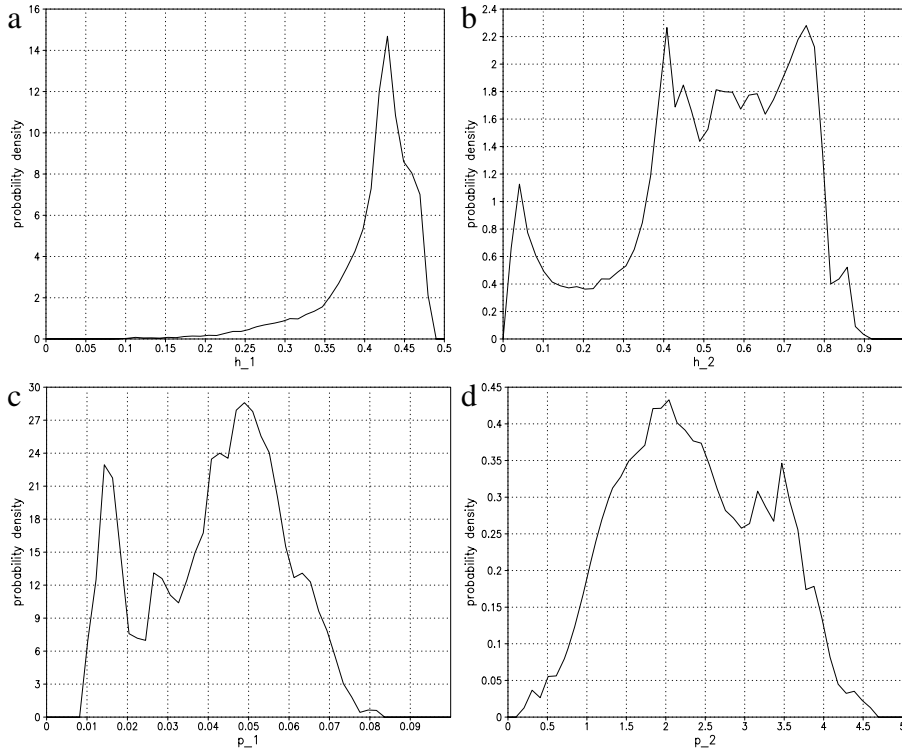


Figure 4.8: Histograms of the different subpopulations a) h_1 , b) h_2 , c) p_1 and d) p_2 , calculated with an integration of 5000 time units long.

4.5 Herbivore conservation in case of a migrating predator

Compared with the configuration of the previous section we add a coupling between the two predator subpopulations. The predator migration from 2 to 1 and vice versa is steered by the size of the predator population at both patches. A net flow of predators from patch 1 to patch 2 occurs when $p_1 > p_2$. Following Janssen (2001) predator migration at a rate v is added: he allowed predator migration in the Rosenzweig-McArthur

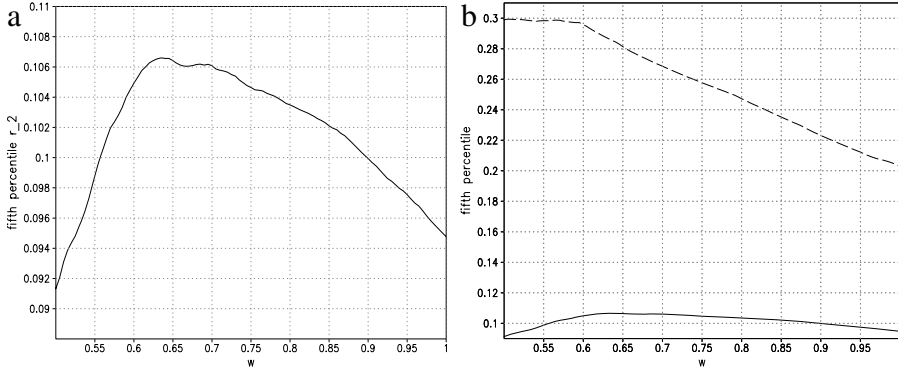


Figure 4.9: For (4.11) the second subpopulation has a fifth percentile of $r_2 = 0.0780$. A change of the parameters b_2 and w with constraint (4.14) yields the optimal value (4.16). a) only the values for r_2 , b) dashed line: r_1 , solid line: r_2 .

model by adding the term $v(p_j - p_i)$ to the right hand side of the time derivative of p_i , $j = 3 - i$, $i = 1, 2$. He then used the carrying capacity and the migration rate as bifurcation parameters and gave an insight into the possible dynamical behaviour of the model. Huang and Diekmann (2001) constructed a predator migration rate that depends upon the density of the herbivore and also added a diffusion rate. They did a thorough bifurcation study of the model, and described changes in the number and the stability of equilibria and limit cycles.

Allowing predator migration as described the system takes the form:

$$\begin{aligned}
 \frac{dh_1}{dt} &= d_1(t) \left(1 - \frac{h_1}{K_1}\right) h_1 - \frac{h_1 p_1}{h_1 + c_1} + w \left(\frac{h_2}{K_2} - \frac{h_1}{K_1}\right), \\
 \frac{dp_1}{dt} &= \frac{h_1 p_1}{h_1 + c_1} - b_1 p_1 + v(p_2 - p_1), \\
 \frac{dh_2}{dt} &= d_2(t) \left(1 - \frac{h_2}{K_2}\right) h_2 - \frac{h_2 p_2}{h_2 + c_2} - w \left(\frac{h_2}{K_2} - \frac{h_1}{K_1}\right), \\
 \frac{dp_2}{dt} &= \frac{h_2 p_2}{h_2 + c_2} - b_2 p_2 - v(p_2 - p_1),
 \end{aligned} \tag{4.17}$$

with

$$b_1 = b_2 = 0.8, \quad c_1 = c_2 = 0.1, \quad w = 0.5, \quad v = 0.1 \tag{4.18}$$

and

$$d_1(t) = q(t), \quad d_2(t) = 3q(t), \quad K_1 = 0.5, \quad K_2 = 1. \tag{4.19}$$

In Figure 4.10 the fluctuation in the herbivore and predator subpopulations at the two patches are given. The fifth percentile of the two herbivore subpopulations are

$$r_1 = 0.104 \quad \text{and} \quad r_2 = 0.447. \tag{4.20}$$

80 Mathematical conservation ecology: supporting a herbivore metapopulation

The fifth percentile r_1 is lower and r_2 is considerably higher than the values we had without migration of the predators. In Table 4.3 minimum, fifth percentile, mean and maximum are given of the herbivores and predators. Compared with the situation of no predator migration, the predator subpopulation at patch 1 is at a much higher level. The fifth percentiles for both predators are much higher than previously. When we compare Figure 4.10 with 4.6, we see that the populations fluctuate with a lower frequency now. Moreover, Figure 4.10 shows much more proportionality, between h_1 and h_2 as well as between p_1 and p_2 . The histograms of the subpopulations are shown in Figure 4.11.

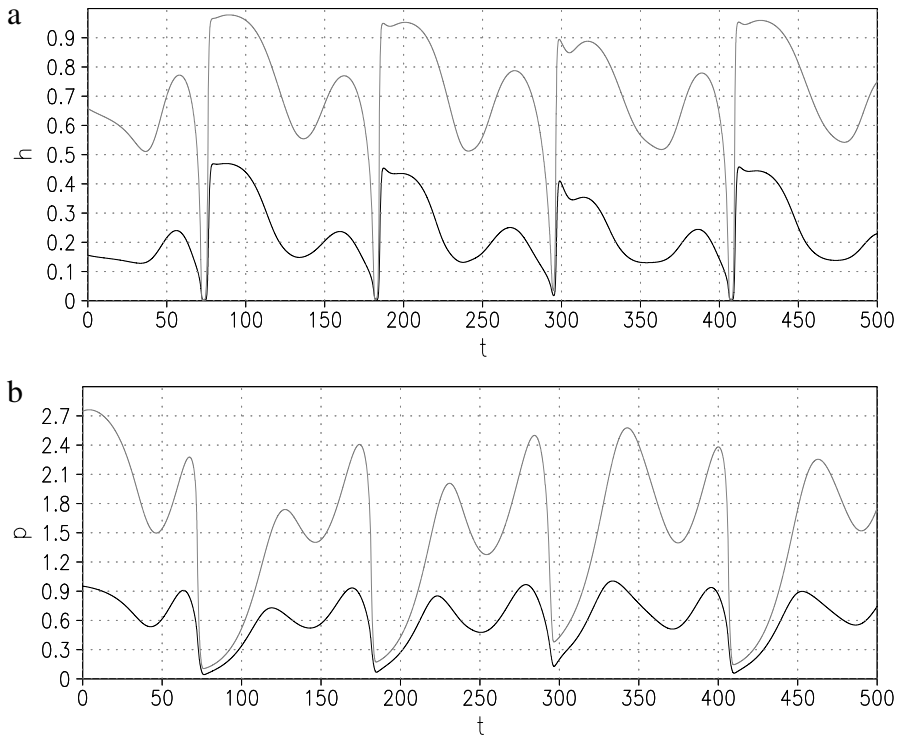


Figure 4.10: *The behaviour of the herbivore and predator populations, where migration between the predators is allowed. Part of the stationary solution of (4.17) is depicted. a) h_1 (black line), h_2 (grey line), b) p_1 (black line), p_2 (grey line).*

To improve r_1 and r_2 the parameters w , v , b_1 and b_2 are varied separately. The results are shown in Figure 4.12. Increasing the predator migration rate v from the value 0.1 up to 0.2, gives rising values for r_2 , whereas the value of r_1 does not change much, see Figure 4.12 a). For values of v between 0 and 0.03 we have that r_1 falls, it then increases until $v = 0.05$ and then remains fairly the same for larger values of v . For v between 0 and 0.01 r_2 falls and grows again for higher values of v . For values

	min	fifth percentile	mean	max
h_1	0.00106	0.104	0.235	0.495
p_1	0.00811	0.0838	0.601	1.03
h_2	0.00130	0.447	0.704	0.995
p_2	0.0179	0.156	1.51	2.78

Table 4.3: *Minimum, fifth percentile, mean and maximum for h_1 , p_1 , h_2 and p_2 for an integration of 5000 time units long, with unperturbed parameters.*

of v below 0.025 we have that the conditions in patch 1 are better for the herbivores, whereas for higher values of v , the herbivores in patch 2 are far better of.

Improving the migration of the herbivore by taking values above $w = 0.5$ yields an increase of r_1 but we see that at the same time r_2 decreases so the positive effect is rather limited, see Figure 4.12 b). A strong decrease of the coupling coefficient w below the value 0.5 has a negative effect upon the herbivore at patch 1, but a strong positive effect upon the herbivore in patch 2. Depending on which herbivore subpopulation needs to be protected, the herbivore migration rate w should be decreased or increased.

An increase of the predator death rate b_1 has hardly any effect at all on the fifth percentiles of the herbivores, increasing b_2 slightly improves the situation for the herbivore subpopulations at both patches, see Figure 4.12 c) and d), where the death rates are varied between 0.80 and 0.82.

4.6 Conclusions

Species conservation in a changing habitat has become an important topic. Degradation of a habitat may bring the size of a local population of a species to a critically low level. Unfortunately, restoring the situation is not always possible: a decrease of the available life space because of human activities cannot be reversed in many cases (Groom et al., 2005). A way to improve the survival chance of a local species is found in the introduction of wildlife corridors facilitating the exchange between subpopulations of a species at different locations. Enhanced migration may improve the survival of the total population. We conclude that at a local level this is not guaranteed using a common type of population model. Factors, not taken in consideration, such as an increase of the genetic diversity may have a positive effect. At the other hand negative effects such as the risk of spread of a disease cannot be excluded either (Gog et al., 2002).

Before we draw more conclusions from our study we remark that the models we investigated, as well as the ones from the literature, indicate that the effect of changes in the model parameters strongly depends on the choice of the model. Two elements are important: the type of interaction between the different species and the way each species disperses in a fragmented habitat.

General rules on the effect of conservation measures are hard to formulate (Etienne and Heesterbeek, 2001). One needs to quantify the amount of effort (the cost)

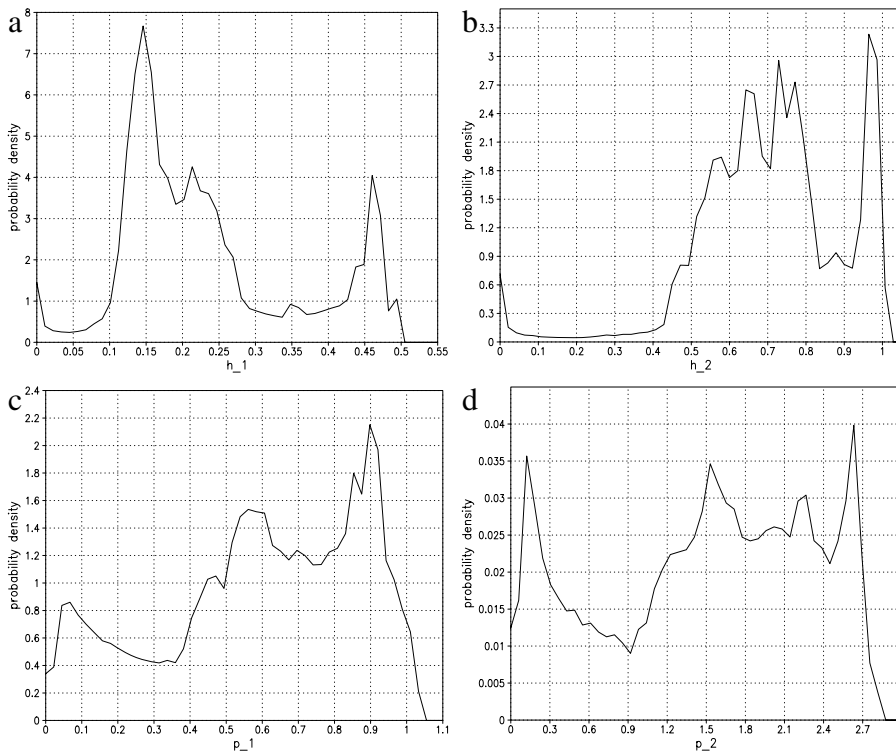


Figure 4.11: Histograms of the different populations a) h_1 , b) h_2 , c) p_1 and d) p_2 , calculated with an integration of 5000 time units long, where migration among the predators is allowed.

that is needed to make certain changes in a metapopulation. The available budget is another factor that has to be taken in consideration. Westphal et al. (2003) find that the effect of conservation strategies, (enlarging existing patches, enhancing corridors between patches, creating new patches) is time dependent: the state of the metapopulation matters for the optimal solution and the sequence of actions is critical. One should not only evaluate what actions should be taken, but also when. Furthermore, general rules cannot be made since they depend on model parameters and the configuration of the metapopulation. This means that an optimal strategy for one particular metapopulation may not be valid for a metapopulation that consists of a different kind of species. This does not make a population viability analysis (PVA) useless but limits its scope, since different populations may behave differently and can therefore not always be compared.

As for our model, a better corridor for a species does not automatically result in less deep dips in the local population. In Section 4.3 we noticed that for a single

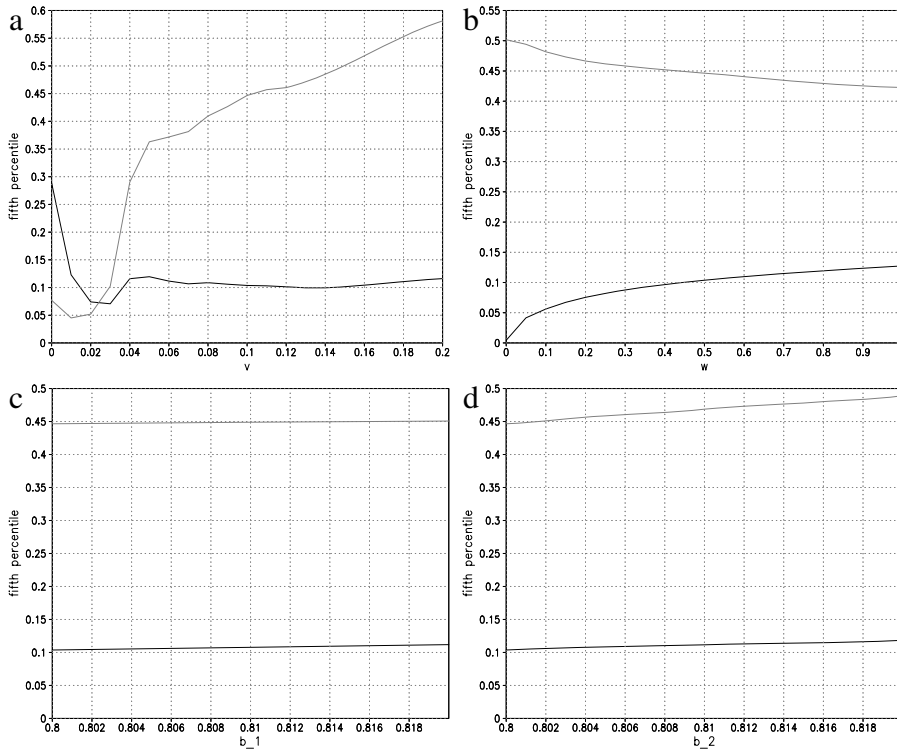


Figure 4.12: Fifth percentiles r_1 (black lines) and r_2 (grey lines) as functions of parameters a) v , b) w , c) b_1 and d) b_2 . In all figures the reference values are $v = 0.2$, $w = 0.5$, $b_1 = b_2 = 0.8$.

species model with uncorrelated climatic fluctuations at the two patches increase of the coupling did not improve the local conditions for the species. This conclusion is only drawn for the model with the given dispersion mechanism. Other types of migration behaviour may have a different effect. In the same section it is also concluded that for the model under consideration the degree of coupling between the two patches does influence the speed of recolonization in case of full local extinction. All the model choices and the results of varying different parameters are given schematically in Table 4.4.

In the more-species model of Section 4.4 a change in some of the parameters induces a qualitative change: the predator at patch 1 dies out. The goal of the parameter changes was to improve the conditions for the herbivore at patch 2 by enlarging the corridor for the herbivore and/or increasing the death rate of the predator at patch 2. Changing different parameters takes different efforts. Let there be an maximum available total effort. If this is completely put in increasing the death rate of the predator

84 Mathematical conservation ecology: supporting a herbivore metapopulation

at patch 2, then the result, that is obtained, can be improved by redirecting a part of the effort towards improving the corridor for the herbivore. In the optimal solution that is derived in this way the predator at patch 1 dies out. Clearly, biodiversity may be influenced by conservation measures in a way that is not easy to foresee.

In Section 4.5 we considered in more detail the effect of changing the parameters of the herbivore and the predator corridors and the death rate of the predators. An increasing migration rate v of the predators has a negative effect on the herbivores in both patches for very small values of v . First the herbivores in patch 1 are better off, but after the predator migration rate has passed a certain value, this changes. For higher values of this migration rate the conditions for the herbivores in patch 2 improve considerably whereas they remain fairly the same in patch 1. Increasing the death rate of the predator in patch 1 has no effect on the conditions of the herbivores and increasing it in patch 2 improves the conditions of the herbivores slightly. In Figure 4.12 it is seen that facilitating the migration of the herbivore indeed improves the situation for the herbivore at patch 1 but worsens the conditions for the herbivore at patch 2. These drawbacks are not as dramatic as in the case of local species extinction, but sufficiently important to stay aware of the possibility that events may occur that are not foreseen and therefore not excluded in the formulation of the optimization problem. Even if the optimal solution has all desired properties it may be so that along the path from the actual situation to the optimal state inevitable events occur that withhold the system from arriving in that state.

Above we have brought up a number of arguments to improve the actual situation for a metapopulation by changing parameters in small steps. In literature there are examples in which it is better to take one large step to escape from an undesirable ecological regime, e.g. Scheffer (1991) explains a way to bring down the turbidity level in a lake using a minimal dynamic model for the fish and algae populations. For more complex models such strategies cannot be developed that easy. Thus, we stay with the strategy of small steps. It means that in parameter space we choose the direction of the highest improvement given a small amount of effort. When this direction is found (gradient method) a small step is made and next the procedure is repeated. For large scale models with many parameters it can be a problem to find this best direction of change. This problem can become unsurpassable if a large computing time is needed to evaluate the outcome for a new set of parameter values. In the present study, where climatic fluctuations are part of the input, a large time interval should be considered requiring a long integration of the full system. It is therefore desirable to find optimal parameter changes with a minimum amount of computation time. In the next chapter we introduce a method from meteorology (chapters 2 and 3) that efficiently selects directions in parameter space that yield a high improvement. Similar to the approach in the climate study where first the method for finding efficient parameter perturbations was tried out in a simple atmospheric model, the Lorenz-63 equations, we will apply the technique in an ecological context to the model we presented here.

model	characteristics	
(4.3)	species configuration climate parameter varied	herbivores, no predators herbivores migrate uncorrelated for both patches acts upon carrying capacities migration rate w
	results	increasing migration rate has no effect it does influence speed of recolonization
(4.10)	species configuration climate parameters varied	both herbivores and predators only herbivores migrate identical for both patches acts upon intrinsic growth rates migration rate w and death rate predator, b_2 with cost function
	results	predator 1 dies out for optimal parameter choice
(4.17)	species configuration climate parameters varied	herbivores and predators herbivores and predators migrate identical for both patches acts upon intrinsic growth rates migration rates w and v , death rates predators b_1 and b_2 separately
	results	increasing predator migration rate \rightarrow positive effect on herbivore 2 for $v > 0.025$ negative effect on both herbivores for smaller values of v , it depends on value of v which patch has the best conditions increasing predator death rates \rightarrow minor positive or no effect on herbivores, increasing herbivore migration rate \rightarrow positive for herbivore 2, negative for herbivore 1

Table 4.4: *Different choices of the model and results of parameter changes.*

4.7 Acknowledgements

We would like to thank Ad van Dommelen, Rampal Etienne and Maarten de Gee for their interest and useful suggestions.

References

- Akçakaya, H.R., 1992. Population viability analysis and risk assessment. in: *Wildlife 2001: Populations*, (eds. D.R. McCullough and R.H. Barrett), Elsevier, Amsterdam, p.148-157.
- Akçakaya, H.R., 2000a. Viability analyses with habitat-based metapopulation models. *Population Ecology*, **42**, 45-53.
- Akçakaya, H.R., 2000b. Population viability analyses with demographically and spatially structured models. *Ecological Bulletins*, **48**, 23-38.
- Akçakaya, H.R. and Sjögren-Gulve, P., 2000. Population viability analyses in conservation planning: an overview. *Ecological Bulletins*, **48**, 9-21.
- Arnott, S.A. and Ruxton, G.D., 2002. Sandeel recruitment in the North Sea: demographic, climatic and trophic effects. *Marine Ecology Progress Series*. **238**, 199-210.
- Becks, L., Miller F.M., Malchov, H., Jürgens, K. and Arndt, H., 2005. Experimental demonstration of chaos in a microbial food web. *Nature*, **435**, 1226-1229.
- Brook, B.W., O'Grady, J.J., Chapman, A.P., Burgman, M.A., Akçakaya, H.R., Frankham, R., 2000. Predictive accuracy of population viability analysis in conservation biology. *Nature*, **404**, 385-387.
- Burgman, M.A., Ferson, S. and Akçakaya, H.R., 1993. Risk Assessment in Conservation Biology. *Chapman & Hall, London*.
- Cushing, J.M., Costantino Brian Dennis, F., Desharnais, R.A. and Henson, S.M., 2003. Chaos in Ecology: Experimental Nonlinear Dynamics. *Theoretical Ecology Series, Academic Press, San Diego*.
- DeAngelis, D.E., Gross, L.J., 1992. Individual-based models and approaches in ecology: populations, communities and ecosystems. *Chapman and Hall, New York*.
- Etienne, R.S., and Heesterbeek, J.A.P., 2001. Rules of thumb for conservation of metapopulations based on a stochastic winking-patch model. *American Naturalist*, **158**, 389-407
- Etienne, R.S., 2002. Striking the Metapopulation Balance: Mathematical Models and Methods meet Metapopulation Management. *PhD Thesis, Wageningen University*.

- Gilpin, M.E., 1990. Extinction of finite metapopulations in correlated environments, in: *Living in a Patchy Environment*, B. Shorrocks and I.R. Swingland, eds., Oxford University Press, 177-186.
- Gog, J., Woodroffe, R. and Swinton, J., 2002. Disease in endangered metapopulations: the importance of alternative hosts. *Proceedings of the Royal Society London B*, **269**, 671-676.
- Grasman, J., and van Straten, G., eds., 1994. Predictability and Nonlinear Modelling in Natural Sciences and Economics. *Kluwer, Dordrecht*, 653pp.
- Grasman, J., and HilleRisLambers, R., 1997. On local extinction in a metapopulation, *Ecological Modelling*, **103**, 71-80.
- Groom, M.J., Meffe, G.K. and Carroll, C.R., 2005. Principles of Conservation Biology. *Sinauer, 3rd Edition*.
- Hanski, I., 1999. Metapopulation Ecology. *Oxford University Press*.
- Harding, K.C. and McNamara, J.M., 2002. A unifying framework for metapopulation dynamics. *The American Naturalist*, **160**, 173-185.
- Holt, R.D., Keitt, T.H., Lewis, M.A., Maurer, B.A., and Taper, M.L., 2005. Theoretical models of species' borders: single species approaches. *Oikos*, **108**, 18-27.
- Hsieh, C.-H., Glaser, S.M., Lucas, A.J., and Sugihara, G., 2005. Distinguishing random environmental fluctuations from ecological catastrophes for the North Pacific Ocean. *Nature*, **438**, 336-339.
- Huang, Y. and Diekmann, O., 2001. Predator migration in response to prey density: What are the consequences? *Journal of Mathematical Biology*, **43**, 561-581.
- Janssen, V.A.A., 2001. The dynamics of two diffusively coupled predator-prey populations. *Theoretical Population Biology*, **59**, 119-131.
- Kareiva, P., 1987. Habitat fragmentation and the stability of predator-prey interactions. *Nature*, **326**, 388-390.
- Levin, S.A., 1992. The problem of pattern and scale in ecology. *Ecology*, **73**, 1943-1967.

88 Mathematical conservation ecology: supporting a herbivore metapopulation

Levins, R., 1969. Some demographic and genetic consequences of environmental heterogeneity for biological control. *Bulletin of the Entomological Society of America*, **15**, 237-240.

Lopez, J.E. and Pfister, C.A., 2001. Local population dynamics in metapopulation models: implications for conservation. *Conservation Biology*, **15**, 1700-1709.

Lorenz, E.N., 1984. Irregularity: A fundamental property of the atmosphere. *Tellus*, **36A**, 98-110.

Lusseau, D., Williams, R., Wilson, B., Grellier, K., Barton, T.R., Hammond, P.S. and Thompson, P.M., 2004. Parallel influence of climate on the behaviour of Pacific killer whales and Atlantic bottlenose dolphins. *Ecology Letters*, **7**, 1068-1076.

Mysterud, A., Stenseth, N.C., Yoccoz, N.G., Langvatn, R. and Steinheim, G., 2001. Nonlinear effects of large-scale climatic variability on wild and domestic herbivores. *Nature*, **410**, 1096-1099.

Pascual, M., Levin, S.A., 1999. From individuals to population densities: searching for the intermediate scale of nontrivial determinism. *Ecology*, **80**, 2225-2236.

Pounds J.A., Fogden, M.P.L., Campbell, J.H., 1999. Biological response to climate change on a tropical mountain. *Nature*, **398**, 611-615.

Rai, V., and Anand, M., 2004. Is dynamic complexity of ecological systems quantifiable? *International Journal of Ecology and Environmental Sciences*, **30**, 123-130.

Reed, J., and Levine, S.H., 2005. A model for behavioral regulation of metapopulation dynamics, *Ecological Modelling*, **183**, 411-423.

Rosenzweig M.L., and MacArthur, R.H., 1963. Graphical representation and stability conditions of predator-prey interactions. *American Naturalist* **97**, 209-223.

Sæther, B.-E., 1997. Environmental stochasticity and population dynamics of large herbivores: a search for mechanisms. *Trends in Ecology and Evolution*, **12**, 143-149.

Scheffer, M., 1991. Fish and nutrients interplay determines algal biomass: A minimal model. *Oikos*, **62**, 271-282.

Sherratt, J.A., Eegan, B.T., and Lewis, M.A., 1997. Oscillations and chaos behind predator-prey invasion: mathematical artifact or ecological reality? *Philosophical Transactions Royal Society London B*, **352**, 21-38.

Stenseth, N.C., Mysterud, A., Ottersen, G., Hurrell, J.W., Chan, K.-S. and Lima, M., 2002. Ecological effects of climate fluctuations. *Science*, **297**, 1292-1296.

Taylor, A.D., 1990. Metapopulations, dispersal, and predator-prey dynamics: An overview, *Ecology*, **71**, 429-433.

Thompson, P.M. and Grosbois, V., 2002. Effects of climate variation on seabird population dynamics. *Directions in Science*, **1**, 50-52.

Urban, F.E., Cole, J.E., Overpeck, J.T., 2000. Influence of mean climate change on climate variability from a 155-year tropical Pacific coral record. *Nature*, **407**, 989-993.

Westphal, M.I., Pickett, M., Getz, W.M. and Possingham, H.P., 2003. The use of stochastic dynamic programming in optimal landscape reconstruction for metapopulations. *Ecological Applications*, **13(2)**, 543-555.

CHAPTER 5

Species conservation by optimal parameter change in a metapopulation model

In this study we carry out a parameter sensitivity analysis for a herbivore-predator metapopulation model, consisting of two patches. Only the herbivores are allowed to migrate between the patches. Furthermore, the intrinsic growth rates of the herbivores depend on climate fluctuations. Our objective is the conservation of the herbivores. We are interested in finding the parameter perturbations that will reduce the extinction risk of one of the subpopulations the most. We make use of the short term behaviour of the model. In the neighbourhood of a short interval of the non-linear reference (unperturbed) orbit the linear error growth can be calculated. The perturbation that causes the largest error growth, the so called first singular vector, can be computed with the use of adjoint equations. The adjoint of a model acts as a backward integration. It turns out that for some cases, the direction of the first singular vector is also as a parameter perturbation effective in changing the dynamics in a long model simulation. The selection is based on the behaviour of this local error growth. This adjoint method is compared to a method where parameter perturbations are randomly chosen. Here we carry out a test for a model with only few parameters. However, it can be applied to models with a very large number of parameters, making the adjoint method an interesting alternative for the random method as then the required number of runs cannot be realized within a realistic computing time. A same argument holds for the use of a systematic method of finding an optimum.

5.1 Introduction

A metapopulation is a set of local populations spread out over different habitat patches, between which migration is possible. Metapopulation models are used to describe the dynamics of spatially distributed populations. In the literature a wide spectrum of mod-

els is found. The models range from occupancy models (describing patches that are either occupied or empty), see e.g. Levins (1970), to individual based models (describing the local population dynamics), see e.g. DeAngelis and Gross (1992). In between a type of structured metapopulation model exists that describes the population dynamics as well as the spatial dynamics by modelling migration and correlation among populations. A good description of these different models and their use can be found in Akçakaya (2000a). Models are an approximation of reality. In this process model structure and model parameters are important features. They determine the reliability of a model. The model parameters are estimated using data or are derived from fundamental physical principles. Inaccurate or insufficient data can result in uncertainty in model parameters. Also, parameter estimation techniques are not flawless. When a certain parameter value is unknown, a realistic upper and lower bound should be given. The uncertainty in model parameters will influence the model output. When analysing population dynamics, this parameter uncertainty should be taken into account (Conroy et al, 1995, Akçakaya, 2000b, Moilanen, 2002, Drechsler et al., 2003).

In metapopulation modelling, parameter estimation may contribute to the practical use of the model output. Moilanen (2002) recognizes that errors, made in data observation, may result in inaccurate parameter estimates which will consequently affect the model predictions. He emphasizes three types of errors that commonly occur in metapopulation data sets. First, patch areas are estimated or measured incorrectly. Second, patches located within or around the study area may be missed. Third, patches may be wrongly observed as empty. Effects of errors can depend on the characteristics of the metapopulation, such as the fragmentation. Moilanen therefore generates, within a stochastic patch occupancy model, a set of different systems, using simulated data. The systems differ in many of their properties such as in the level of patch aggregation, the distribution of migration distances and the rate at which local populations go extinct and empty patches become colonized (turnover rate). Next, errors are added to the data set of each system. These errors are randomly drawn from a uniform distribution. Incorrect estimation of a patch area influences the extinction risk, missing patches cause overestimation of migration distances and finally wrongly describing patches as empty can have a large effect on all these factors. It is therefore important to specify the data errors that can occur and the effect they can have on the parameterization, especially when the metapopulation model is used to make conservation management decisions.

5.1.1 Species conservation and sensitivity analysis

Conservation of a metapopulation can be enhanced by increasing the area of patches (either by a fixed area or a fixed percentage) or the connectivity between certain patches. These measures may decrease the risk of extinction of local populations and increase the probability of re-colonization of empty patches. Conservation managers are interested in finding the optimal strategy for metapopulation persistence. Etienne (2004) examines a detailed stochastic patch occupancy model to evaluate whether rules of thumb can be formulated for optimal strategies. He suggests that the largest patch should be enlarged if a fixed percentage of area can be added, the smallest patch should

be enlarged if a fixed amount of area can be added and lastly, the distance between the two largest patches should be reduced when given the choice between all distances among pairs of patches. He points out that the strength of his rules strongly depends on parameter values such as patch clustering and dispersal distance.

In this study we search for optimal parameter changes to conserve a specified species within a predator-prey metapopulation model. This model describes the local dynamics of both populations divided over two patches. The herbivores are allowed to migrate between the two patches. Furthermore, the influence of climate upon the intrinsic growth rates is taken into account. In chapter 4 this model has been used to find the optimal management strategy given a fixed investment. Restricted by a cost function small changes in the death rate of the predator in one of the patches and in the migration rate of the herbivores are made.

The model used in this study contains a reasonably small number of parameters. For more realistic and thus more complex models, the number of parameters will be much larger. A large parameter set makes a parameter change analysis computationally demanding. Not only for the purpose of conservation management such an analysis is made, also for model sensitivity analysis we have to deal with large scale computations when changing parameter values. When dealing with uncertainty in parameters, sensitivity analysis can help to identify the parameters that have a strong effect and therefore should be given priority for a better estimation, i.e. by collecting more data. If in addition to a large number of parameters long simulation runs are required, then a full scale sensitivity analysis may become problematic. In this study a large time integration is needed to include a sufficient number of extreme weather conditions in the evaluation of a choice of the ecological parameter values.

5.1.2 Finding effective parameter changes

In this study we test a method from meteorology that efficiently selects directions in parameter space that cause a large change in a specific output variable related to the climate. First this method is introduced using the example of a simple atmospheric model (chapter 2) and next applied to a more realistic atmospheric model (chapter 3). The method may have a wider application, and could be used in metapopulation analysis as well. We therefore want to test it for a simple metapopulation model. When proven successful, the effectiveness of the method can be applied to a more realistic ecological model. Five model parameters will be perturbed: the carrying capacities of the patches for the herbivores, the death rates of the predators, and the migration rate of the herbivores. They form the parameter vector α . We are interested in finding the combination of perturbed parameter values that will most strongly affect the population dynamics, as simulated with the model. In this study our objective will be the conservation of the herbivores at each of the patches.

First, a model run with the original, unperturbed, parameter values is made. This run is used as a reference to compare with model runs where the parameters are perturbed. The model runs cover a sufficiently large time interval so that extreme weather conditions are likely included. The change in the population viability is monitored

by observing the fifth percentile of the different populations. This is the value below which the subpopulation is found 5 out of 100 times in a series of values taken at fixed time intervals. The higher this fifth percentile, the better the conditions are for this population and the smaller the risk of extinction. It is assumed that the effort to change a parameter is the same for each parameter. The set of possible perturbations of the parameter vector lies on a hypersphere centred around the original reference parameter vector α_r and with radius 0.05 times the length of α_r . Once a perturbation $\delta\alpha$ has been chosen, it can be added to α_r , resulting in the new parameter vector $\alpha_r + \delta\alpha$. A new model run with these perturbed parameters can then be made and so on. The key question is how to detect from the set just those perturbations that are highly favourable for the purpose in mind. The goal is to improve the conditions of a selected population. In this chapter we explore and compare several methods to find these perturbations.

In this study our aim is the conservation of the herbivores: we want to find parameter perturbations that favour the herbivore (sub)populations the most; this will result in a lower extinction risk. In order to choose from the numerous possible combinations of parameter perturbations, we develop an efficient method as an alternative to a random method, because for large parameter sets a systematic method for computing the gradient as a function of these parameters is not within reach. Presumably, our method will reduce the computing time considerably. The idea is that parameters, that are likely to be effective, are selected on the basis of the short term behaviour of the system. This means that the search is done using short simulations only, rather than making long simulations without knowing whether the added parameter vector perturbation will have a large effect on the model outcome. To test the effectiveness of the method for our model, we will collect a set with parameter perturbations chosen with our proposed method and a set of randomly chosen ones. By comparing the two sets, the effectiveness of our method will be monitored. For each perturbed simulation within both sets, the fifth percentiles for the herbivores at both patches are calculated. The success rate of both methods is evaluated by the number of fifth percentiles within each set that are higher than the one of the reference run.

For the selection process that uses the short term behaviour of the model, we introduce the tangent linear and adjoint model (see Errico, 1997, for a clear description). Adjoint models have been commonly used for perturbations of initial conditions in for instance climate models (see Courtier et al, 1993, for an overview), and more recently for parameter perturbations (see e.g. Barkmeijer et al, 1996, Moolenaar and Selten, 2004). Because of the non-linear dynamics of the system, the tangent linear and adjoint models can only be used as approximations on a short time scale. Since we are interested in perturbations in parameters, the variable space consists of the state space extended with the parameter space. With the use of the tangent linear and adjoint model the perturbation in the parameters can be found that results in the largest deviation from the reference orbit in state space over a short time interval. This parameter perturbation vector is called the first right singular vector and the vector containing the error in the state variables at end time, the first left singular vector.

In this paper, a method is described that finds in an efficient way, parameter perturbations that cause a large shift in the fifth percentile of the herbivore subpopulations

for a long run. Because the parameter perturbation is small, a large negative effect is accompanied by a large positive effect in the opposite direction. Based on work done by Moolenaar and Selten (2004) we select certain (scaled) left singular vectors as parameter perturbation vectors that are likely to cause a large positive change in the extinction risk for a predefined species in the long run. The selection of these singular vectors is based on the first singular value being related to the direction of the largest error growth in the state vector. The best choice of the singular vector is at the moment just after the singular value has peaked. In this way, effective parameter perturbations can be selected on the basis of the short term behaviour. This selection process saves computing time compared to random selection of parameter perturbation, where the rate of success of selecting an effective parameter perturbation is extremely low.

5.1.3 Overview

This study is built up as follows. In Section 5.2 the models are formulated: the metapopulation model driven by the climate model. A reference run with unperturbed parameters is made and the distribution in time of the local populations is described. The fifth percentiles of the different subpopulations are given indicating the most vulnerable subpopulation. In Section 5.3 the tangent linear and the adjoint equations of the model are introduced. It is explained how they can be used to find the parameter perturbation that causes the largest error growth in state space for a short integration. This perturbation is called the first singular vector. It is described how our proposed method selects singular vectors from the evolution of the corresponding first singular value. We will analyse whether these singular vectors are successful in increasing the fifth percentiles of the considered subpopulations. In Section 5.4 parameter perturbations are added at random, in order to make a comparison with the constructed adjoint method. By comparing the success rates of the different methods, the efficiency of the adjoint method is evaluated. Finally, Section 5.5 contains our concluding remarks.

5.2 Distribution in time of the local population size

In this section, we describe a herbivore-predator metapopulation model containing two patches, between which only the herbivores can migrate. We use the Rosenzweig-MacArthur model (1963) for each patch. A migration term is added for the herbivores. The system of coupled differential equation reads:

$$\begin{aligned}
 \frac{dh_1}{dt} &= d_1(t)\left(1 - \frac{h_1}{K_1}\right)h_1 - \frac{h_1p_1}{h_1 + c_1} + w\left(\frac{h_2}{K_2} - \frac{h_1}{K_1}\right), \\
 \frac{dp_1}{dt} &= \frac{h_1p_1}{h_1 + c_1} - b_1p_1, \\
 \frac{dh_2}{dt} &= d_2(t)\left(1 - \frac{h_2}{K_2}\right)h_2 - \frac{h_2p_2}{h_2 + c_2} - w\left(\frac{h_2}{K_2} - \frac{h_1}{K_1}\right),
 \end{aligned}
 \tag{5.1}$$

$$\frac{dp_2}{dt} = \frac{h_2 p_2}{h_2 + c_2} - b_2 p_2,$$

where the state variables h_i and p_i denote the biomass of the herbivores and predators in patch i respectively. This type of herbivore-predator model is commonly used, see e.g. Sherratt et al. (1997), Rai and Anand (2004), Janssen (2001), Huang and Diekmann (2001). The parameters d_i are the intrinsic growth rates and K_i the carrying capacities of the herbivores; b_i are the death rates of the predators. The predator-prey interaction is of Holling type II (DeAngelis, 1992). The parameter c represents the reciproke of the slope at the origin of the functional response. Finally, w is the migration rate. Migration among habitat patches is of ecological interest, see e.g. Hanski et al. (2000), Ovaskainen and Hanski (2004), Ovaskainen (2004). Change of the migration rate may affect the local dynamics of populations and ultimately the entire metapopulation. The parameters are set at the following values:

$$b_1 = b_2 = 0.8, \quad c_1 = c_2 = 0.1, \quad w = 0.5, \quad K_1 = 0.5, \quad K_2 = 1. \quad (5.2)$$

In our model, we include the influence of climate fluctuations upon the herbivore population. To that end, the intrinsic growth rates d_1 and d_2 are made time dependent. The effect of climate fluctuations, especially climate change, upon population dynamics has a growing interest (i.e. Stenseth et al, 2002, Araújo et al, 2004, Preisser and Strong, 2004). The influence of the climate upon the metapopulation model is an external forcing and can lead to periods with low population sizes. A sudden extinction at such a stage from a catastrophic event is not taken in consideration. Such a behaviour should be described in a stochastic model (Burgman et al., 1993).

To mimic the climate, the Lorenz 84 equations (Lorenz, 1984) are introduced. It is a simple model of the atmospheric flow. The Lorenz 84 model is a strongly truncated spectral model of the atmospheric flow. It is defined by three coupled nonlinear differential equations

$$\begin{aligned} \frac{dx}{dt} &= e(-y^2 - z^2 - Ax + AF), \\ \frac{dy}{dt} &= e(xy - Bxz - y + G), \\ \frac{dz}{dt} &= e(Bxy + xz - z). \end{aligned} \quad (5.3)$$

The component x represents the strength of the zonal flow (westerly wind current) and the components y and z represent the strength of the amplitudes of respectively the cosine and sine phases of a chain of large superposed waves. The parameter F is a forcing from the north-south temperature gradient and G is a forcing from the continent-ocean temperature contrast. Parameter B represents the strength of the advection of the waves by the westerly current. The parameter e is introduced to alter the time scale of the climate model. In the original form of the model it is set $e = 1$. We choose e such that the influence of the climate upon the model is large. The model shows chaotic behaviour

for a large set of values in parameter space, from which we choose

$$A = 0.25, \quad B = 4, \quad F = 8, \quad G = 1 \quad e = 0.025. \quad (5.4)$$

The models (5.1) and (5.3) are coupled by assuming the following dependency of the intrinsic growth rates upon the climate:

$$d_1(t) = z(t; x_0, y_0, z_0) + \gamma, \quad d_2(t) = 3d_1(t), \quad (5.5)$$

where $\gamma = 2.5$, which is chosen such that $z(t) + \gamma > 0$ for all t . The vector (x_0, y_0, z_0) denotes the starting point in the Lorenz 84 model. Note that the time series for $z(t)$ is the same for both patches. Different time series could be taken, by taking a different starting point in each patch. This could be a choice when the two patches are at a large distance from each other, whereas for patches close together the same starting point could be taken.

We make a long run of 5000 time units, with the parameters set at the values mentioned above. This time interval, starting after a spin up, is sufficiently large to get a good insight in the viability of both herbivores and predators, taking the influence of climate into account. The evolution of the first 500 time units is shown in Figure 5.1. Out of the herbivores, the subpopulation in patch 2 is the most vulnerable to fluctuations although the carrying capacity is twice as high as in patch 1. However, the climate has a larger influence upon patch 2. As can be seen in Figure 5.1, h_2 has a higher maximum and a lower minimum than h_1 . Predator-prey interactions cause this large fluctuation of the herbivore at patch 2. As for the predators, the values of p_1 are a factor 100 smaller than those of p_2 .

In Table 5.1 minimum, fifth percentile, mean and maximum for h_1, p_1, h_2 and p_2 are given. The fifth percentile is the value below which the subpopulation is found 5 out of 100 times in a series of values calculated at fixed time intervals. The fifth percentiles of h_i and p_i are called r_{hi} and r_{pi} respectively and are calculated from the time series of 5000 time units. For each time unit 100 integration steps were used, so for each run we have a time series of 500000 points. Out of the herbivores, the one in patch 2, has the largest extinction risk, which is pointed out by the values $r_{h1} = 0.294$ and $r_{h2} = 7.80 \cdot 10^{-2}$. These fifth percentiles will be used to monitor the change in population dynamics when searching for the optimal parameter change, in the subsequent sections. The higher the fifth percentile, the better the conditions are for the corresponding subpopulation and the smaller the risk of local extinction.

To quantify the distribution of the size of a subpopulation, we calculate the histograms of the subpopulations. Figure 5.2 shows these histograms for h_1, p_1, h_2 and p_2 . These graphs are obtained by sampling the attractor of the system (5.1) at 500000 points with step size 0.01. The areas that contain the first 5% of the histograms are indicated. The histograms for the two herbivores, h_1 and h_2 , are shaped quite differently. The histogram of h_1 shows one peak at the larger values and shows a very small area in the neighbourhood of zero, whereas the histogram of h_2 shows another peak at the small values.

	min	fifth percentile	mean	max
h_1	$9.98 \cdot 10^{-2}$	0.294	0.408	0.479
p_1	$1.02 \cdot 10^{-2}$	$1.46 \cdot 10^{-2}$	$4.23 \cdot 10^{-2}$	$8.10 \cdot 10^{-2}$
h_2	$2.33 \cdot 10^{-2}$	$7.80 \cdot 10^{-2}$	0.518	0.883
p_2	0.269	0.979	2.36	4.57

Table 5.1: Minimum, fifth percentile, mean and maximum for h_1 , p_1 , h_2 and p_2 for an integration of 5000 time units long, with unperturbed parameters.

5.3 A method to select effective perturbations in a large parameter set

In this section, we analyse the effect of parameter perturbations upon the subpopulations. The perturbations that will improve the conditions of the population the most are of greatest interest. The parameters under consideration are b_1 , b_2 (the death rates of the predators), K_1 , K_2 (the carrying capacities of the herbivores) and w (the migration rate). The unperturbed (reference) parameter vector is represented by

$$\alpha_{\mathbf{r}} = (b_{1r}, b_{2r}, K_{1r}, K_{2r}, w_r)^T = (0.8, 0.8, 0.5, 1, 0.5)^T. \quad (5.6)$$

The parameter perturbations lie on a hypersphere, centred around $\alpha_{\mathbf{r}}$. The length of a perturbation vector $\delta\alpha = (\delta b_1, \delta b_2, \delta K_1, \delta K_2, \delta w)^T$ is limited. We choose to restrict it to 5% of the length of the reference parameter vector. This may be written as

$$\langle \delta\alpha, \delta\alpha \rangle^{1/2} = 0.05 \langle \alpha_{\mathbf{r}}, \alpha_{\mathbf{r}} \rangle^{1/2}, \quad (5.7)$$

where \langle, \rangle is the Euclidian inner product:

$$\langle x, y \rangle = \sum_i x_i y_i. \quad (5.8)$$

A perturbed vector in parameter space will take the form

$$\alpha_{\mathbf{p}} = \alpha_{\mathbf{r}} + \delta\alpha = (b_{1r} + \delta b_1, b_{2r} + \delta b_2, K_{1r} + \delta K_1, K_{2r} + \delta K_2, w_r + \delta w)^T. \quad (5.9)$$

The choice of this type of perturbation means that realisation of a change of each of the parameters with one unit costs a same (financial) effort. The method then yields combinations of parameter changes that are highly effective given a fixed small (financial) budget. In Section 5.5 it is discussed how to handle in case the effort per unit parameter change differs for each parameter.

A position in the state space is indicated by the vector

$$\mathbf{x} = (x, y, z, h_1, p_1, h_2, p_2)^T. \quad (5.10)$$

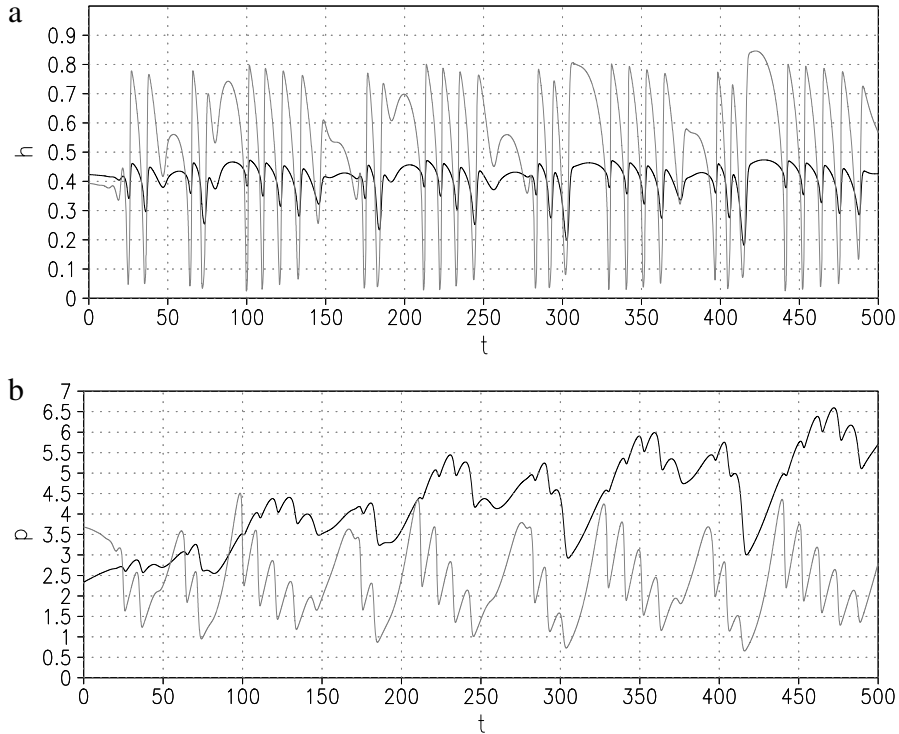


Figure 5.1: *a) Evolution of h_1 (black) and h_2 (gray) for 500 time units. b) Evolution of $100 \cdot p_1$ (black) and p_2 (gray) for 500 time units.*

The aim of this study is to find the parameter perturbations that will improve the chance of survival of a subpopulation most. Different objectives can be taken in consideration. We choose a single subpopulation: either the herbivore at patch 1 or the herbivore at patch 2. Other objectives may be chosen as well. Global species conservation may be the goal, then we have to consider a weighted sum of densities of species over all patches. If biodiversity should be maintained, then the minimum of all (sub)populations should be taken.

In this section we describe a method to select parameter perturbations within the large set formed by the hypersphere. This method needs to be effective in the sense that it has to have a high probability of drawing parameter perturbations that cause a large change in the output. In this case the output is the fifth percentile of the herbivore subpopulations. As remarked before a large negative effect is accompanied by a large positive effect with the perturbation vector pointing in the opposite direction.

With a high probability a parameter perturbation with a large effect is found from a linear analysis of the system behaviour near the reference orbit. For this purpose, the

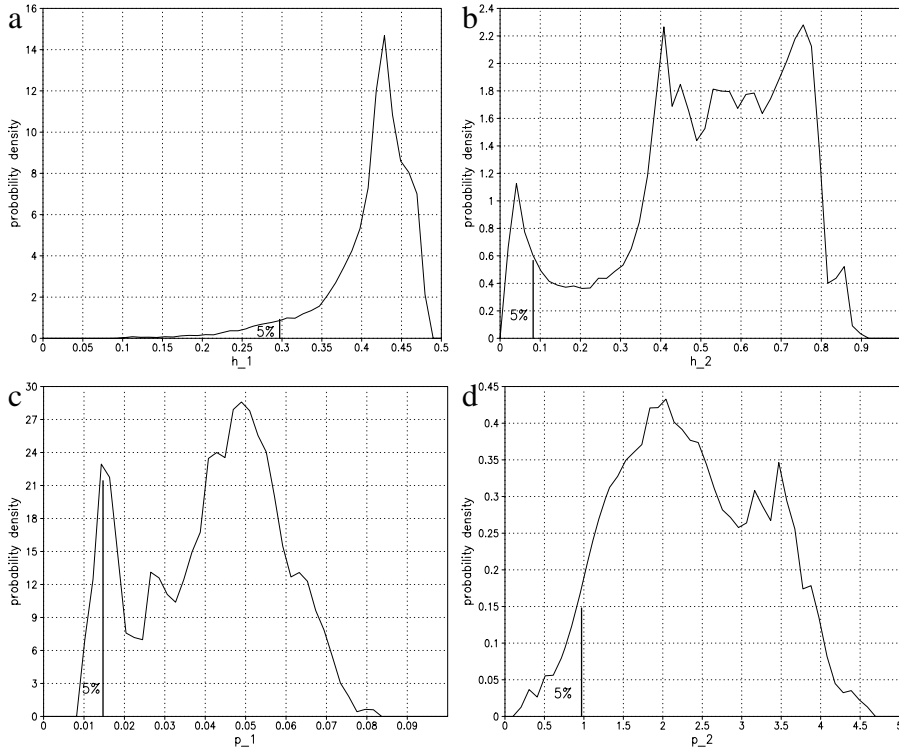


Figure 5.2: Histograms of the different subpopulations a) h_1 , b) h_2 , c) p_1 and d) p_2 , calculated with an integration of 5000 time units long.

tangent linear and adjoint equations that correspond with the system (5.1) are introduced. The system (5.1) has only a few parameters, it is presented as a case study here. The technique described can be used for dynamical systems with a much larger number of parameters. Then no alternative exists that selects an effective parameter perturbation within a realistic computing time. The idea is to use the short term behaviour of the model to obtain an indication of the long term behaviour of the model for a new set of parameters. If it is possible to identify on the basis of the short integrations, the parameter perturbations that will likely cause a large change in a long term integration, then this would save a considerable amount of computation time. Of course, due to the chaotic behaviour of the model, this cannot be achieved in an exact way, because the strange attractor cannot be scanned over its full (infinite) length. Moolenaar and Selten (2004) developed a method where certain points at the attractor were chosen, for which the parameter perturbations that caused the largest error growth on the short term, were also effective in changing the long term integration of the model. The short term integration can be carried out efficiently using the tangent linear and adjoint equations

of the model. This method was tested in the atmospheric Lorenz 63 model. We will now apply this method to the metapopulation model (5.1), coupled to the Lorenz 84 atmospheric model (5.3).

In Section 5.3.1 the tangent linear and the adjoint equations are formulated and a singular vector decomposition is made. In Section 5.3.2 it is explained how singular vectors can be used as parameter perturbations. In Section 5.3.3 the simulation results are discussed. A large set of likely effective perturbations is selected for which long integrations are made and it is verified whether these perturbations are indeed effective in the sense that the herbivore subpopulations are better conserved. In Section 5.3.4 it is shown why the singular value of the adjoint method is of importance for choosing a singular vector as a parameter perturbation vector.

5.3.1 Tangent linear and adjoint equations

The tangent linear and adjoint equations are useful tools to calculate the maximum error growth over a time interval sufficiently short for the linear approximation to hold. This can be applied to error growth due to small perturbations in the initial conditions. The method is commonly used for this purpose. It also applies to error growth due to small perturbations in the parameters. The tangent linear equations calculate the error growth over a short time period. With the corresponding adjoint operator, a singular value decomposition (SVD) can be made. The singular vector corresponding to the largest singular value is the vector that causes the maximum error growth.

First a short reference orbit with unperturbed parameters is calculated, using the nonlinear equations (5.1). These nonlinear equations are of the general form

$$\dot{\mathbf{x}} = \mathbf{F}_1(\mathbf{x}, \alpha), \quad (5.11)$$

where \mathbf{x} is a vector in state space, α a parameter vector and \mathbf{F}_1 contains the right hand side of the differential equations of the model. In order to allow perturbations in the parameters and to calculate the error growth they can cause, we need to extend the state vector \mathbf{x} with the parameter vector α , resulting in the vector \mathbf{q} :

$$\mathbf{q} = \begin{pmatrix} \mathbf{x} \\ \alpha \end{pmatrix}. \quad (5.12)$$

The extended version of the system equations are:

$$\dot{\mathbf{q}} = \begin{pmatrix} \dot{\mathbf{x}} \\ \dot{\alpha} \end{pmatrix} = \begin{pmatrix} \mathbf{F}_1(\mathbf{x}, \alpha) \\ \mathbf{F}_2(\alpha) \end{pmatrix} = \begin{pmatrix} \mathbf{F}_1(\mathbf{x}, \alpha) \\ \mathbf{0} \end{pmatrix} = \mathbf{F}(\mathbf{q}). \quad (5.13)$$

The parameters remain constant in time, that is why $\mathbf{F}_2(\alpha) = \mathbf{0}$. The parameter perturbations will however, cause a deviation in state space. This deviation from the reference orbit can be approximated using the tangent linear equations. The tangent linear equations are obtained by linearizing equation (5.13) around a reference (unperturbed) orbit

\mathbf{q}_r :

$$\begin{aligned}\dot{\mathbf{q}} &= \mathbf{F}(\mathbf{q}) \Rightarrow (\mathbf{q}_r + \delta \dot{\mathbf{q}}_r) = \mathbf{F}(\mathbf{q}_r + \delta \mathbf{q}_r) \approx \mathbf{F}(\mathbf{q}_r) + J\delta \mathbf{q}_r + \mathcal{O}(|\delta \mathbf{q}_r|^2) \\ &\Rightarrow \dot{\mathbf{q}}_r + \delta \dot{\mathbf{q}}_r \approx \mathbf{F}(\mathbf{q}_r) + J\delta \mathbf{q}_r, \\ &\Rightarrow \delta \dot{\mathbf{q}}_r \approx J\delta \mathbf{q}_r\end{aligned}\tag{5.14}$$

where J is the Jacobi matrix:

$$J = \frac{\partial \mathbf{F}(\mathbf{q})}{\partial \mathbf{q}} \Big|_{\mathbf{q}_r} = \begin{pmatrix} \frac{\partial \mathbf{F}_1(\mathbf{x}, \alpha)}{\partial \mathbf{x}} & \frac{\partial \mathbf{F}_1(\mathbf{x}, \alpha)}{\partial \alpha} \\ \frac{\partial \mathbf{F}_2(\alpha)}{\partial \mathbf{x}} & \frac{\partial \mathbf{F}_2(\alpha)}{\partial \alpha} \end{pmatrix} \Big|_{\mathbf{q}_r} = \begin{pmatrix} \frac{\partial \mathbf{F}_1(\mathbf{x}, \alpha)}{\partial \mathbf{x}} & \frac{\partial \mathbf{F}_1(\mathbf{x}, \alpha)}{\partial \alpha} \\ \mathbf{0} & \mathbf{0} \end{pmatrix} \Big|_{\mathbf{q}_r}.\tag{5.15}$$

The equation

$$\delta \dot{\mathbf{q}}_r(t) = J\delta \mathbf{q}_r(t)\tag{5.16}$$

is called the tangent linear equation. The evolution $\delta \mathbf{q}_r(t)$ in extended state space caused by a small initial perturbation $\delta \mathbf{q}_r(0)$ can be approximated using this tangent linear equation. However, we do not intend to perturb the initial state vector $\mathbf{x}_r(0)$, but only the parameter vector α_r . The perturbation $\delta \alpha_r$ is transformed into a perturbation $\delta \mathbf{q}_r(0)$ using a prolongation matrix P_2 :

$$\delta \mathbf{q}_r(\mathbf{0}) = P_2 \delta \alpha = \begin{pmatrix} \mathbf{0} \\ \delta \alpha \end{pmatrix}.\tag{5.17}$$

The evolution of this perturbation according to the tangent linear equation (5.16) may be denoted by the propagation matrix (also called the resolvent operator) R :

$$\delta \mathbf{q}_r(T) = R(0, T)\delta \mathbf{q}_r(0).\tag{5.18}$$

Since the perturbations in the parameters remain constant during the integration, we can write:

$$\delta \mathbf{q}_r(T) = \begin{pmatrix} \delta \mathbf{x}(T) \\ \delta \alpha(T) \end{pmatrix} = \begin{pmatrix} \delta \mathbf{x}(T) \\ \delta \alpha(0) \end{pmatrix}.\tag{5.19}$$

A projection matrix P_1 is used to extract the state space $\delta \mathbf{x}$:

$$P_1 \mathbf{q} = P_1 \begin{pmatrix} \mathbf{x} \\ \alpha \end{pmatrix} = \mathbf{x}.\tag{5.20}$$

The linear evolution of the error in the state variables can be formulated with the propagation matrix R :

$$\delta \mathbf{q}_r(T) = R(0, T) \cdot \delta \mathbf{q}_r(0).\tag{5.21}$$

Thus we have

$$\delta \mathbf{x}(T) = P_1 \delta \mathbf{q}_r(T) = P_1 R(0, T)\delta \mathbf{q}_r(0) = P_1 R P_2 \delta \alpha = M \delta \alpha,\tag{5.22}$$

where

$$M = P_1 R(0, T) P_2.\tag{5.23}$$

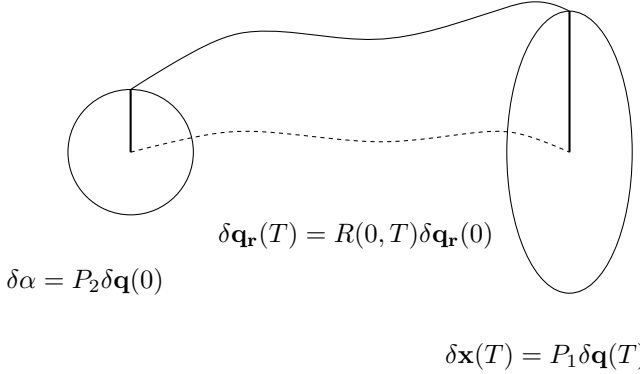


Figure 5.3: Schematic picture of the evolution of a perturbation in parameter space at initial time, into a deviation from the reference orbit in state space.

To recapitulate, the above matrix M is used to approximate the effect $\delta \mathbf{x}(T)$ on the final state vector caused by a perturbation $\delta \alpha_r$ of the parameter vector. This is depicted in Figure 5.3.

The adjoint of M , the operator M^* acts as a backward integration. Since M a real matrix, the adjoint is equal to M^T . The adjoint determines a perturbation at initial time given the output at end time. We are interested in the parameter perturbation that evolves into the singular vector corresponding to the largest singular value. This perturbation can be found as follows. For the length of $\delta \mathbf{x}(T)$ we have:

$$\frac{\langle \delta \mathbf{x}(T), \delta \mathbf{x}(T) \rangle^{1/2}}{\langle \delta \alpha(0), \delta \alpha(0) \rangle^{1/2}} = \frac{\langle M \delta \alpha(0), M \delta \alpha(0) \rangle^{1/2}}{\langle \delta \alpha(0), \delta \alpha(0) \rangle^{1/2}} = \frac{\langle M^T M \delta \alpha(0), \delta \alpha(0) \rangle^{1/2}}{\langle \delta \alpha(0), \delta \alpha(0) \rangle^{1/2}}, \quad (5.24)$$

where M^T is the transpose of M and \langle, \rangle is the Euclidian inner product. The factor (5.24) is maximized when $\delta \mathbf{q}_r(0)$ is the eigenvector of $M^T M$ with the largest eigenvalue. The eigenvalue problem becomes:

$$M^T M \mathbf{v} = \lambda \mathbf{v}. \quad (5.25)$$

These eigenvectors are called singular vectors of M . Singular vectors can be calculated by making a Singular Value Decomposition of matrix M :

$$M = U W V^T, \quad (5.26)$$

where U is a column-orthogonal matrix (containing the left singular vectors), W is a diagonal matrix with non-negative elements (the singular values) and V^T is the transpose of the orthonormal matrix V (containing the right singular vectors). These singular vectors are the eigenvectors of $M^T M$:

$$M^T M V = (U W V^T)^T (U W V^T) V = V W U^T U W V^T V = V W^2 V^T V = V W^2 \quad (5.27)$$

and the eigenvalues are equal to the squares of the singular values in W . The matrix M projects the right singular vectors (in parameter space) onto the left singular vectors (in state space).

$$MV = UWW^TV = UW. \quad (5.28)$$

When the elements of W are put in increasing order, the first left singular vector is the vector that maximizes (5.24). It is the first principal axis of the ellipsoid of Figure 5.3. The first right singular vector in parameter space is the perturbation vector that caused this largest deviation. For further reading on adjoint equations we refer to Errico (1997) and to Lawson et al. (1995), who also apply this method to a model in population dynamics.

5.3.2 Singular vectors as parameter perturbations

We will now use the mathematical techniques described in the previous section, on the metapopulation model (5.1)-(5.5). In this case, the vector \mathbf{x} in state space and the vector α in parameter space read:

$$\mathbf{x} = (x, y, z, h_1, p_1, h_2, p_2)^T, \quad \alpha = (b_1, b_2, K_1, K_2, w)^T. \quad (5.29)$$

The tangent linear equations for x , y and z do not have to be considered because these variables do not depend on the parameter vector α . For the other variables we have:

$$\begin{aligned} \frac{d\delta h_1}{dt} = & [(z + 2.5)(1 - 2\frac{h_1}{K_1}) - \frac{p_1}{h_1 + c_1} + \frac{h_1 p_1}{(h_1 + c_1)^2} - \frac{w}{K_1}] \delta h_1 + \quad (5.30) \\ & [-\frac{h_1}{h_1 + c_1}] \delta p_1 + [\frac{w}{K_2}] \delta h_2 + [(z + 2.5)(\frac{h_1}{K_1})^2 + w \frac{h_1}{K_1^2}] \delta K_1 + \\ & [-w \frac{h_2}{K_2^2}] \delta K_2 + [\frac{h_2}{K_2} - \frac{h_1}{K_1}] \delta w, \end{aligned}$$

$$\frac{d\delta p_1}{dt} = [\frac{p_1}{h_1 + c_1} - \frac{h_1 p_1}{(h_1 + c_1)^2}] \delta h_1 + [\frac{h_1}{h_1 + c_1} - b_1] \delta p_1 + [-p_1] \delta b_1, \quad (5.31)$$

$$\begin{aligned} \frac{d\delta h_2}{dt} = & [\frac{w}{K_1}] \delta h_1 + \quad (5.32) \\ & [3(z + 2.5)(1 - 2\frac{h_2}{K_2}) - \frac{p_2}{h_2 + c_2} + \frac{h_2 p_2}{(h_2 + c_2)^2} - \frac{w}{K_2}] \delta h_2 + \\ & [-\frac{h_2}{h_2 + c_2}] \delta p_2 + [-w \frac{h_1}{K_1^2}] \delta K_1 + [3(z + 2.5)(\frac{h_2}{K_2})^2 + w \frac{h_2}{K_2^2}] \delta K_2 + \\ & [\frac{h_1}{K_1} - \frac{h_2}{K_2}] \delta w, \end{aligned}$$

$$\frac{d\delta p_2}{dt} = [\frac{p_2}{h_2 + c_2} - \frac{p_2 h_2}{(h_2 + c_2)^2}] \delta h_2 + [\frac{h_2}{h_2 + c_2} - b_2] \delta p_2 + [-p_2] \delta b_2, \quad (5.33)$$

$$\frac{d\delta b_1}{dt} = 0, \quad (5.34)$$

$$\frac{d\delta K_1}{dt} = 0, \quad (5.35)$$

$$\frac{d\delta b_2}{dt} = 0, \quad (5.36)$$

$$\frac{d\delta K_2}{dt} = 0, \quad (5.37)$$

$$\frac{d\delta w}{dt} = 0. \quad (5.38)$$

For each short model run, starting at a certain point at the attractor, the corresponding first singular vector and singular value are calculated. The runs must be short enough so that the linear approximation is sufficiently accurate. In this case the time interval is taken 200 time units long. The singular vectors and their singular values depend on the starting point of the run. We make a short model run, calculate the first singular vector and its singular value, and next make another short model run, starting at the end point of the previous run. By plotting the consecutive singular values, we obtain the evolution of the first singular value, see Figure 5.4.

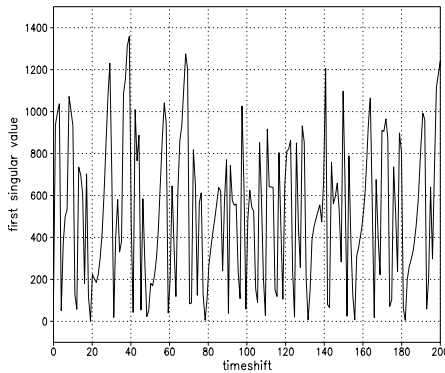


Figure 5.4: *Evolution of the first singular value*

As can be seen, the first singular value fluctuates rapidly. When the singular value is large (in a high peak), the maximum error growth is large and it can be said that the corresponding reference orbit is then very sensitive to parameter perturbations. Our hypothesis, based on the study Moolenaar and Selten (2004) with the Lorenz 63 model, is that a singular vector corresponding to the singular value in the first local minimum after a high peak, is likely to be a direction for a parameter perturbation that causes a large change in a long model run. For a peak in the evolution of the first singular value, we require that it has exceeded the value 1000. The singular vector that corresponds to the singular value in the first local minimum after this peak, will then be selected. A parameter perturbation will now be added to the model for which a large run will be made. It is in the same direction as the selected singular vector in the short run of the

linearized system, but its length will be scaled:

$$\langle \delta\alpha, \delta\alpha \rangle^{1/2} = 0.05 \langle \alpha_{\mathbf{r}}, \alpha_{\mathbf{r}} \rangle^{1/2}, \quad (5.39)$$

where $\delta\alpha$ is the perturbation vector and $\alpha_{\mathbf{r}}$ is the parameter vector containing the original values.

In order to test whether our hypothesis holds for the model (5.1), 25000 long runs will be made, each time with a different singular vector as parameter perturbation. This singular vector has a singular value in a local minimum, and will be scaled such that its length is 5% of the length of the original parameter, see (5.39). In order to find different singular vectors that we can use, we computed a long sequence of singular values. A peak of value 1000 or higher occurred on average every 15 runs, so for 25000 useful singular vectors, around 375000 consecutive short integrations and singular value decompositions are needed. The simulation results are described in Section 5.3.3. For comparison, again 25000 perturbed long runs will be made, but this time with different randomly directed parameter vector perturbations scaled to the same length, as in (5.39). The efficiency of this random method is described in Section 5.4, where we compare it with the efficiency of our method.

5.3.3 Simulation results

In this section we apply the adjoint method for finding effective parameter perturbations. We compute 25000 long runs each with a different first singular vector, corresponding to a singular value in a local minimum, as a parameter perturbation. All long runs are integrated over 5000 time units and start after a spin up. For each perturbed run, the fifth percentiles of the different subpopulations are calculated, so for each population group we have 25000 different fifth percentiles. The probability densities of these fifth percentiles are shown in the histograms of Figure 5.5. The values for the fifth percentiles for the unperturbed run are pointed out in the Figure by `h1_ref`, `h2_ref`, `p1_ref` and `p2_ref`.

Figure 5.5 a) shows the result for herbivore h_1 . This histogram has only a small range and is bounded by 0.330 and 0.415 on the horizontal axis. All the fifth percentiles in this histogram are larger than reference value, `h1_ref`, meaning all perturbation vectors lead to an improvement of h_1 . The histogram is skew and has its maximum towards the right indicating that the majority of the parameter perturbations have a fifth percentile that is close to the maximum. The maximum for r_{h_1} , 0.415, is 1.4 times larger than the reference value, 0.294. The histogram for the second herbivore population is shown in Figure 5.5 b). The histogram is bounded by 0.228 and 0.470. This has a wider range than the histogram for herbivore h_1 . The histogram is skew with its maximum towards the right. So, even though all these values are larger than the reference value `h2_ref`, not all of all of them are close to the maximum. The maximum of r_{h_2} found, 0.470, is six times larger than the reference value, $7.80 \cdot 10^{-2}$, which shows that a large improvement is possible for the conditions of herbivore h_2 , more so than for h_1 .

Figures 5.5 c) and d) show the histograms for the predators p_1 and p_2 . Since we are only interested in improving the conditions for the herbivores, we will not go into detail here. Two remarks will be made however. For the predator p_1 , 88% of the selected singular vectors, worsen the conditions for p_1 , whereas, 69% of the selected singular vectors improve the conditions for p_2 . So the chosen parameter perturbations are likely to be favourable for predator p_2 and at the same time disagreeable for predator p_1 . Secondly, perturbations are drawn that result in the extinction of p_1 . Without a predator in patch 1, the herbivore in this patch has a greater chance of survival. More herbivores will migrate to patch 2, which is favourable for the predators in that patch.

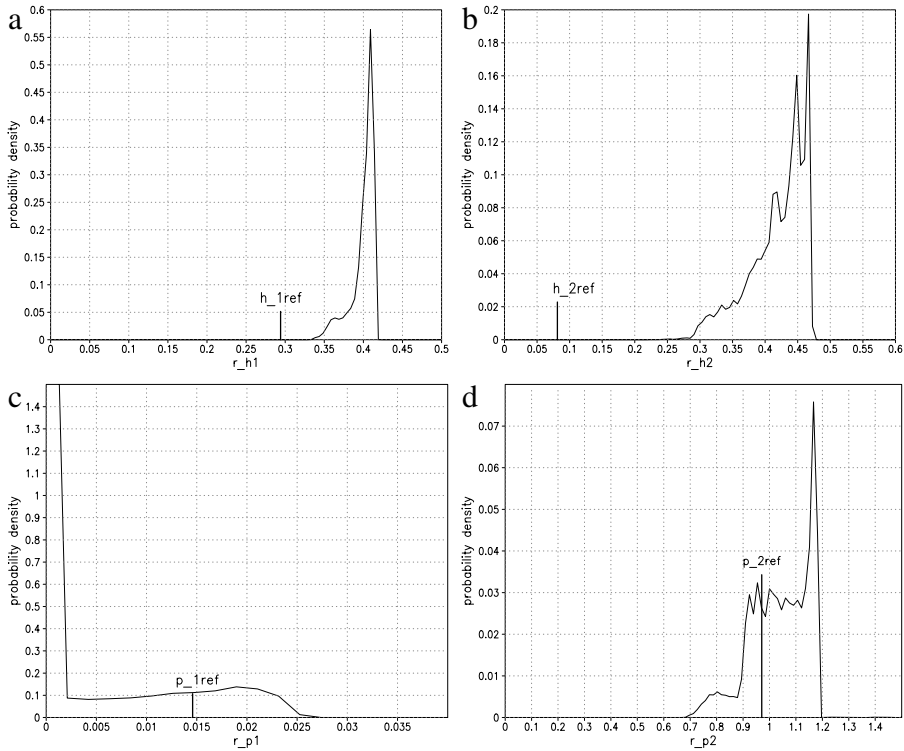


Figure 5.5: Histograms of the fifth percentiles, where the direction of the first singular vector (with small singular value) is used as parameter perturbation. For each histogram 25000 long integrations are made. a) h_1 b) h_2 c) p_1 d) p_2 .

In Figure 5.6 the values for r_{h1} are plotted against the values of r_{h2} . For each perturbed run both r_{h1} and r_{h2} were calculated and these two values can be plotted in a (r_{h1}, r_{h2}) -plane. This figure shows that the selected parameter perturbations that yield the larger values for r_{h1} also yield larger values for r_{h2} . Thus, effective parameter perturbations are in fact favourable for both herbivores.

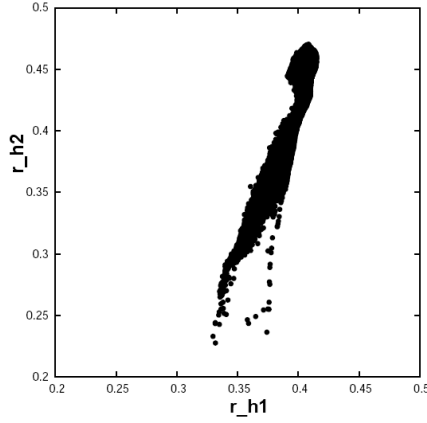


Figure 5.6: (r_{h1}, r_{h2}) -plane for the model runs with selected singular vectors as parameter perturbations.

The parameter perturbation vector, found with this adjoint method, that gave the best improvement for the **herbivore subpopulation at patch 1** is the vector

$$(\delta b_1, \delta b_2, \delta K_1, \delta K_2, \delta w) = (2.88 \cdot 10^{-2}, 6.30 \cdot 10^{-2}, 3.82 \cdot 10^{-2}, 2.27 \cdot 10^{-2}, 1.36 \cdot 10^{-2}). \quad (5.40)$$

The parameters are then set as

$$(b_1, b_2, K_1, K_2, w) = (0.829, 0.863, 0.538, 1.023, 0.514). \quad (5.41)$$

The fifth percentile r_{h1} changes from 0.294 (reference orbit) to 0.415. In Figure 5.7 the evolution of the different populations computed with these new parameters are shown for the first 500 time units (dashed lines). As a reference the evolutions calculated with the unperturbed parameters are plotted as well (solid lines). Table 5.2 gives the minimum, fifth percentile, mean and maximum for the different populations, computed for a run of 5000 time units. Figure 5.7 a) shows the results for the herbivores h_1 (black) and h_2 (grey). It can be seen that for both populations the perturbed run has less fluctuations, the trajectories stay longer at high values and there are less local minimum. Figure 5.7 b) shows the results for the predators p_1 (black) and p_2 (grey). Note that for the reference evolution (solid line) p_1 is multiplied by a factor 100 and that for the perturbed evolution (dashed line) p_1 is multiplied by a factor 1000. This shows that p_1 has decreased remarkably. Its values still fluctuate, but this can't be seen well at this scale. For p_2 it can be seen that the fluctuations have become less rapid. Comparing the results of Tables 5.1 and 5.2 we see that for both herbivores the minimum as well

as the maximum values have increased. For this parameter perturbation that gave the largest r_{h1} , also resulted in a large r_{h2} . In fact, this r_{h2} is 97% of the largest r_{h2} found. For p_1 conditions have deteriorated, the minimum and maximum value have decreased much and so has r_{p1} . The minimum value for p_2 has increased, but its maximum has decreased. However, taking our indicator as measure conditions seem to have improved for this population, since r_{p2} has a slightly larger value.

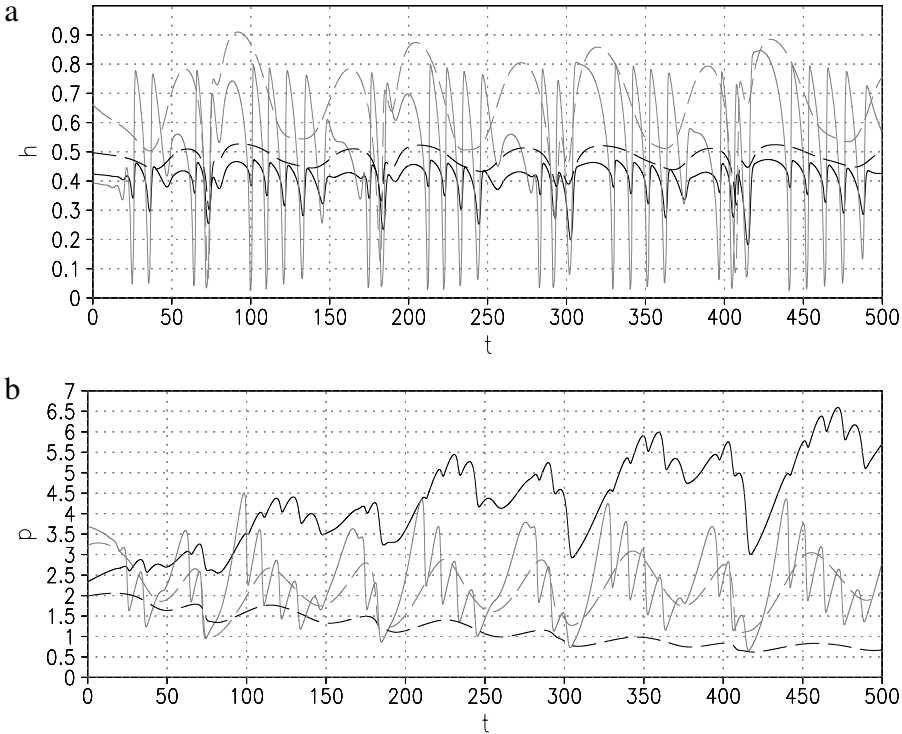


Figure 5.7: a) Evolution of h_1 (black) and h_2 (grey) for first 500 time units out of a 5000 time unit integration. b) Evolution of p_1 (black) and p_2 (grey) for first 500-time units out of a 5000 time unit integration. Solid lines are the evolutions with the unperturbed parameters, dashed lines are the evolutions perturbed with the singular vector (with a singular value that occurred after a high peak) that yielded the largest r_{h1} . Note that p_1 is multiplied by a factor 100 for the solid line and by a factor 1000 for the dashed line.

The parameter perturbation vector, found with the adjoint method, that gave the best improvement for the **herbivore subpopulation in patch 2** is the vector

$$(\delta b_1, \delta b_2, \delta K_1, \delta K_2, \delta w) = (3.44 \cdot 10^{-2}, 6.74 \cdot 10^{-2}, 2.91 \cdot 10^{-2}, 1.38 \cdot 10^{-2}, 1.38 \cdot 10^{-2}). \quad (5.42)$$

	min	fifth percentile	mean	max
h_1	0.183	0.415	0.479	0.528
p_1	$1.46 \cdot 10^{-8}$	$2.22 \cdot 10^{-8}$	$1.84 \cdot 10^{-4}$	$2.06 \cdot 10^{-3}$
h_2	$4.58 \cdot 10^{-2}$	0.456	0.674	0.951
p_2	0.341	1.00	2.11	3.30

Table 5.2: Minimum, fifth percentile, mean and maximum for h_1 , p_1 , h_2 and p_2 for the integration of 5000 time units long, with the first singular vector with small singular value as parameter perturbation, that yields the largest r_{h_1} .

The parameters are now set as

$$(b_1, b_2, K_1, K_2, w) = (0.834, 0.867, 0.529, 1.014, 0.514). \quad (5.43)$$

The value of r_{h_2} changes from 0.0780 (reference orbit) to 0.478. Figure 5.8 shows the evolution of the first 500 time units for a) the herbivores, and b) the predators. These evolutions are quite similar to the ones in Figure 5.7, except for p_1 , which is now multiplied by a factor 100000 for the perturbed simulation. Table 5.3 shows the minimum, fifth percentile, mean and maximum for the simulation with the perturbation that yields the largest r_{h_2} . Again, this parameter perturbation also yields a large improvement for the herbivore h_1 , in the other patch, which is shown by r_{h_1} which is 98% of the maximum r_{h_1} found.

	min	fifth percentile	mean	max
h_1	0.166	0.408	0.475	0.521
p_1	$9.27 \cdot 10^{-27}$	$7.56 \cdot 10^{-25}$	$1.02 \cdot 10^{-7}$	$4.74 \cdot 10^{-6}$
h_2	$4.79 \cdot 10^{-2}$	0.470	0.697	0.954
p_2	0.301	0.887	1.96	3.06

Table 5.3: Minimum, fifth percentile, mean and maximum for h_1 , p_1 , h_2 and p_2 for the integration of 5000 time units long, with the first singular vector with small singular value as parameter perturbation, that yields the largest r_{h_2} .

In Figure 5.9 histograms of the distribution in time of the subpopulations sizes are shown. The histograms of the reference simulation are shown (solid grey lines), along with the histograms where the model is perturbed with the singular vector that yields either the largest r_{h_1} (solid black lines) or the largest r_{h_2} (dashed black lines). In Figure 5.9 a) the different histograms for h_1 are shown. It is clear that both perturbations result in a shift of the histogram towards the right. The histograms of h_2 are shown in Figure 5.9 b). These histograms also show a shift to the right and the peak between the values 0 and 0.1 that is clearly present in the unperturbed histogram has nearly vanished in the perturbed histograms. In the perturbed runs there are for h_2 much less values that are lower than 0.5. Figure 5.9 c) shows the histograms for p_1 . Conditions have worsened

considerably in the perturbed runs for this predator. Both histograms lie far left in this figure. For the second predator, p_2 , the ranges of the perturbed histograms have become smaller especially at the upper bound, as can be seen in Figure 5.9 d).

The two differences between the two patches are that the intrinsic growth rate, which depends on the climate fluctuations, of patch 2 is 3 times higher and its carrying capacity is twice as high as in patch 1. The optimal parameter perturbation for the herbivores in patch 1 (5.41) have higher predator death rates than the optimal parameter perturbation for the herbivores in patch 2 (5.43), whereas the carrying capacities are higher for patch 2. For both parameter perturbation vectors, the perturbation in the death rate of the predator in patch 2 is the largest component. The migration rates are approximately the same.

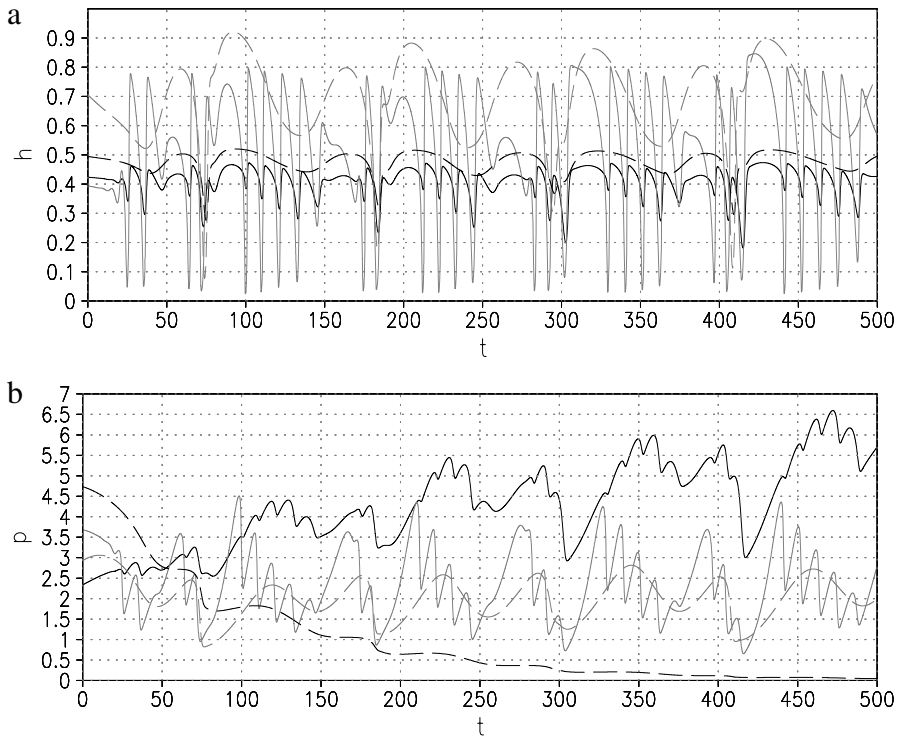


Figure 5.8: *a) Evolution of h_1 (black) and h_2 (grey) for first 500 time units out of a 5000 time unit integration. b) Evolution of p_1 (black) and p_2 (grey) for first 500-time units out of a 5000-time unit integration. Solid lines are the evolutions with the unperturbed parameters, dashed lines are the evolutions perturbed with the singular vector (with a singular value that occurred after a high peak) that yielded the largest r_{h_2} . Note that p_1 is multiplied by a factor 100 for the solid line and by a factor 1000000 for the dashed line.*

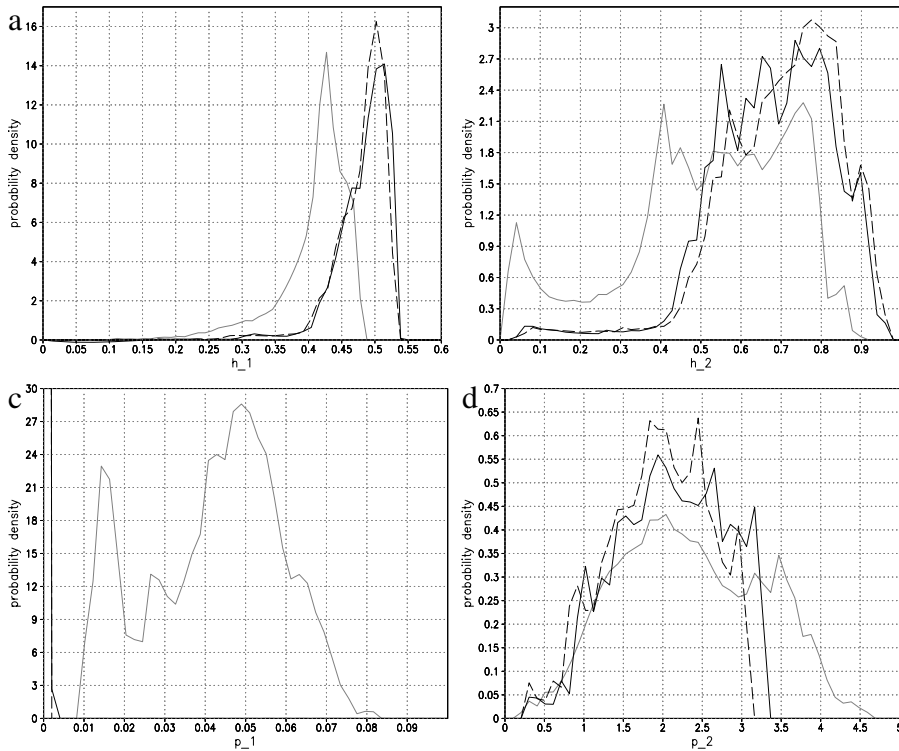


Figure 5.9: Histograms of the different subpopulations a) h_1 . b) h_2 . c) p_1 . d) p_2 . Grey: unperturbed, black solid: perturbed with singular vector that yielded largest r_{h1} , black dashed: perturbed with singular vector that yielded largest r_{h2} .

5.3.4 Importance of the singular value

In the previous subsection we showed that the first singular vector that correspond to a singular value that occurs just after a high peak in its evolution, has a high probability to be a parameter perturbation that is effective in improving the conditions for the herbivores. This method of finding effective parameter perturbations was first evaluated for the Lorenz 63 model (Moolenaar and Selten, 2004) and now proves to be effective in a metapopulation model as well. The method was first developed on the basis of empirical findings, see Section 1.3. The question why these particular singular vectors are effective remains to be answered. We can however, compare the singular vectors that correspond to a singular value *after* a high peak, with the singular vectors that correspond to a singular value *in* a high peak. A high singular value means that the short run is very sensitive to small parameter perturbations. Thus, one might be tempted to choose the perturbations in the direction of the singular vectors that correspond to

singular values *in* a high peak.

In Figure 5.10 the histograms of the fifth percentiles for the different populations are shown for this alternative method (dashed dotted lines). The solid black lines are the histograms that correspond with the results of the adjoint method described in the previous section. Now, 25000 long term integrations were made with different singular vectors corresponding to singular values in a high peak. The histograms for the herbivores are shown in Figure 5.10 a) and b) for h_1 and h_2 respectively. It can be seen immediately that these perturbations are not as effective as the singular vectors chosen with the previous adjoint method. The histograms for the herbivores are much closer to the reference values, $h1_ref$ and $h2_ref$ and they do not reach the largest values of r_{h1} and r_{h2} by far. For the predators these newly selected singular vectors have mainly a positive effect on p_1 , but a negative effect on p_2 .

The above considerations land us to the conclusion that the singular vectors corresponding to singular values that occur *after* a high peak, that is after a sensitive area, are far more likely to be parameter perturbations that are effective in improving the conditions for the herbivores, than the singular vectors corresponding to singular values *in* a high peak, that is exactly in a sensitive area.

5.4 Random selection of parameter perturbations

In this section, the adjoint method is compared with a random method. For the random method, perturbation vectors are drawn at random from a uniform hypersphere in parameter space, centred at the reference parameters. Again we require that the length of the perturbation vectors, $\delta\alpha$ is 5% of the length of the parameter vector that contains the unperturbed parameters, α_r , so

$$\langle \delta\alpha, \delta\alpha \rangle^{1/2} = 0.05 \langle \alpha_r, \alpha_r \rangle^{1/2}, \quad (5.44)$$

where \langle, \rangle is the Euclidian inner product.

Figure 5.11 shows the histograms of all the populations for both the adjoint method from Section 5.3.3 and the random method. The solid lines are the histograms of the adjoint method and the dashed lines depict the histograms of the random method. Figure 5.11 a) shows the two different histograms for herbivore h_1 . The random method gives values for r_{h1} between 0.038 and 0.426. It looks like a unimodal function with 36% of its values on the right hand side of $h1_ref=0.294$, which is the value of r_{h1} when using the unperturbed parameters. This means that only 36% of the randomly chosen perturbation vectors yield an improvement. The range of the histogram of the adjoint method lies at the very right of the histogram that belongs to the random method. This clearly shows that the adjoint method has a much higher probability of drawing parameter perturbations that will improve the population of h_1 than the random method does.

The histograms for the different methods for the second herbivore population are shown in Figure 5.11 b). Here, for the random method, the values of r_{h2} lie between 0.0141 and 0.562. The reference value, $h2_ref=7.80 \cdot 10^{-2}$ lies much to the left of

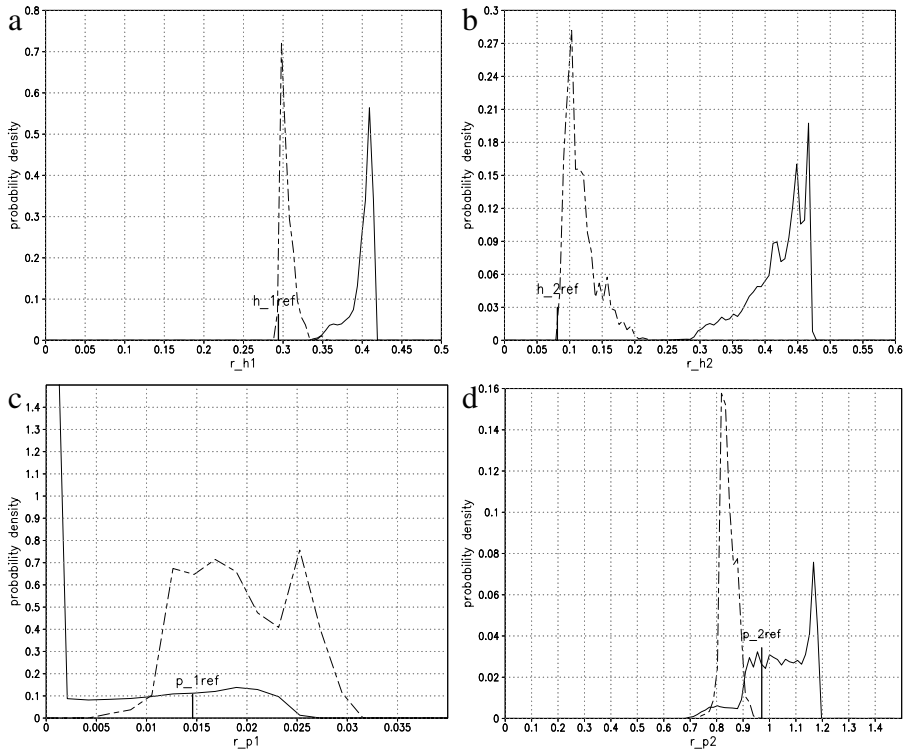


Figure 5.10: Histograms of the fifth percentile of different methods, solid black line is first singular vector (with small singular value after a peak) as perturbation and dashed-dotted black line is first singular vector (with large singular value in a peak). For each histogram 25000 long integrations are made. a) h_1 b) h_2 c) p_1 d) p_2 .

this histogram, however 46% of the drawn vectors give a value for r_{h2} that is larger than $h2_{ref}$. The histogram shows that much improvement is possible for this herbivore subpopulation, since the largest r_{h2} found is seven times larger than $h2_{ref}$. The histogram of the adjoint method lies in the right side of the histogram of the random method, but does not quite reach its largest value. However, it can be said again that the adjoint method has a higher probability of drawing parameter perturbations that will improve the population of h_2 , than the random method.

Figures 5.11 c) and d) show the different histograms for the predators p_1 and p_2 . For predator p_1 we have that 52% of the random perturbation vectors worsen its conditions, compared to 88% of the perturbation vectors drawn with the adjoint method. This means that the adjoint method is more likely to draw perturbation vectors that worsen the conditions for p_1 . The random method has a higher probability to draw perturbation vectors that worsen the conditions for p_2 than to improve them. Here, 73%

of the perturbation vectors worsen the conditions of p_2 . So for this predator the adjoint method is more beneficial than the random method.

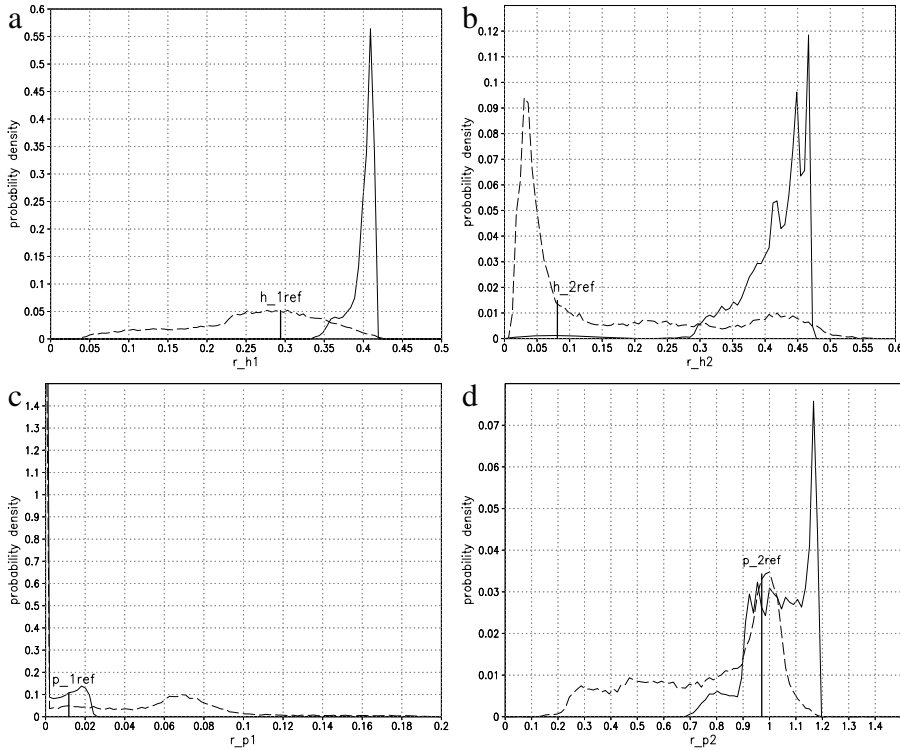


Figure 5.11: Histograms of the fifth percentile of different methods, solid black line is first singular vector (with small singular value after a peak) as perturbation, dashed line is random perturbation, For each histogram 25000 long integrations are made. a) h_1 b) h_2 c) p_1 d) p_2 .

Let us first consider the parameter choice that leads to the largest improvement for the **herbivore subpopulation at patch 1**. The randomly chosen parameter perturbation vector, that yields the largest r_{h1} ($= 0.424$) is

$$(\delta b_1, \delta b_2, \delta K_1, \delta K_2, \delta w) = (3.50 \cdot 10^{-2}, 5.02 \cdot 10^{-2}, 5.58 \cdot 10^{-2}, -9.54 \cdot 10^{-3}, -7.42 \cdot 10^{-4}). \quad (5.45)$$

Note that this vector contains both positive and negative values. The new parameters are:

$$(b_1, b_2, K_1, K_2, w) = (0.835, 0.850, 0.556, 0.990, 0.499). \quad (5.46)$$

For this parameter perturbation, the perturbation in the carrying capacity of herbivore 1 is the largest component. The perturbation in the death rate of predator 2 is not as large as the ones in the optimal parameter changes found with the adjoint method. Furthermore, the changes in the carrying capacity of herbivore 2 and the migration rate are in the negative direction and a factor 10 and 100 respectively smaller than the other changes.

For the **herbivore subpopulation at patch 2** we obtain the following. The randomly chosen parameter perturbation vector, that yields the largest r_{h2} ($= 0.562$) is

$$(\delta b_1, \delta b_2, \delta K_1, \delta K_2, \delta w) = (7.26 \cdot 10^{-3}, 8.28 \cdot 10^{-2}, 4.15 \cdot 10^{-3}, -3.96 \cdot 10^{-3}, 1.56 \cdot 10^{-3}). \quad (5.47)$$

Note again that this vector contains both positive and negative values. The new parameters are:

$$(b_1, b_2, K_1, K_2, w) = (0.807, 0.883, 0.504, 0.996, 0.502). \quad (5.48)$$

In this perturbation vector is dominated in the positive b_1 direction by far, it is a factor 10 higher than the perturbations in the other directions.

As in the previous case, the value of r_{h2} exceeds the largest value found with the singular vectors as parameter perturbations. Thus, the best improvements for both herbivore subpopulations obtained with the random method are just better than the ones obtained with the adjoint method. However, when drawing a random parameter perturbation and a perturbation selected with the adjoint method we see from the Figures 5.11 a,b that the probability that the random one is better is extremely small.

5.5 Concluding remarks

This study is set out to find parameter perturbations that optimally change the population dynamics in a metapopulation model, in the sense that locally herbivores have a better chance of survival. The parameters in the model we use are not based on data. In fact the herbivores and predators of our model do not represent real world biological species. The parameters are chosen within realistic boundaries in order to capture different characteristic dynamics. It is assumed that the cost of changing a parameter is the same for each parameter. The maximum change is 5% of the length of the original parameter vector. This can be thought of as having a perturbation set that lies in a unit hypersphere that is centred around the original parameter values. A perturbation that is drawn from this unit sphere is then scaled such that the length of this vector is 0.05 times the length of the vector containing the original parameter values as its elements. Of course, this results in a numerous amount of possible parameter perturbations. Assumingly a lot of the perturbation vectors will not have much effect on the dynamics for a long simulation. It is of interest to find the parameter perturbations that will change the population dynamics the most for a long simulation, especially in terms of conservation of populations. Conservation of a population was measured using the

fifth percentile of each population group. The higher this fifth percentile, the better the change of survival for this particular population. The method we developed can also be used for the purpose of making a sensitivity analysis. It shows which parameters affect the output the most in case parameters change their value. It also answers the question about the uncertainty in the model output given the uncertainty in the parameter values. For realistic models, parameter values are estimated with the use of data and knowledge of the underlying (physical) processes. However, this data can be insufficient and inaccurate, leading to errors in the parameter estimates (Moilanen, 2002, Conroy et al., 1995, Akçakaya, 2000, Drechsler et al., 2003).

A method to find optimal parameter perturbations for conserving populations was presented in Section 5.3. The tangent linear and adjoint model were used to calculate singular vectors. The first right singular vector lies a unit sphere in parameter space, centred around the reference parameter values. It evolves into the first left singular vector that gives the largest deviation from the reference solution at end time. These calculations are made for a short time period, because the linear approximation of the model needs hold with a sufficient accuracy. In the adjoint method that is tested in this study, certain parameter perturbations that are optimal in changing the population dynamics in a short model run, turned out to also be optimal in a long model run. The selection of the singular vectors was based on the singular value. When computing consecutive runs, where the initial condition of a next run is the end point of the previous run, the evolution of the singular value can be observed. It turned out that the singular vector corresponding to a singular value that occurred after a high peak was likely to be an optimal parameter perturbation in terms of conserving the herbivores. All the perturbations selected by this method resulted in fifth percentiles that were larger than the original fifth percentiles, for the herbivores. The largest fifth percentile found for the herbivore in patch 1 was 1.4 times larger than the original value. For the herbivore in patch 2 the possibility for improvement turned out to be even larger, the largest fifth percentile found for this population was 6 times larger than the original value.

To test the above selection procedure, also singular vectors were selected that correspond to a singular value in a high peak. The larger a singular value, the more sensitive the (linear) model is to parameter perturbations, for a short integration time. However, these perturbation vectors were not as effective in a long simulation as the previous ones. They did yield improvement for the herbivores. All the fifth percentiles were larger than the original value, however, they were smaller than the ones found with the singular vectors corresponding to a value in a local minimum, after a high peak. This same result was found in Moolenaar and Selten (2004) where these techniques were applied to a simple atmospheric model.

The adjoint method was also compared to a random method. In the random method, parameter perturbations were drawn from the unit sphere centred around the original values, with a uniform distribution. These perturbations yielded to both improved and worsened conditions for the herbivores. For the first herbivore only 36% lead to an improvement, whereas 46% improved the conditions for the second herbivore. Figure 5.11 shows the histograms of the fifth percentiles for both the adjoint and the random method for the different populations. It can be seen that for the herbivores, the

adjoint method draws parameter perturbations that yield fifth percentiles that lie on the right side of the histogram corresponding to the fifth percentiles calculated with the randomly chosen parameter perturbations. It can be concluded that the parameter perturbation vectors drawn with the adjoint method have a higher probability to be effective in improving the conditions for the herbivores, than the random method.

In this study it is assumed that the cost to change a parameter is the same for all. We may drop this assumption and allow to parameters, for which the change by one unit costs less effort, a larger range than for the others. This can be done by adding a matrix containing weights to the norm. The unit sphere in parameter space will be scaled. It will still be a unit sphere, only with respect to a different norm. Initially we had

$$\langle \delta\alpha, \delta\alpha \rangle = 1, \quad (5.49)$$

where $\delta\alpha$ is the vector containing the parameter perturbations. A diagonal matrix D will be added, with as its diagonal elements ϵ_i the weighing factors. If for instance, we want to allow the first parameter α_1 a perturbation twice as large as the for the other parameters, we take $\epsilon_1 = \frac{1}{2}$ and the value 1 for the other diagonal elements. We now have for the unit sphere at initial time:

$$\langle D\delta\alpha, D\delta\alpha \rangle = 1. \quad (5.50)$$

The optimization problem now becomes:

$$\frac{\langle \delta\mathbf{x}(T), \delta\mathbf{x}(T) \rangle^{1/2}}{\langle D\delta\alpha(0), D\delta\alpha(0) \rangle^{1/2}} = \frac{\langle D^T M^T M D \delta\alpha_{\mathbf{r}}(0), \delta\alpha_{\mathbf{r}}(0) \rangle^{1/2}}{\langle D\delta\alpha(0), D\delta\alpha(0) \rangle^{1/2}}, \quad (5.51)$$

and a singular value decomposition needs to be made with $D^T M^T M D$. Proceeding with the computations in this way we find that the parameter perturbation vector then becomes $D^{-1}v$.

The adjoint technique proved to be very useful for finding optimal parameter changes for species conservation a metapopulation model. Although already widely used in meteorology (i.e. Courtier et al., 1993, Barkmeijer et al., 2002, Moolenaar and Selten, 2004), it is a fairly unknown technique in metapopulation modelling. The method shown in this article was first tested in an atmospheric model (Moolenaar and Selten, 2004) and proved to be successful for an metapopulation model as well. In this study a metapopulation was used that was coupled to an atmospheric model. We chose to only perturb the parameters in the metapopulation model. However, perturbations in the climate model could have been taken into consideration as well. For this, the tangent linear equation would have to be extended with the equations for the atmospheric model. In this way, uncertainty in the climate model, or even the effect climate change could have on a metapopulation could be estimated. When first determining boundaries in which the climate parameter models are uncertain, the extreme changes for the dynamics of the populations can then be calculated. The interest in the effect of climate change upon ecosystems is strongly growing (i.e. Stenseth et al., 2002, Araújo et al., 2004, Preisser and Strong, 2004). The adjoint method proposed in this study

opens new possibilities for conservation management and sensitivity studies of large scale models.

5.6 Acknowledgement

We would like to thank Maarten de Gee for his interest and useful comments.

References

- Akçakaya, H.R., 2000a. Viability analyses with habitat-based metapopulation models. *Population Ecology*, **42**, 45-53.
- Akçakaya, H.R., 2000b. Population viability analyses with demographically and spatially structured models. *Ecological Bulletins*, **48**, 23-38.
- Araújo, M.B., Cabeza, M., Thuiller, W., Hannah, L., 2004. Would climate change drive species out of reserves? An assessment of existing reserve-selection methods. *Global Change Biology* **10**, 1618-1626.
- Barkmeijer, J., Iversen T., Palmer, T.N., 2003. Forcing singular vectors and other sensitive model perturbations. *Quarterly Journal of Royal Meteorological Society*, **129**, 2401-2424.
- Burgman M.A., Ferson, S. and Akçakaya, H.R., 1993. Risk Assessment in Conservation Biology. *Chapman and Hall, London*.
- Conroy, M.J., Cohen, Y., James, F.C., Matsinos, Y.G., Maurer, B.A., 1995. Parameter estimation, reliability and model improvement for spatially explicit models of animal populations. *Ecological Applications*, **5**, 17-19.
- Courtier, P., Derber, J., Errico, R., Louis, J-P, Vukicevic, T., 1993. Important literature on the use of adjoint, variational methods and the Kalman filter in meteorology. *Tellus*, **45**, 342-357.
- DeAngelis, D.E., Gross, L.J., 1992. Individual-based models and approaches in ecology: populations, communities and ecosystems. *Chapman and Hall, New York*.
- DeAngelis, D.E., 1992. Dynamics of Nutrient Cycling and Food Webs. *Chapman and Hall, London*.
- Drechsler, M., Frank, K., Hanski, I., O'Hara, R.B., Wissel, C., 2003. Ranking metapopulation extinction risk: from patterns in data to conservation management decisions. *Ecological Applications*, **13**, 990-998.
- Errico, R.M., 1997. What is an adjoint model? *Bulletin of the American Meteorological Society*, **78**, 2577-2591.
- Etienne, R.S., 2004. On optimal choices in increase of patch area and reduction of interpatch distance for metapopulation persistence. *Ecological Modelling*, **179**, 77-90.

- Hanski, I., Alho, J., Moilanen, A., 2000. Estimating the parameters of survival and migration of individuals in metapopulations. *Ecology*, **81**(1), 239-251.
- Huang, Y. and Diekmann, O., 2001. Predator migration in response to prey density: What are the consequences? *Journal of Mathematical Biology* **43**, 561-581.
- Janssen, V.A.A., 2001. The dynamics of two diffusively coupled predator-prey populations. *Theoretical Population Biology*, **59**, 119-131
- Lawson, L.M., Y.H. Spitz, E.E. Hofmann and R.B. Long, 1995. A data assimilation technique applied to a predator-prey model. *Bulletin of Mathematical Biology*, **57**:4, 593-617.
- Levins, R., 1970. Extinction. in: Some Mathematical Problems in Biology. Gertenhaber, M. (Ed.), *American Mathematical Society*, 75-107.
- Lorenz, E.N., 1984. Irregularity: A fundamental property of the atmosphere. *Tellus*, **36A**, 98-110.
- Moilanen, A., 2002. Implications of empirical data quality to metapopulation model parameter estimation and application. *Oikos*, **96**, 516-530.
- Moolenaar, H.E., Selten, F.M., 2004. Finding the effective parameter perturbations in atmospheric models: the LORENZ63 model as case study. *Tellus* **56A**, 47-55.
- Ovaskainen, O., 2004. Habitat-specific movement parameters estimated using mark-recapture data and a diffusion model. *Ecology* **85**(1), 242-257.
- Ovaskainen, O., Hanski, I., 2004. From individual behavior to metapopulation dynamics: unifying the patchy population and classic metapopulation models. *The American Naturalist*, **164**, 364-377.
- Press, W.H., Flannery, B.P., Teukolsky, S.A., Vetterling, W.T., 1986. Numerical Recipes. *Cambridge University Press*.
- Preisser, E.L., Strong, D.R., 2004. Climate affects predator control of an herbivore outbreak. *The American Naturalist*, **163**, 754-762.
- Rai, V., Anand, M., 2004. Is dynamic complexity of ecological systems quantifiable? *International Journal of Ecology and Environmental Sciences* **30**, 123-130.

Sherratt, J.A., Eagan, B.T., Lewis, M.A., 1997. Oscillations and chaos behind predator-prey invasion: mathematical artifact of ecological reality? *Philosophical Transactions Royal Society London B*, **352**, 21-38.

Stenseth, N.C., Mysterud, A., Ottersen, G., Hurrell, J.W., Chan, K.-S., Lima, M., 2002. Ecological effects of climate fluctuations. *Science*, **297**, 1292-1296.

Rosenzweig M.L., and MacArthur, R.H., 1963. Graphical representation and stability conditions of predator-prey interactions. *American Naturalist* **97**, 209-223.

Summary

Uncertainty in the outcome of climate and ecosystem models is widely recognized. A contributing factor is uncertainty in the value of parameters as well as uncertainty in the understanding of physical processes within these systems. Because of this uncertainty a range of outcomes is usually given. This range can be too large to gain insight in the possible evolutions, for instance in terms of climate change. Policy making might be hindered by this uncertainty, for instance policies on reducing greenhouse gases emissions. It is evident that the parameters, the model is most sensitive to, need to be identified. Within an uncertainty study, a parameter sensitivity study is inevitable.

Numerical models are used to simulate physical processes such as the atmospheric circulation and the dynamics of metapopulations. The physical processes can be expressed in mathematical equations, forming a numerical model. By numerically approximating the solution, a prediction can be made of the future state of the model. Small-scale processes are captured in so-called model parameters. Parameters are constant values in the model. They can be estimated using observed data and/or fundamental physical principles. Inaccurate or insufficient data can lead to uncertainties in the parameters, which can influence the model forecast. It is important to verify how much small changes in parameters can change a model outcome. Especially parameter perturbations that have the largest effect on the outcome of the model are of importance. The model is most sensitive to these parameter perturbations, which we call effective parameter perturbations.

The more complex the model and the larger the amount of parameters, the more difficult it is to find the most effective parameters. A random method, where parameters are perturbed at random, is then unfeasible. It is therefore useful to develop a method that finds effective parameter perturbations in an efficient way. In this thesis we describe a method that selects parameter perturbations that have a high probability to cause a large change in the long term behaviour of the model. Use is made of the short term dynamic behaviour of the model. A short part of the non-linear (unperturbed) reference orbit is considered. The error growth in the neighbourhood of this reference orbit can be calculated with the use of the so-called tangent linear equations. The parameter perturbation that causes the largest deviation from the reference orbit in this short term, can be determined with the use of the so-called adjoint equations acting as a backward integration. This perturbation is called the first singular vector.

In this thesis we carry out a parameter sensitivity analysis in two atmospheric mod-

els; the Lorenz 63 model and the quasi-geostrophic three-level T21QG model. Moreover, we consider a metapopulation model, the Rosenzweig-McArthur model coupled to the atmospheric Lorenz 84 model. In chapter 2 the Lorenz 63 model is used as a case study. In the atmospheric circulation preferred patterns occur, referred to as regimes. The atmosphere exhibits irregular regime changes. Climate is described by the strength of the occurring regimes and by the frequency of transitions from one regime to the other. Climate change will be looked at in terms of change in the strength of preferred circulation patterns. The Lorenz 63 system contains only two regimes, making it easy to analyse. When the parameters are set at their original values, these regimes are equally visited in a long simulation and the model is symmetric. Parameter perturbations are introduced that cause asymmetry in the model. One regime can be visited more at the expense of the other and climate change occurs. We assume that the parameters contain 5% uncertainty.

We develop a method that selects parameter perturbations that have a high probability to cause a large change in the climate, using the short term dynamic behaviour of the model. We start with a direct method, where the parameter perturbations are selected at random. This is feasible because it is a simple model that does not require much computing time. We select 50000 different random perturbations and make a long simulation with the perturbed model. The probability density function (PDF) of the rate of asymmetry that the parameter perturbations can cause is unimodal with a maximum at zero (no asymmetry). Next we select the parameter perturbations that caused the largest climate change. With these parameter perturbations we make short simulations. The short simulations are short enough for the linearity of the model to be accurate enough. It appears that for some intervals of the attractor, these parameter perturbations collide with the first singular vector. This occurs just *after* the reference orbit has passed a highly sensitive area. This means that after the singular value (the length of the singular vector) has peaked at a high value, it has shrunk again. Again we make 50000 long simulations, this time with parameters perturbed in the direction of the singular vectors, that are selected on the basis of the singular value. We compare the two methods and it appears that the adjoint method is more efficient in selecting effective parameter perturbations and hardly draws any perturbations that cause just a small amount of climate change.

After these findings in a simple atmospheric model, we test the adjoint method in a more realistic model, the quasi-geostrophic three-level T21QG model, described in chapter 3. The T21QG model integrates prognostic equations for potential vorticity. It contains several regimes, that can be identified with Empirical Orthogonal Functions (EOFs). The first EOFs indicate the preferred patterns, such as the NAO (North Atlantic Oscillation) and the PNA (Pacific North Atlantic oscillation). By using these EOFs the dimension of the state space of the model can be reduced considerably. Changes in regime behaviour indicate changes in the climate. In this study only the forcing parameters are perturbed. Again we assume that the forcing parameters contain 5% uncertainty.

We compare the random method and the adjoint method, developed in the context of the Lorenz 63 model, as they are applied to the T21QG model. The vector con-

taining the forcing parameters has a dimension of 1449 (degrees of freedom). This is considerably larger than in the simple Lorenz 63 model. Since the T21QG model requires more computing time, only 1000 different model simulations are feasible for both methods. To carry out these simulations we use the high performance computing facility at the European Centre for Medium range Weather Forecasts (ECMWF), where it is possible to make parallel runs. One simulation takes approximately 7 hours in real time and we are able to make 32 runs simultaneously. The climate change is measured with the use of the first few EOFs. For every integration step the streamfunction is projected onto the EOFs. This gives an anomaly in the direction of every EOF. A time series of the anomalies can be calculated for every EOF. Next a PDF is computed of the time series of the anomalies. A change in the PDF, such as a shift or change in shape, indicates climate change. It turns out that the parameter perturbations that give the largest climate change in terms of the sum of absolute changes in PDF1 to PDF6 also give the largest change in only PDF1. So only changes in this PDF can be used as an indicator of climate change. When comparing the random method with the adjoint method, it turns out that the parameter perturbations drawn with the random method hardly cause any change at all. The chosen singular vectors are more effective in changing the regime behaviour, 35.7% of the found perturbations are more effective than all the random perturbations. This also means that the random method does not approach the optimal climate change. This is because of the large parameter space, in which a numerous combinations are possible. Finding the most effective parameter perturbation might not be within reach in this model with the adjoint method. However, we show that although hampered by the large parameter set, the adjoint method comes closer to selecting the parameter perturbation causing the largest climate change than the random method.

In chapters 4 and 5 we use a metapopulation model, coupled to the simple atmospheric Lorenz 84 model. The effect of climate variability and change upon ecological systems is gaining attention. Here we use a herbivore-predator model, containing two patches. The intrinsic growth rates and/or the carrying capacities of the herbivores depend on the climate fluctuations. Fifth percentiles are used to indicate the state of the populations with respect to their risk of extinction. The fifth percentile is the threshold below which 5 out of a 100 values from a long time series are found. The higher this fifth percentile, the lower the risk of extinction. A rise in the fifth percentile indicates that the conditions of the corresponding population are improved.

In chapter 4 different versions of the model are investigated. We start with the model where predators are absent and the herbivores can migrate between the patches. The carrying capacities of the herbivores depend of the climate fluctuations. We use two different, uncorrelated, time series of the climate for the patches. We analyse the influence of the migration rate. It turns out that an increasing migration coefficient does not improve the local conditions for a species. The degree of coupling between the two patches does however influence the speed of recolonization in cause of a complete local extinction. Next predators are added to the model. This time climate time series are the same in the different patches and the intrinsic growth rates of the herbivores depend on the climate. The goal is to improve the conditions of the most vulnerable herbivore

subpopulation by increasing the migration rate of the herbivores and/or the death rate of the predators. For the optimal solution we found that the predator dies out in one patch. Lastly the model is adjusted by also allowing migration between the predators at the two patches. An increase in the migration rate between the predators, v , has a negative effect on the herbivores for small values of v . It depends on the value of v which patch has the highest improvement of conditions for the herbivores. Increasing the death rates of the predators has little or no effect on the herbivores. Increasing the migration rate of the herbivores has a positive effect on the herbivores in one patch, but a negative effect on the herbivores in the other patch. It turns out that general rules are hard to formulate. The type of choices that is made depends on the population that needs to be supported. Changes in favour of a specific population can have unforeseen negative consequences for other populations, with extinction as extreme.

In chapter 5 the second version of the model is used, so only the herbivores can migrate between the patches and their intrinsic growth rates are influenced by the climate. We consider a set of five parameters that can be perturbed: the intrinsic growth rates, the death rates of the predators and the migration rate. The adjoint method as used in atmospheric models in chapters 2 and 3, is now tested in this metapopulation model. We want to find the ecological parameter perturbations that decrease the risk of extinction of the herbivores as much as possible. It turns out that a parameter perturbation in the direction of a selected singular vector improves the conditions for both herbivores. In addition parameters in the driving climate model could be perturbed as well. In this way the effect of climate change upon ecological systems could be analysed. The adjoint method as described in this thesis opens new possibilities for conservation management and sensitivity analysis of large scale models.

Samenvatting

Onzekerheid in uitkomsten van klimaat- en ecosysteemmodellen wordt algemeen erkend. Oorzaak hiervan is onzekerheid over de waarde van parameters en tevens onzekerheid over het begrip van fysische processen binnen deze systemen. Door deze onzekerheid wordt meestal een bereik van verschillende uitkomsten gegeven. Dit bereik kan te groot zijn om een betekenisvol inzicht te krijgen in mogelijke evoluties, bijvoorbeeld met betrekking op klimaatverandering. Beleidsvoering kan door deze onzekerheid belemmerd worden, bijvoorbeeld beleidsmaatregelen om de uitstoot van broeikasgassen te verminderen. Het is duidelijk dat het nodig is de parameters te identificeren waar een model het meest gevoelig voor is. Binnen een onzekerheidsstudie is een parametergevoeligheidsanalyse onvermijdelijk.

Numerieke modellen worden gebruikt om fysische processen, zoals de atmosferische circulatie en de dynamica van metapopulaties, te simuleren. De fysische processen kunnen worden uitgedrukt in wiskundige vergelijkingen, die een numeriek model vormen. Door de oplossing numeriek te benaderen, kunnen we een voorspelling maken van de toestand van het model in de toekomst. Kleinschalige processen worden samengevat in zogenaamde modelparameters. Parameters zijn constante waarden in het model. Ze worden geschat met gebruik van geobserveerde data en/ of met behulp van fundamentele fysische principes. Onnauwkeurige of onvolledige data kunnen tot onzekerheden in de parameters leiden, wat de modelvoorspelling kan beïnvloeden. Het is belangrijk om te bepalen in hoeverre kleine veranderingen in parameters een model uitkomst kan veranderen. Vooral de mogelijke parameter verstoringen die het grootste effect hebben op de uitkomst van het model zijn van belang. Het model is het meest gevoelig voor deze parameter verstoringen, die we effectieve parameter verstoringen noemen.

Hoe complexer het model en hoe groter de hoeveelheid parameters, des te moeilijker is het om de meest effectieve parameters te vinden. Een random methode, waarmee parameters willekeurig worden verstoord, is dan niet haalbaar. Het is daarom nuttig om een methode te ontwikkelen die op een efficiënte manier de meest effectieve parameter verstoringen vindt. In dit proefschrift beschrijven we een methode die parameter verstoringen selecteert die een hoge waarschijnlijkheid hebben een grote verandering in het lange termijn gedrag van het model te veroorzaken. Het korte termijn dynamische gedrag van het model wordt gebruikt. Een korte sectie van de niet-lineaire (onverstoorde) referentie baan wordt beschouwd. De foutengroei in de omgeving van

dit deel van de referentiebaan kan uitgerekend worden met behulp van de zogenaamde tangent lineaire vergelijkingen. De parameter verstoring die op dit korte interval de grootste afwijking ten opzichte van de referentiebaan veroorzaakt, kan worden bepaald met behulp van de zogenaamde adjoint vergelijkingen; deze procedure werkt als een integratie terug in de tijd. Deze verstoring heet de eerste singuliere vector.

In dit proefschrift voeren we een parametergevoeligheids analyse uit voor twee atmosferische modellen; het Lorenz 63 model en het quasi-geostrofe drie-lagen T21QG model. Tevens beschouwen we een metapopulatie model, het Rosenzweig-McArthur model dat gekoppeld is aan het atmosferische Lorenz 84 model. In de atmosferische circulatie komen voorkeurspatronen voor, ook wel regimes genoemd. De atmosfeer vertoont onregelmatige regime's overgangen. Klimaat wordt beschreven door de verschijning van de verschillende regimes met een bepaalde sterkte en door de frequentie van transitie van het ene regime naar het andere. Klimaatverandering wordt bekeken in termen van verandering in de sterkte van voorkeurspatronen in de circulatie. Het Lorenz 63 model, bestudeerd in hoofdstuk 2, heeft maar twee regimes, wat het makkelijk maakt om te analyseren. Wanneer de parameters hun originele waarden hebben, worden deze twee regimes even vaak bezocht in een lange simulatie en het model is symmetrisch. Parameter verstoringen kunnen asymmetrie in het model veroorzaken. Het ene regime kan vaker worden bezocht ten koste van het andere en er treedt klimaatverandering op. We nemen aan dat de parameters 5% onzekerheid bevatten.

We ontwikkelen een methode die parameter verstoringen selecteert die zeer waarschijnlijk een grote verandering in het klimaat veroorzaken, gebruik makend van het korte termijn dynamische gedrag van het model. We beginnen met een directe (random) methode, waar de parameter verstoringen willekeurig worden geselecteerd. Dit is haalbaar omdat het een simpel model is, dat niet veel rekentijd vergt. We selecteren 50000 verschillende willekeurige verstoringen en maken een lange simulatie met het verstoorde model. De functie van de waarschijnlijkheidsdichtheid (PDF) van de mate van asymmetrie die de parameter verstoringen kunnen veroorzaken is unimodaal met een maximum bij het punt nul (geen asymmetrie). Vervolgens selecteren we de parameter verstoringen die de meeste klimaatverandering hebben veroorzaakt. Met deze parameter verstoringen maken we korte simulaties. De korte simulaties zijn zo kort dat de lineariteit van het model nog nauwkeurig genoeg is. Het blijkt dat voor sommige intervallen van de attractor, deze parameter verstoringen samenvallen met de richting van de eerste singuliere vector. Dit gebeurt net *nadat* een referentie baan een zeer gevoelig gebied heeft gepasseerd. Dit houdt in dat nadat de singuliere waarde (de lengte van de singuliere vector) een grote waarde heeft bereikt, deze weer sterk is gekrompen. We maken opnieuw 50000 lange simulaties, waar deze keer de parameters zijn verstoord in de richting van de singuliere vectoren, geselecteerd op basis van de singuliere waarde. We vergelijken de twee methoden en het blijkt dat de adjoint methode veel efficiënter is in het selecteren van effectieve parameter verstoringen en dat deze vrijwel geen verstoringen trekt die slechts een kleine hoeveelheid klimaatverandering veroorzaken.

Na deze bevindingen in een simpel atmosferisch model, testen we de adjoint methode in een realistischer model, het quasi-geostrofe drie-lagen T21QG model, beschreven in hoofdstuk 3. Het T21QG model integreert prognostische vergelijkingen

voor potentiële vortciteit. Het bevat verschillende regimes, die kunnen worden geïdentificeerd met Empirische Orthogonale Functies (EOFs). De eerste EOFs geven de voorkeurspatronen aan, zoals de NAO (Noord Atlantische Oscillatie) en de PNA (Pacific Noord Atlantische oscillatie). Door het gebruik van deze EOFs kan de dimensie van de toestandsruimte van een model aanzienlijk worden verkleind. Veranderingen in het regimegedrag geven veranderingen in het klimaat aan. In deze studie worden alleen de forceringsparameters verstoord. Opnieuw nemen we aan dat de forceringsparameters 5% onzekerheid bevatten.

We vergelijken de random methode met de adjoint methode ontwikkeld in de context van het Lorenz 63 model, wanneer we deze toepassen op het T21QG model. De vector die de forceringsparameters bevat heeft een dimensie van 1449 (aantal vrijheidsgraden). Dit aantal is aanzienlijk meer dan in het simpele Lorenz 63 model. Aangezien het T21QG meer computer tijd vergt, zijn slechts 1000 verschillende model simulaties per methode haalbaar. Om deze simulaties uit te voeren gebruiken we de high performance computer faciliteit van het European Centre for Medium range Weather Forecasts (ECMWF), waar het mogelijk is om parallel te rekenen. Eén simulatie vergt ongeveer 7 uur in echte tijd en we kunnen 32 simulaties tegelijk uitvoeren. De klimaatverandering wordt gemeten aan de hand van de eerste paar EOFs. Voor elke integratiestap wordt de stroomfunctie geprojecteerd op de EOFs. Dit geeft een anomalie in elke EOF richting. Een tijdreeks van de anomalieën kan berekend worden voor elke EOF. Vervolgens wordt een PDF gemaakt van de tijdreeks van de anomalieën. Een verandering in de PDF, zoals een verschuiving of een verandering in de vorm, geeft klimaatverandering aan. Het blijkt dat de parameter verstoringen die de grootste klimaatverandering teweeg brengt in termen van de som van absolute veranderingen in PDF1 tot en met PDF6 ook de grootste verandering veroorzaakt in alleen de eerste PDF. Dus veranderingen in alleen deze PDF kunnen gebruikt worden als indicator voor klimaatverandering. Wanneer we de random methode met de adjoint methode vergelijken, blijkt dat de parameter verstoringen die getrokken worden met de random methode amper een verandering veroorzaken. De gekozen singuliere vectoren zijn effectiever in het veranderen van het regime gedrag, 35.7% van de gevonden verstoringen zijn meer effectief dan alle random verstoringen. Dit betekent ook dat de random methode niet de optimale klimaat verandering benadert. Dit komt door de grote parameter ruimte, waarin een groot aantal combinaties mogelijk zijn. Het vinden van de meest effectieve parameter verstoring is misschien nog steeds niet haalbaar in dit model met de adjoint methode. We laten echter zien dat, ondanks de beperking door de grootte van de parameter set, de adjoint methode dichtbij het selecteren van de parameter verstoring die de grootste klimaatverandering veroorzaakt komt, dan de random methode.

In de hoofdstukken 4 en 5 gebruiken we een metapopulatie model, gekoppeld aan het simpele atmosferische Lorenz 84 model. Het effect van klimaat variabiliteit en de daarmee samenhangende verandering in ecologische systemen krijgen steeds meer aandacht. Hier gebruiken we een herbivoor-predator model, wat twee gebieden omvat. De intrinsieke groeicoëfficiënten en/of de draagkrachten van de herbivoren zijn afhankelijk van de klimaatfluctuaties. Vijfde percentielen worden gebruikt om de toestand van de populaties met betrekking tot hun risico van uitsterving aan te tonen. Het

vijfde percentiel is de drempelwaarde waaronder 5 van de 100 waarden van een lange tijdreeks worden gevonden. Hoe hoger dit vijfde percentiel, des te lager is het risico van uitsterving. Een groei in het vijfde percentiel geeft aan dat de condities van de bijbehorende populatie zijn verbeterd.

In hoofdstuk 4 worden verschillende versies van het model onderzocht. We beginnen met het model waar predatoren afwezig zijn en de herbivoren kunnen migreren tussen de gebieden. De draagkrachten van de herbivoren zijn afhankelijk van de klimaatfluctuaties. We gebruiken twee verschillende, ongecorreleerde, tijdreeksen van het klimaat voor de gebieden. We analyseren de invloed van de migratiecoëfficiënt. Het blijkt dat een toenemende migratiecoëfficiënt niet de lokale condities van een soort verbeterd. De mate van koppeling tussen de twee gebieden beïnvloedt echter wel de snelheid van rekolonisatie in het geval van een volledige lokale uitsterving. Vervolgens worden predatoren toegevoegd aan het model. Tevens worden dezelfde klimaat-tijdreeksen gebruikt in de verschillende gebieden en de intrinsieke groeicoëfficiënten van de herbivoren zijn afhankelijk van het klimaat. Het doel is om de condities van de meest kwetsbare herbivoor subpopulatie te verbeteren door de migratiecoëfficiënt van de herbivoren en/of de sterftecoëfficiënt van de predatoren te vergroten. Voor de door ons gevonden optimale oplossing sterft de predator in één gebied uit. Als laatste wordt het model aangepast door ook migratie tussen de predatoren toe te laten. Een toename in de migratie mate tussen de predatoren, v , heeft een negatief effect op de herbivoren voor kleine waarden van v . Het hangt af van de waarde van v in welk gebied de grootste verbetering in condities voor de herbivoren optreedt. Toename van de sterftecoëfficiënten van de predatoren heeft weinig of geen effect op de herbivoren. Toename van de migratiecoëfficiënt van de herbivoren heeft een positief effect op de herbivoren in het ene gebied maar een negatief effect op de herbivoren in het andere gebied. Het blijkt dat algemene regels moeilijk op te stellen zijn. Het type keuzes die gemaakt moeten worden hangen af van de populatiegroep die versterkt moet worden. Veranderingen ten gunste van een bepaalde populatie, kunnen onvoorziene negatieve gevolgen hebben voor andere populaties, met als extreem uitsterving.

In hoofdstuk 5 wordt de tweede variant van het model gebruikt, dus alleen de herbivoren kunnen migreren tussen de gebieden en hun intrinsieke groeicoëfficiënten worden beïnvloed door het klimaat. We nemen een set van vijf parameters in acht die verstoord kunnen worden: de intrinsieke groeicoëfficiënten, de sterftecoëfficiënten van de predatoren en de migratiecoëfficiënt. De adjoint methode, zoals deze is gebruikt in atmosferische modellen in hoofdstukken 2 en 3, wordt nu getest in dit metapopulatie model. We willen de ecologische parameter verstoringen vinden die het uitstervingsrisico voor de herbivoren zoveel mogelijk zal verminderen. Het blijkt dat de geselecteerde singuliere vectoren de condities voor beide herbivoren verbeteren. Tevens kan er voor gekozen worden ook de parameters in het drijvende klimaat model te verstoren. Op deze manier zou bijvoorbeeld het effect van klimaatverandering op ecologische systemen kunnen worden geanalyseerd. De adjoint methode zoals deze is beschreven in dit proefschrift opent nieuwe mogelijkheden voor natuurbeheer en gevoeligheidsstudies van grootschalige modellen.

Word of thanks

I would like to thank my supervisors Prof. Johan Grasman and Dr. Frank Selten for their continuous support and motivation. Also thanks to my colleagues at KNMI and Wageningen University for their interest, especially Dr. Jan Barkmeijer and Dr. Maarten de Gee for their useful suggestions.

Thanks to my parents for believing in me. Thanks to Johan, you are always there for me. Thanks to Sytske, you have always been my role model (and a very good one). Thanks to Nienke, for all the chatting to cheer me up.

Most of all, thanks to Richard. It would have been impossible if it hadn't been for you.

"Ever since I've been with you, you hold me up when I'm falling down"¹

¹Joseph Arthur: Honey and the moon; Redemption's son

Curriculum Vitae

Personal details	
Name	Hanneke Elisabeth Moolenaar
Date of birth	August 25, 1979
Place of birth	Zoetermeer

Education	
1991-1995	Oranje Nassau College, Zoetermeer
1995-1997	Christelijk Lyceum Zeist, Zeist
1997-1998	Mathematics (propedeuse) Utrecht University
1998-2001	Mathematics (M.Sc.) University of Groningen
2001-2006	Ph.D. in applied mathematics Wageningen University in collaboration with KNMI
